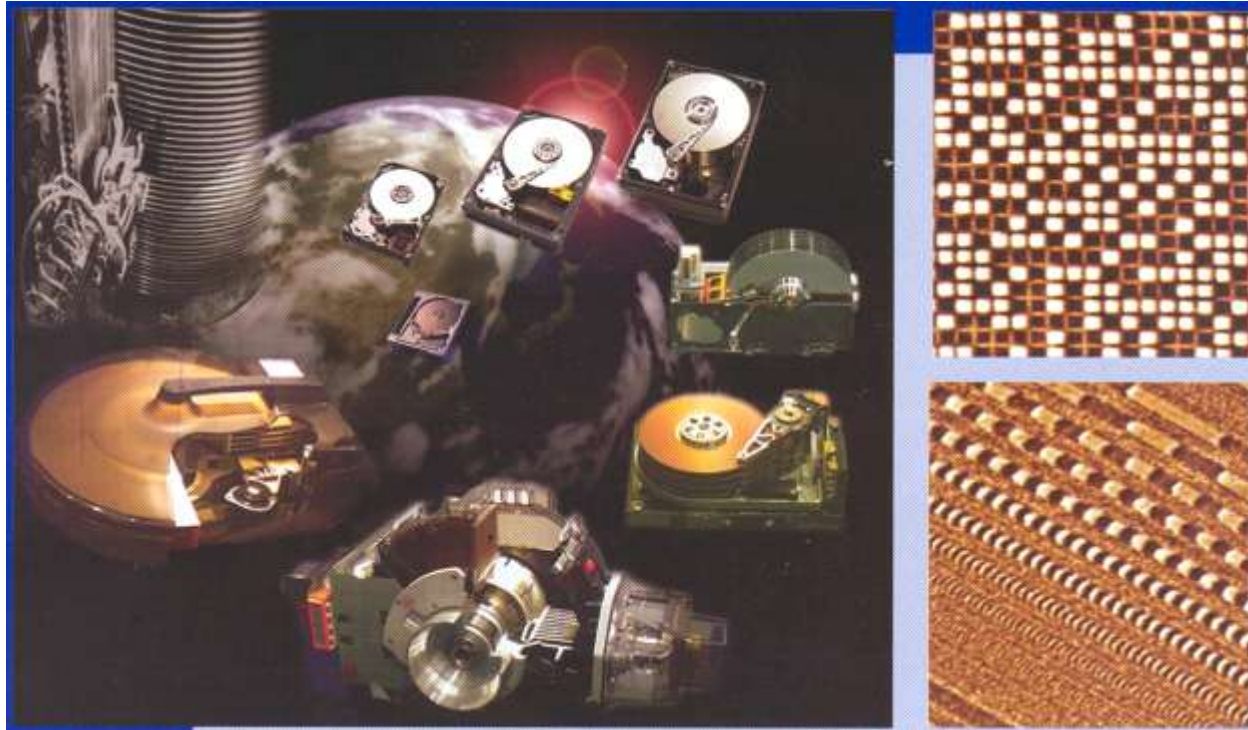


Magnetic Recording



Stella Z. Wu

Seagate Technology



IEEE Magnetics Society Summer School
Assisi, June 9-14, 2013



Acknowledgement

Jan-Ulrich Thiele

Roger Wood

Kaizhong Gao

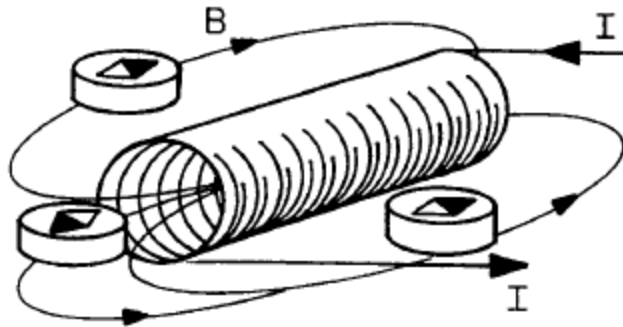
Ganping Ju

Shuaigang Xiao

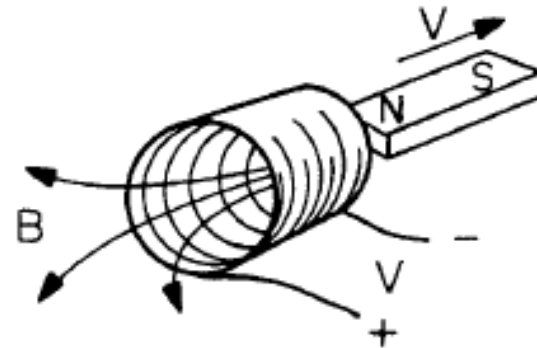
And many more of my Seagate colleagues

Elements of a magnetic recording system

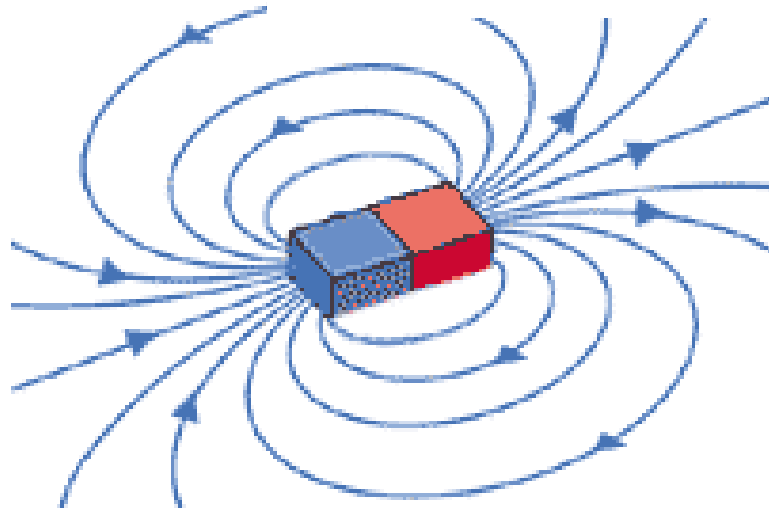
write



read



store



115 years ago

Magnetic Recording Invented

Valdemar Poulsen



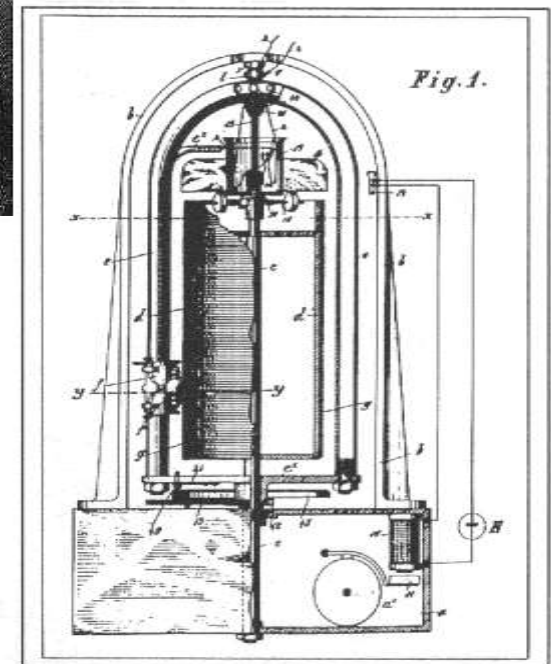
Valdemar Poulsen's wire recorder from 1898
(Danish technical museum www.tekniskmuseum.dk)



1898

MAGNETIC RECORDING

Invented by Valdemar Poulsen
Copenhagen, Denmark 1898



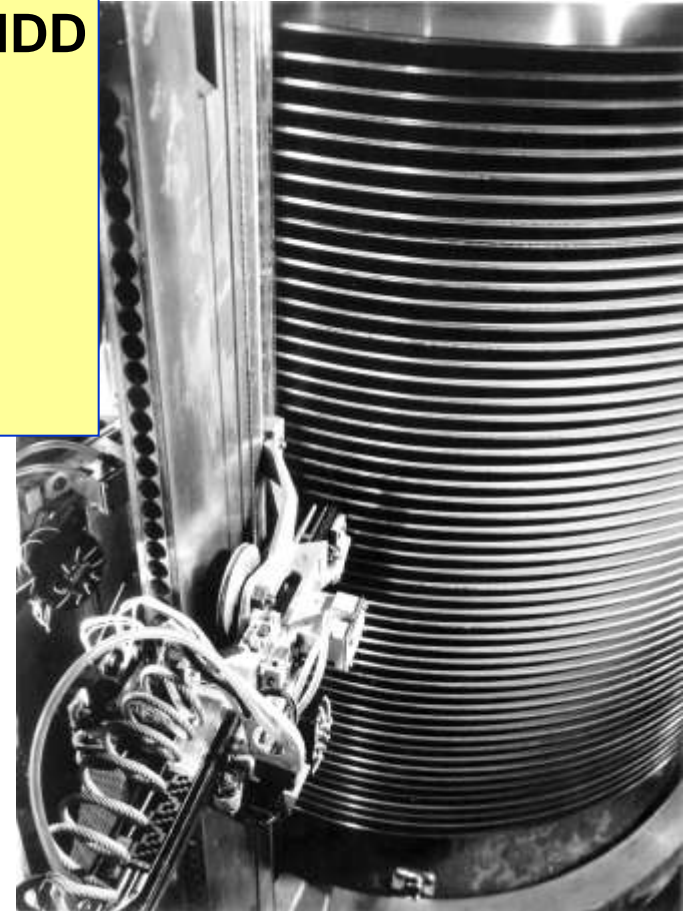
"Method of Recording and
Reproducing Sounds or Signals."

57 years ago

1956

IBM RAMAC - first HDD

- 5 MegaBytes
- Fifty 24" disks
- 1200 RPM
- 2 kbits/sq.in.
- 100 BPI x 20 TPI
- 150 kbit/s



\$10,000/Mbyte

32 years ago



1981



3380 system

- 1.26 GigaBytes (GB)
- Nine 14" disks
- 3600 RPM
- 12.2 Mbits/sq.in.
- 15.25 kBPI x 800 TPI
- 20 Mbit/s
- **Thin-film head !**

\$15,000 to make / sold for \$100,000

19 years ago

1994

2.5" form-factor x 12.5 mm high



TravelStar LP

2.5-inch low-profile (12.5 mm)

2 disks, 4 heads, 4200 RPM

- Capacity 720 MB
- 644 Mb/sq in
- 101 kBPI x 6.35 kTPI
- 39.5 Mbits/sec
- thin-film media
- MR head
- PRML channel
- non-op. shock 500g

13 years ago

2000

1 GigaByte microdrive



1 GB Microdrive

1-inch form-factor (5 mm)

1 disks, 2 heads, 3600 RPM

- Capacity 1 GB
- 15.2 Gbit/sq in
- 435 kBPI x 35 kTPI
- 38.8 Mbits/sec
- **GMR head**

Data Storage...It's all going digital



Digital Imaging



Home Media Server



Digital Video Recorder



Game Consoles



HDTV w/ built-in DVR



Personal Computer



Handheld / Portable



Automobile

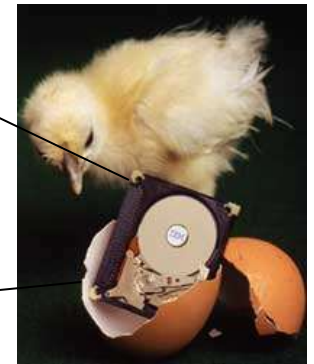
Product scaling



160 Gbyte
mobile drive



10 Gbyte



2 kbits/in²
70 kbits/s
50x 24" in dia disks
\$10,000/Mbyte

135 Gbits/in²
500 Mb/s
2 x 2.5" glass disks
<\$0.005/Mbyte

Microdrive
100 Gbits/in²
1 x 1" dia disk

Price scaling

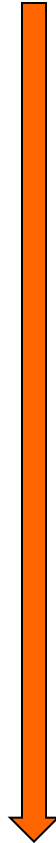
1956 IBM RAMAC - first HDD: \$10,000,000/GB

Digital Storage Cost per GB 1981 – 2012

1981	\$300,000
1987	\$50,000
1990	\$10,000
1994	\$1,000
1997	\$100
2000	\$10
2004	\$1
2012	\$0.10

Timeline

Sony walkman holds 90min of music	1979
Seagate ships 1st hard drive	1980
IBM launches 1st personal computer	1981
Time magazine names computer: Machine of the Year	1982
Introduction of Microsoft Word	1983
Apple introduces the Macintosh	1984
Blockbuster opens 1st store	1986



Seagate ships 5M hard drives	1988
WWW established with HTML	1990
Seagate ships 100M hard drives	1996
More emails than snail mails	
Xbox 360 unveiled w Seagate drive	2005
Seagate ships 1 billion hard drives	2008
World's largest data center opens in Nevada	
Seagate ships 2 billion hard drives	2013



It takes **29** years to reach first billion hard drive shipment

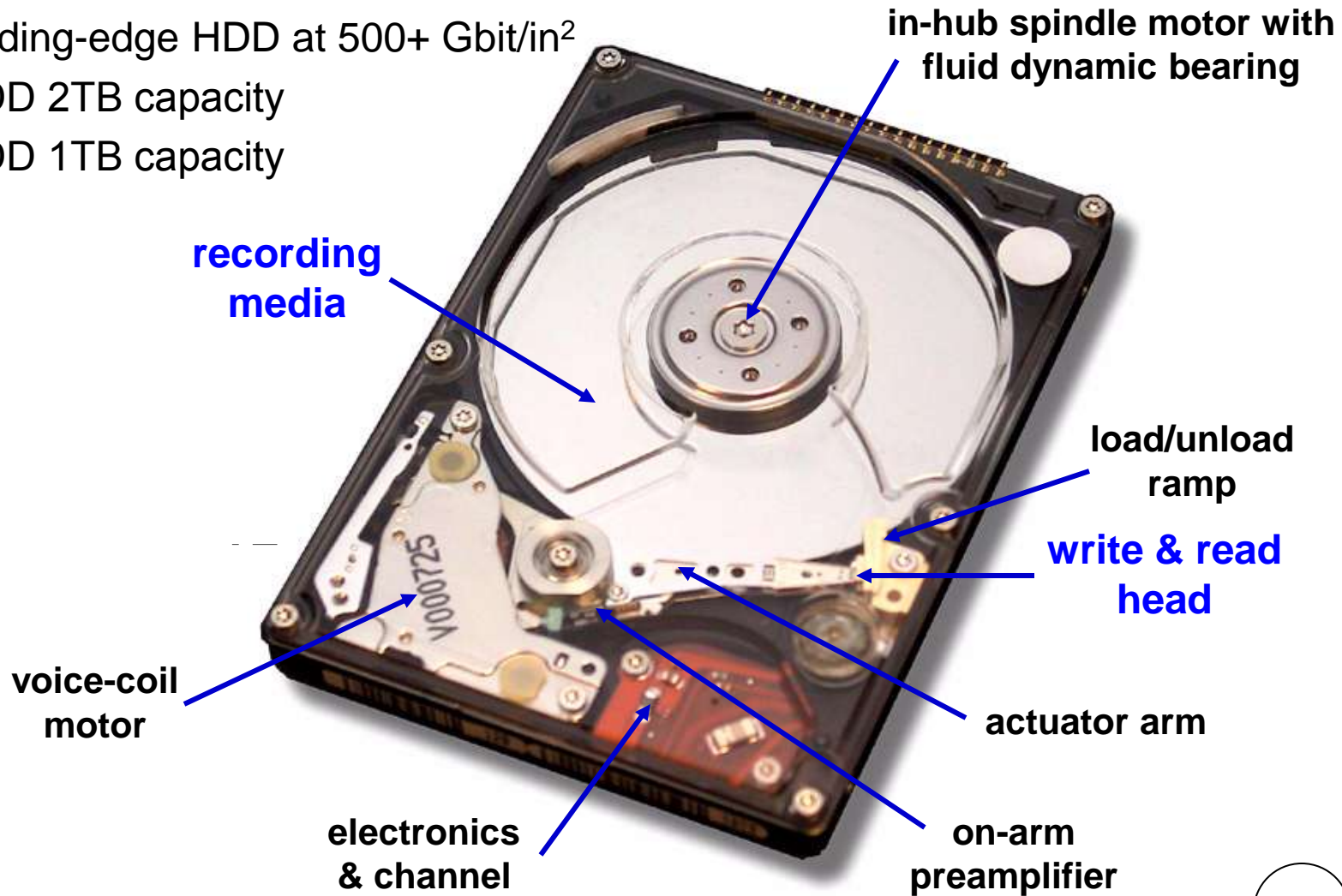
It takes only **4** years to reach second billion hard drive shipment

(3/12/2013 Seagate press release)

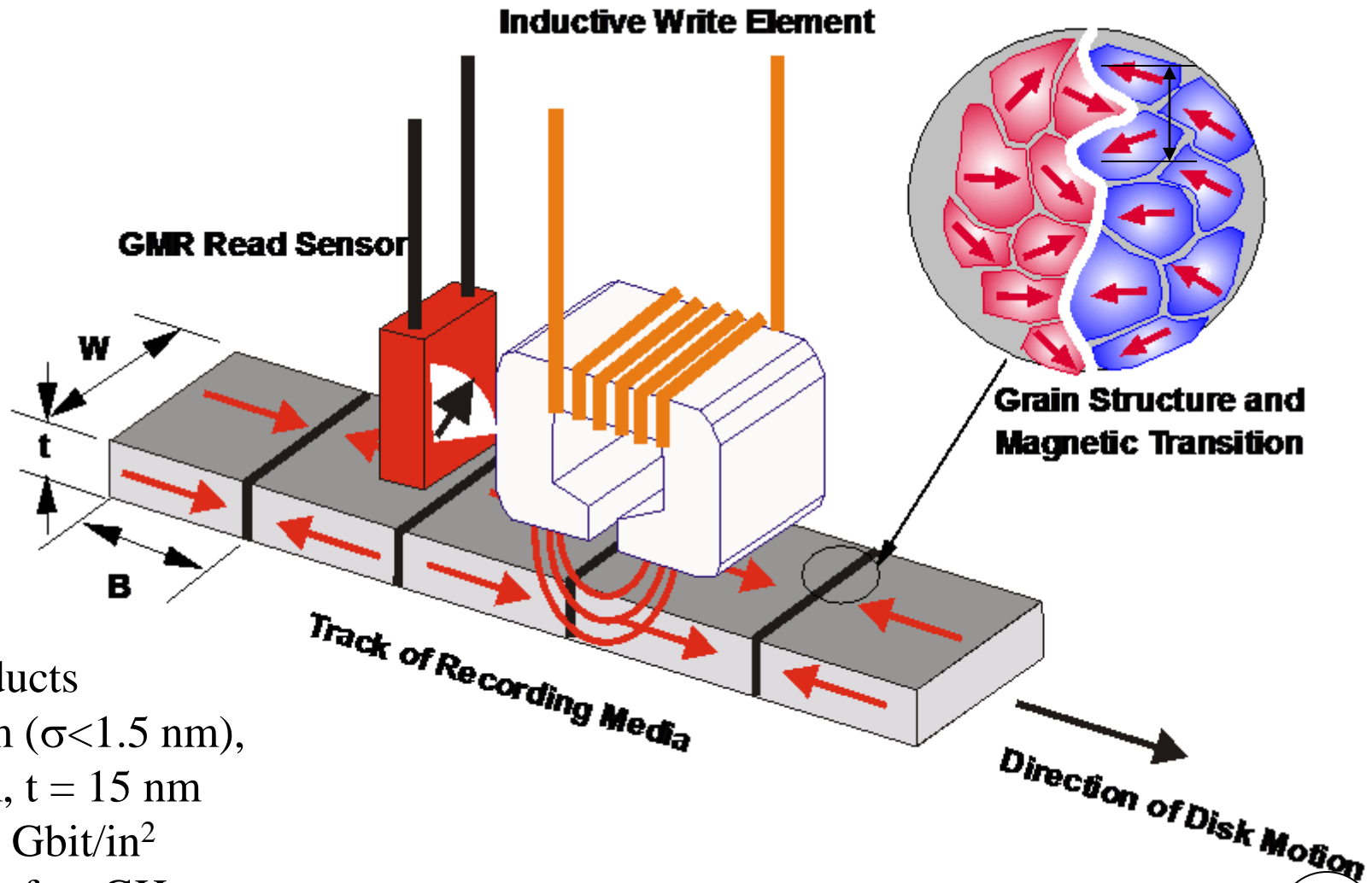
Components of a Hard Disk Drive

current leading-edge HDD at 500+ Gbit/in²

- 3.5" HDD 2TB capacity
- 2.5" HDD 1TB capacity



Recording basics



2009 products

$B = 15 \text{ nm}$ ($\sigma < 1.5 \text{ nm}$),

$W = 80 \text{ nm}$, $t = 15 \text{ nm}$

AD $\sim 500 \text{ Gbit/in}^2$

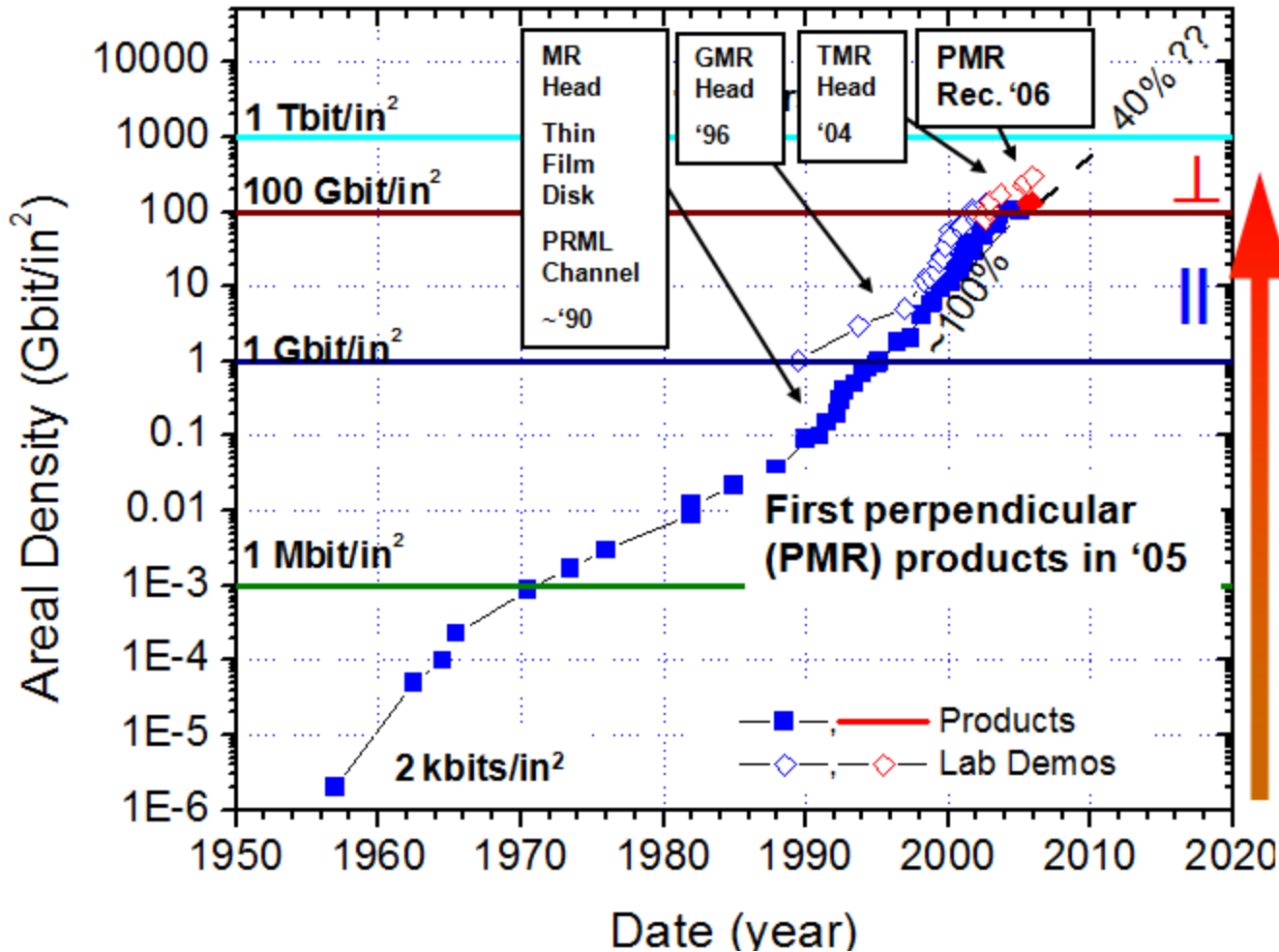
data rate \sim few GHz

HDD Industry Roadmap: Areal Density Growth

Commercial product
720 Gbits/in², 500 GB/2.5" Platter

Demonstration
~1 Tbits/in²

Research frontier
1.5-10 Tbits/in²

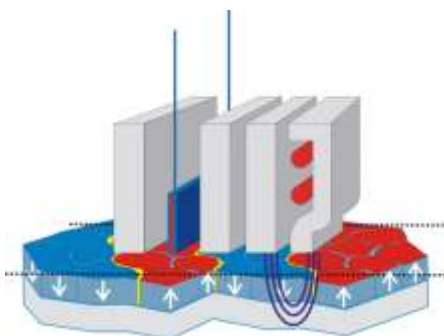
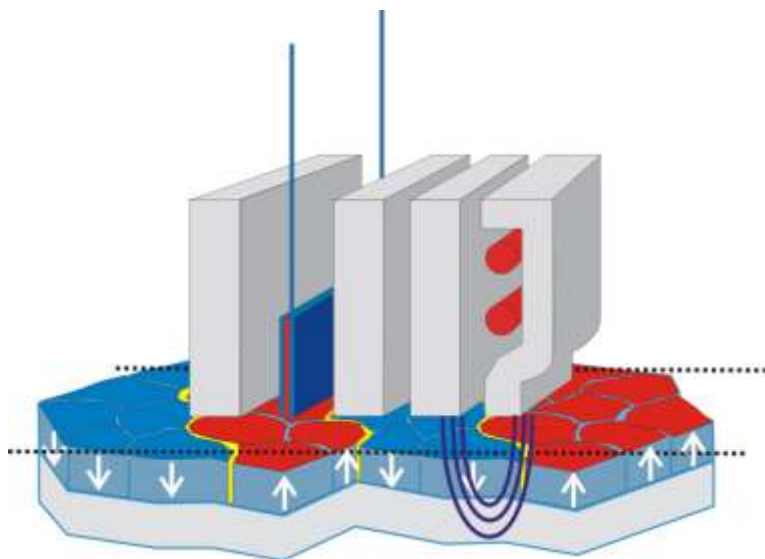


Technology Options:

- Longitudinal
- Perpendicular
- Heat Assist**
- Patterned Media**

Scaling

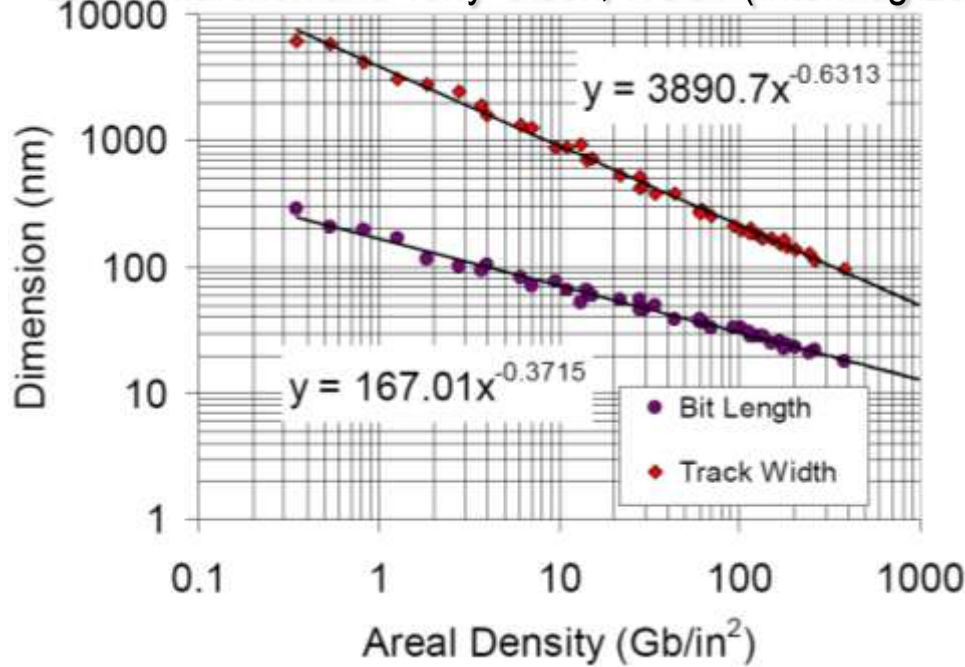
- Worked successfully for 50 years
 - Write head lithography/materials improved
 - Sensors improved - Inductive \Rightarrow AMR \Rightarrow GMR \Rightarrow TMR \Rightarrow ...
 - Media with smaller more isolated grains
 - Fly height reduced from μm to $\sim 10\text{nm}$



- Shrink all dimensions by s
- Increase density by $1/s^2$

CC-01: Magnetic Spacing Trends: From LMR to PMR and Beyond

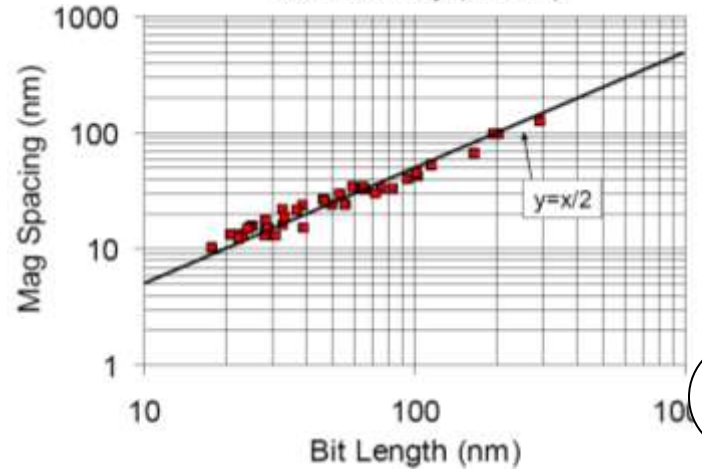
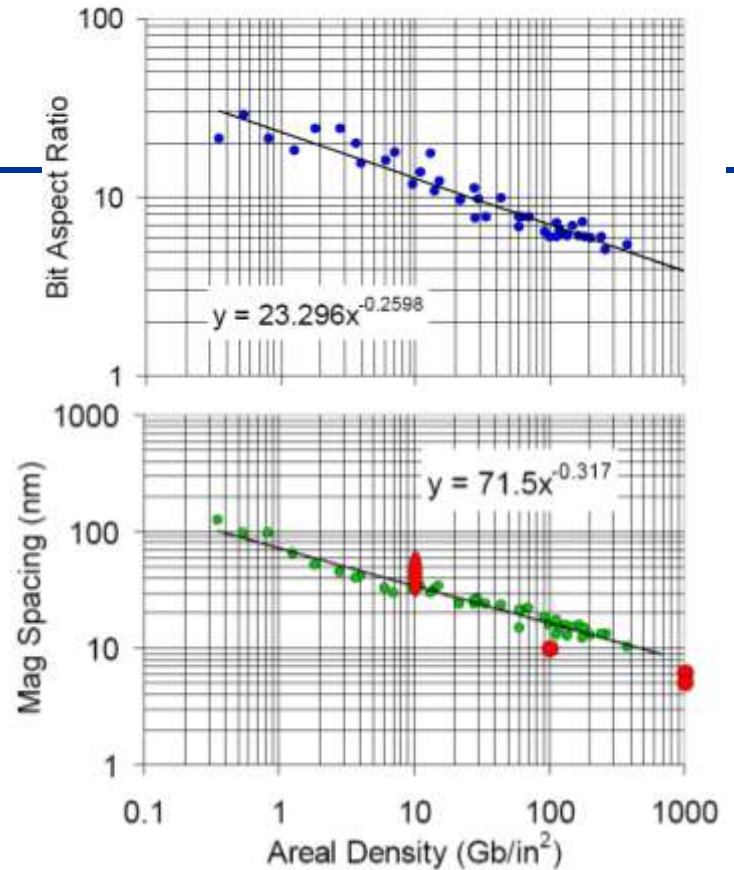
Bruno Marchon and Terry Olson, HGST (Intermag 2009)



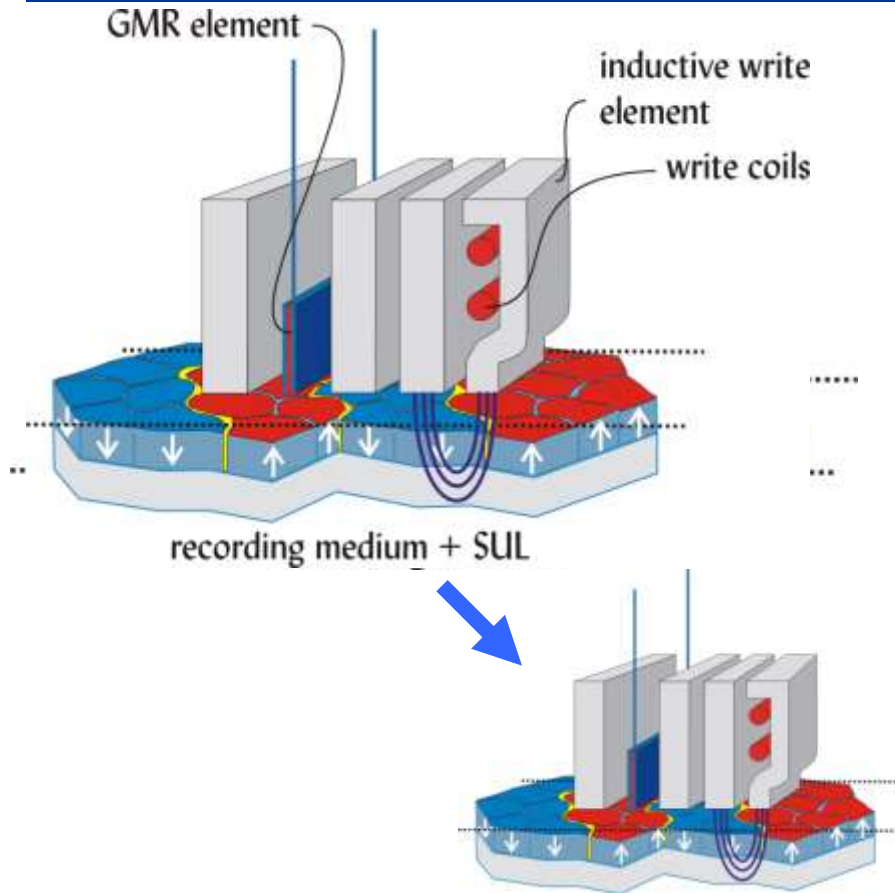
- The scaling trends have held from below 1Gb/in² until today's densities, with no significant discontinuities when crossing major technology changes.
- HMS scaling may be rationalized based on a readback argument.

$$HMS\% = 1 - (1 - AD\%)^{-0.32}$$

AD (Gbps)	1,000	2,000	10,000
HMS (nm)	8.0	6.4	3.9
BAR	3.9	3.3	2.1



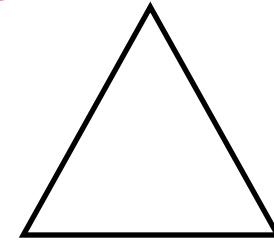
Limits to 'conventional' scaling in magnetic recording



$$\text{SNR}_p \propto 10 \cdot \log_{10}(N)$$

$$\cong 30 \text{ dB for } N=1000$$

Signal-to-Noise Ratio



**thermal
stability**

writeability

$$\text{stability} \sim \frac{K_u V^*}{k_B T}$$

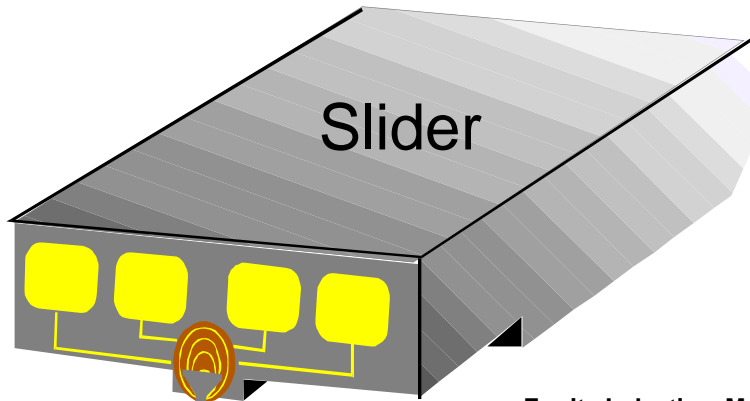
$$B_{S, \max} = 2.4 \text{ T}$$

The achievable areal density using 'conventional' scaling is limited by trade-off between **SNR**, **thermal stability** and **writeability**

Write Element



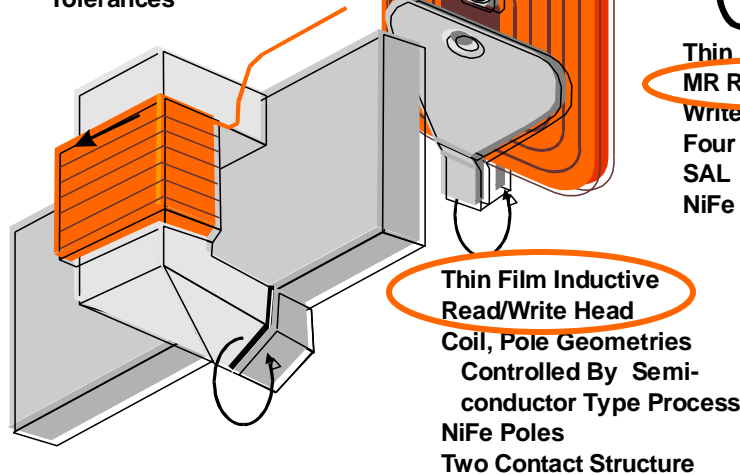
Evolution of Recording Heads



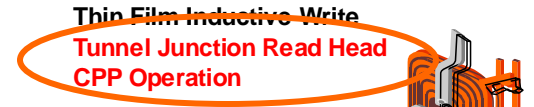
Slider

Head

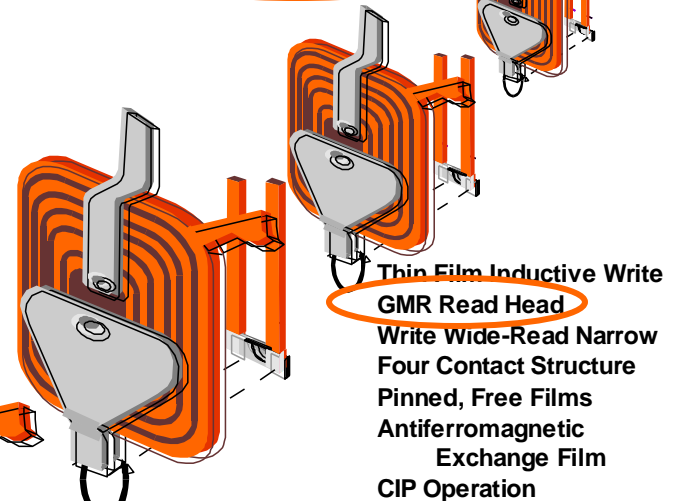
Ferrite Inductive MnFe
Read/Write Head
Wire wound coil
Machined Pole Pieces
Gap Width Controlled
By Films And Assembly
Tolerances



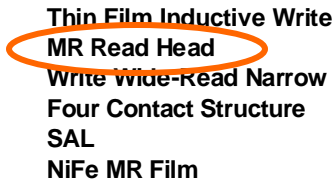
Thin Film Inductive
Read/Write Head
Coil, Pole Geometries
Controlled By Semi-
conductor Type Process
NiFe Poles
Two Contact Structure



Thin Film Inductive Write
Tunnel Junction Read Head
CPP Operation



Thin Film Inductive Write
GMR Read Head
Write Wide-Read Narrow
Four Contact Structure
Pinned, Free Films
Antiferromagnetic
Exchange Film
CIP Operation



Thin Film Inductive Write
MR Read Head
Write Wide-Read Narrow
Four Contact Structure
SAL
NiFe MR Film

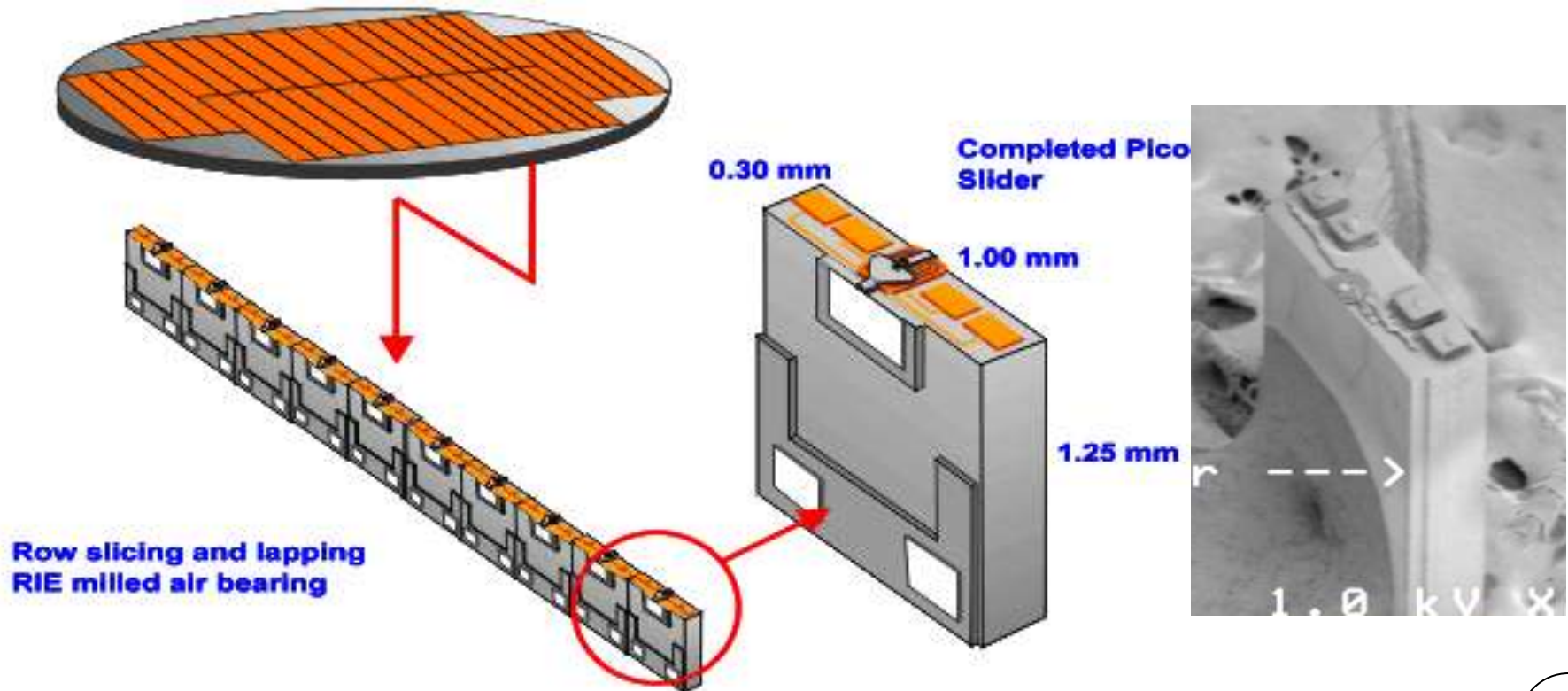
Thin Film Head Process – Wafer to Row to Slider

HEAD

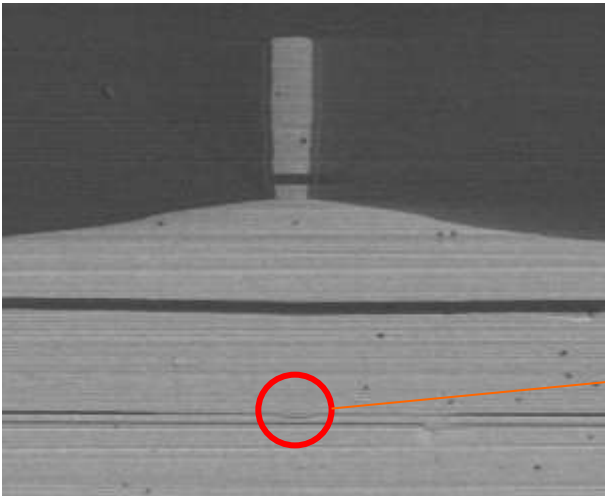
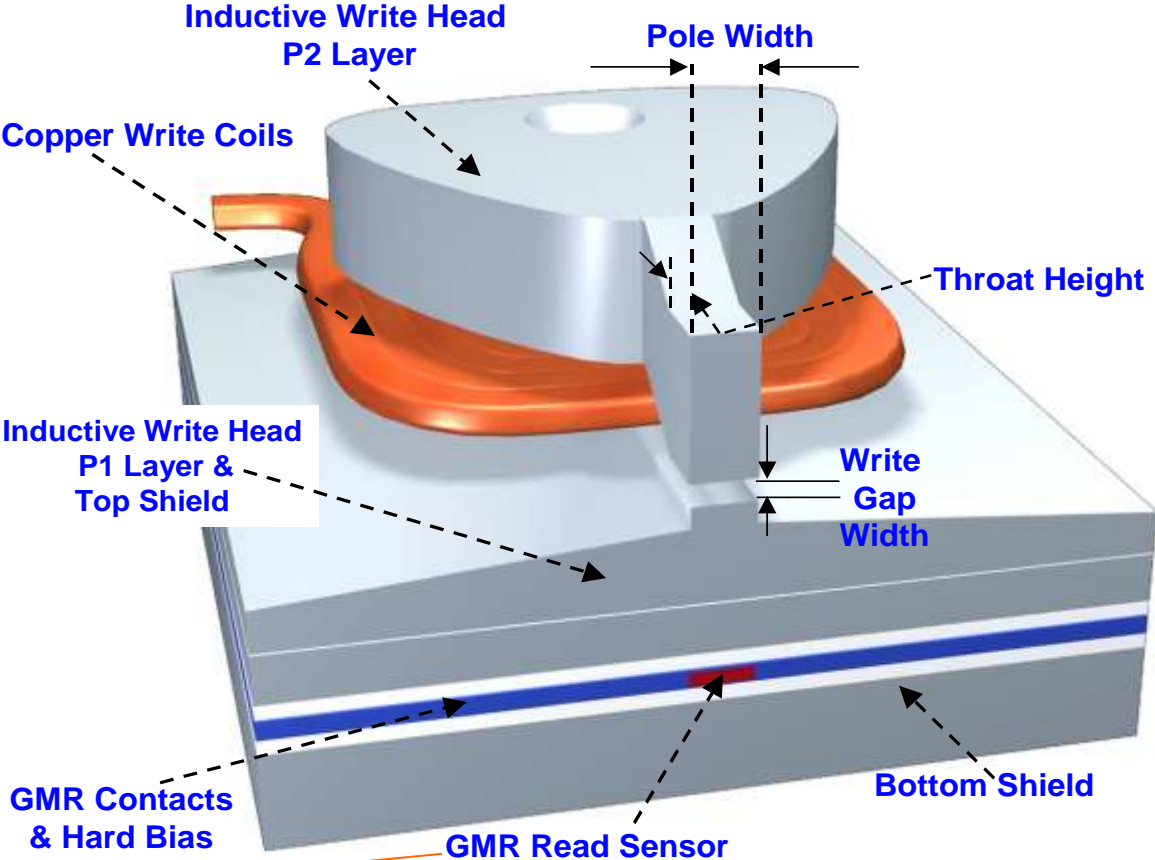
- 3 minimum features / mm^2
- 10^5 features / 200 mm wafer

IC

- 10^6 -- 10^7 minimum features / mm^2
- 10^{10} -- 10^{11} features / 200 mm wafer



Thin Film Recording Head (longitudinal)



Scaling the write head

- resolution limited by lithography (and inability to continue scaling of fly height)
- maximum field limited by materials availability to $\sim 2.4\text{T}$

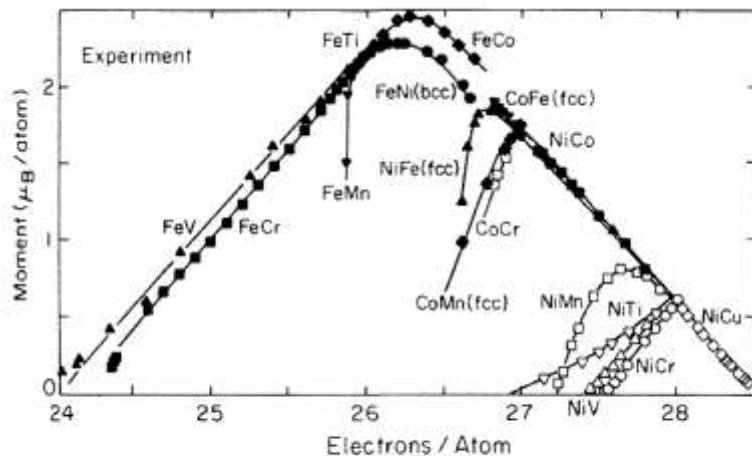
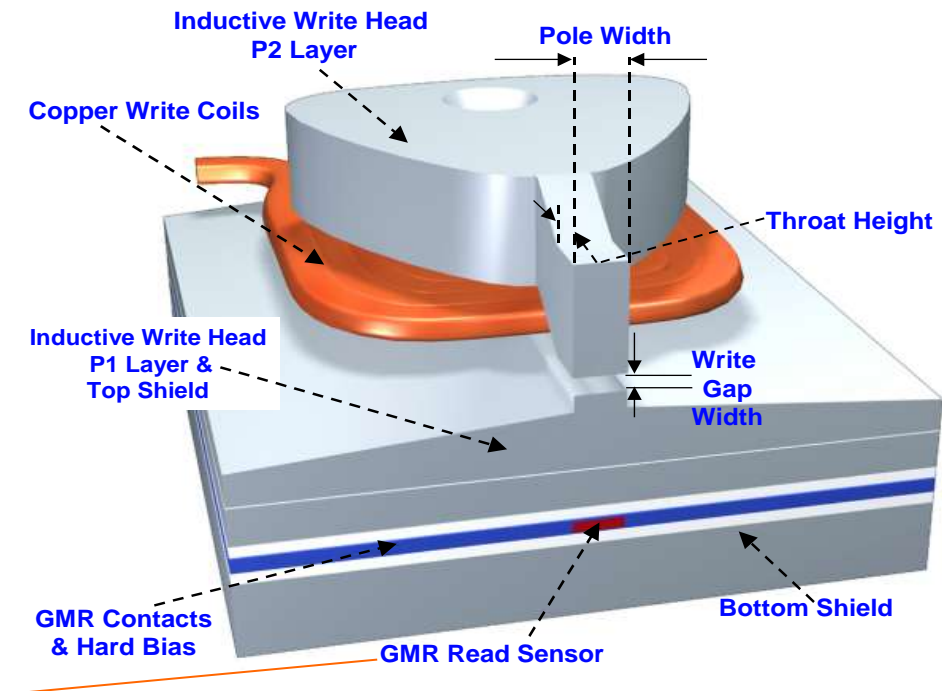
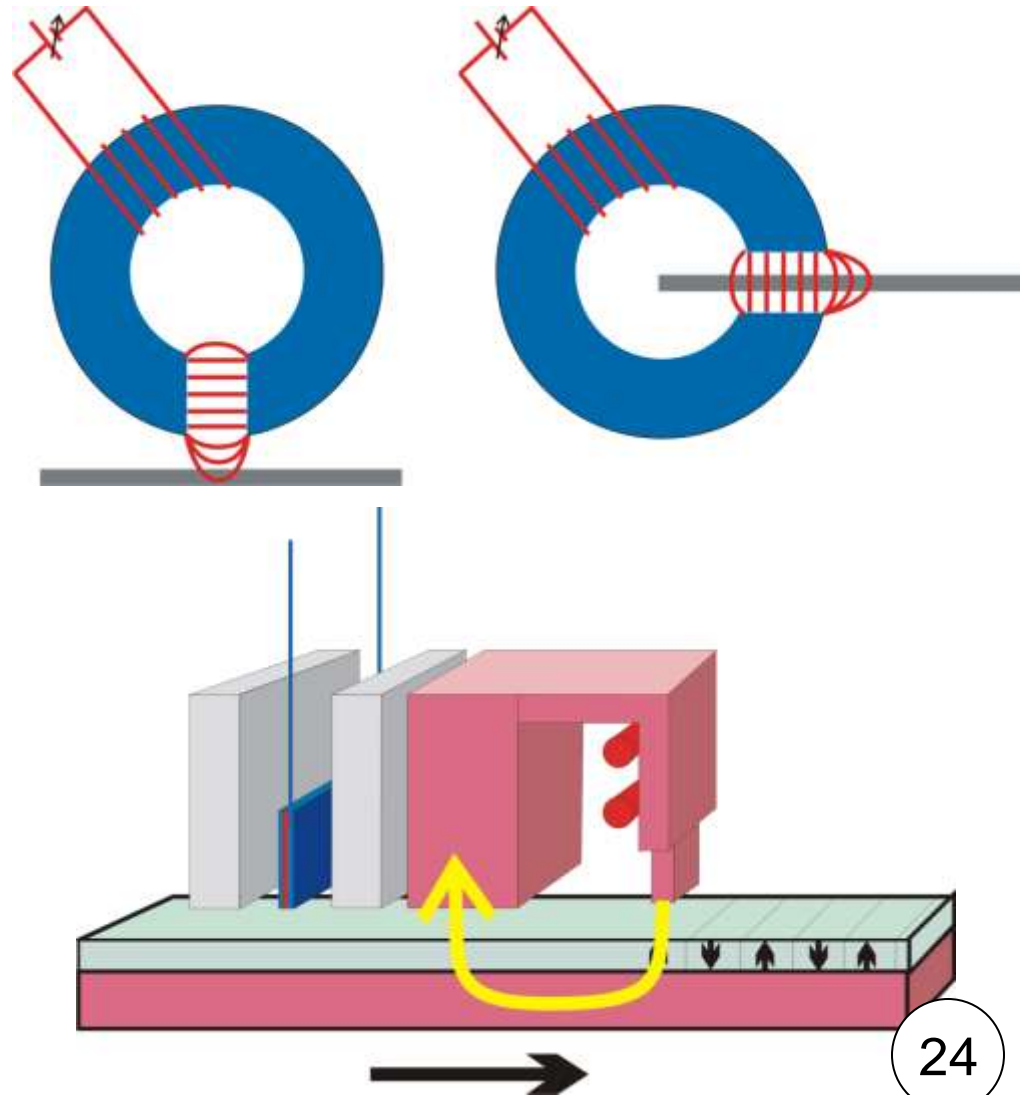


Figure 5.1 The Slater–Pauling curve showing moment per atom (in Bohr magnetons) for metallic alloys as a function of valence electron concentration or alloy composition. [After Dederichs et al. (1991).]

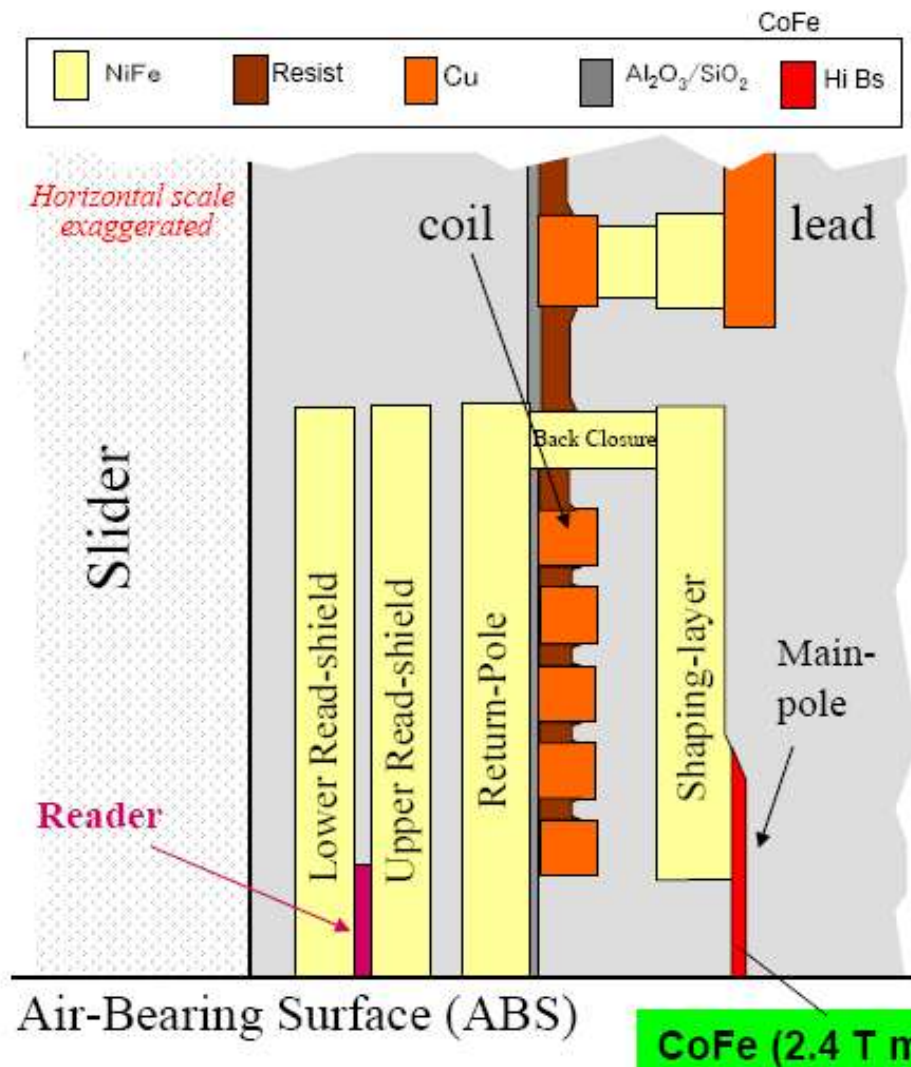


Longitudinal & perpendicular recording

- In longitudinal recording bit transitions are written by the fringing fields, in perpendicular recording the media is directly in the magnetic circuit
- In principle this allows larger fields to be applied and sharper field gradients
- Ideally need to match the head and media soft underlayer (SUL)
- Single pole design means much thinner pole tips
- Easier to scale to narrow dimensions
- Max. B_s of CoFe-alloy pole tip materials $\sim 2.4\text{T}$, however max. write field in the media $\sim 1\text{-}1.2\text{T}$

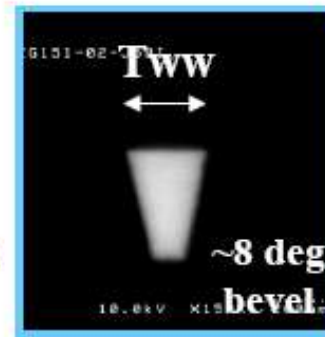


Example Perpendicular Write-Head Structure

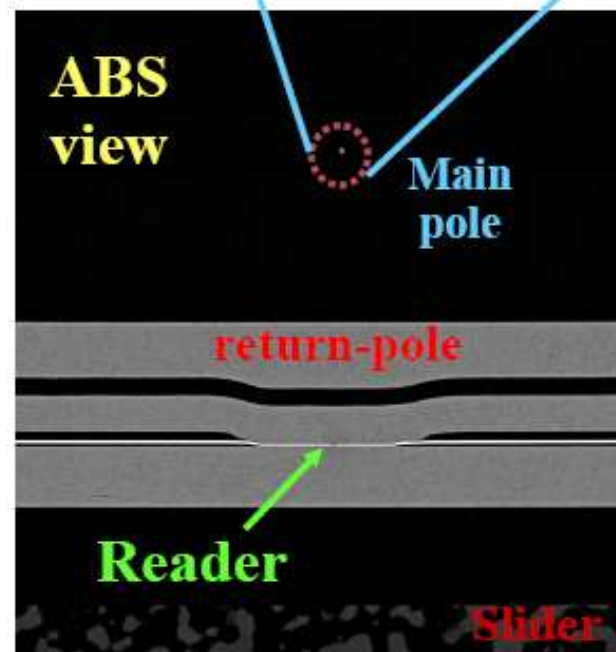


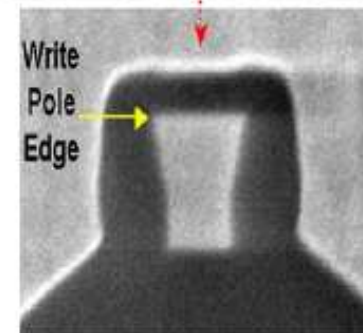
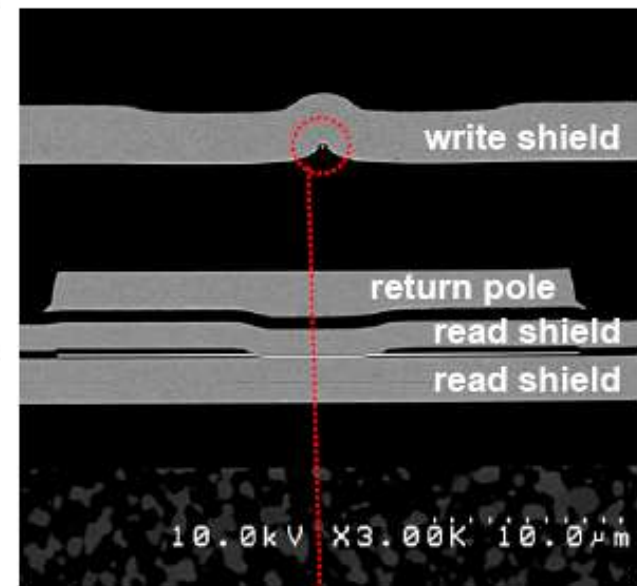
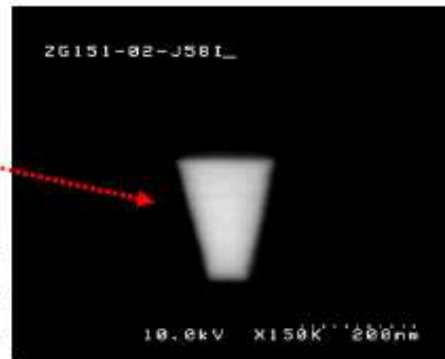
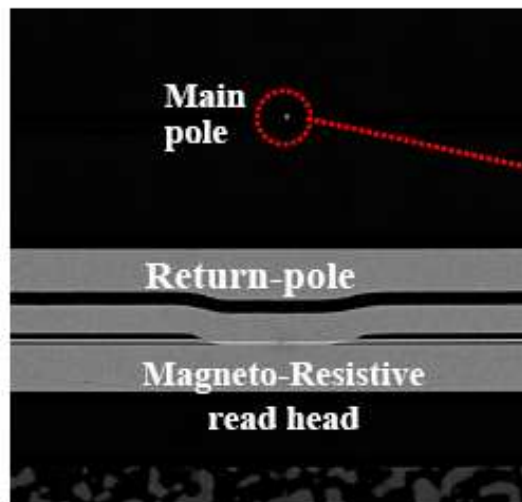
Main pole

$T_{ww} = \sim 180nm$



ABS view





**Conventional
Trapezoidal Structure**
(Field gradient: 80-100 Oe/nm)

Trailing-Shield enhances write-field gradients

Side-shields confine side-writing fields
and prevent adjacent track erasure (ATE)

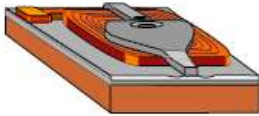
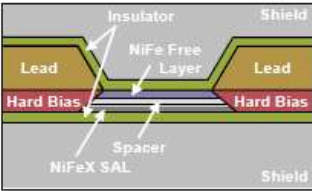
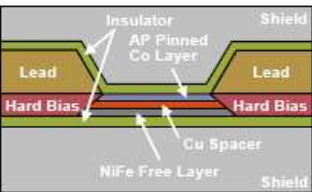
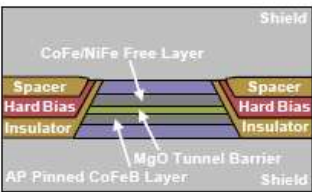
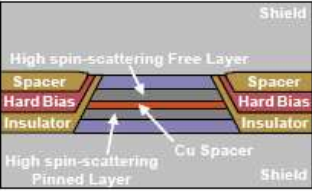
(side leakage of fields can cause erasure of
data on adjacent tracks,)

New Trailing & Side-Shield Structure
(Field gradient: 150-200 Oe/nm)

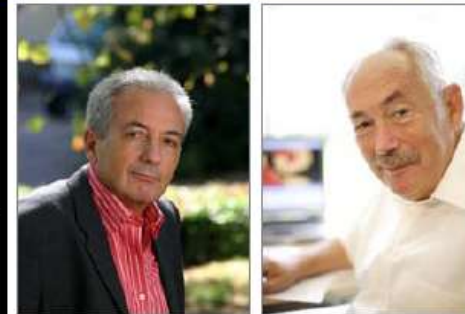
Read Sensor



Progress in Read Head Sensor Technologies

Year	Density (Gb/in ²)	Sensor Technology	Structure	MR Effect	Current Geometry
1979	0.01 Gb/in ²	Thin-film Inductive		N/A	N/A
1991	0.1 Gb/in ²	MR Sensor		Anisotropic MR	CIP
1997	2 Gb/in ²	Spin Valve		Giant MR	CIP
2006	100 Gb/in ²	Tunnel Valve		Tunneling MR	CPP
2011	1 Tb/in ²	CPP GMR		Giant MR	CPP

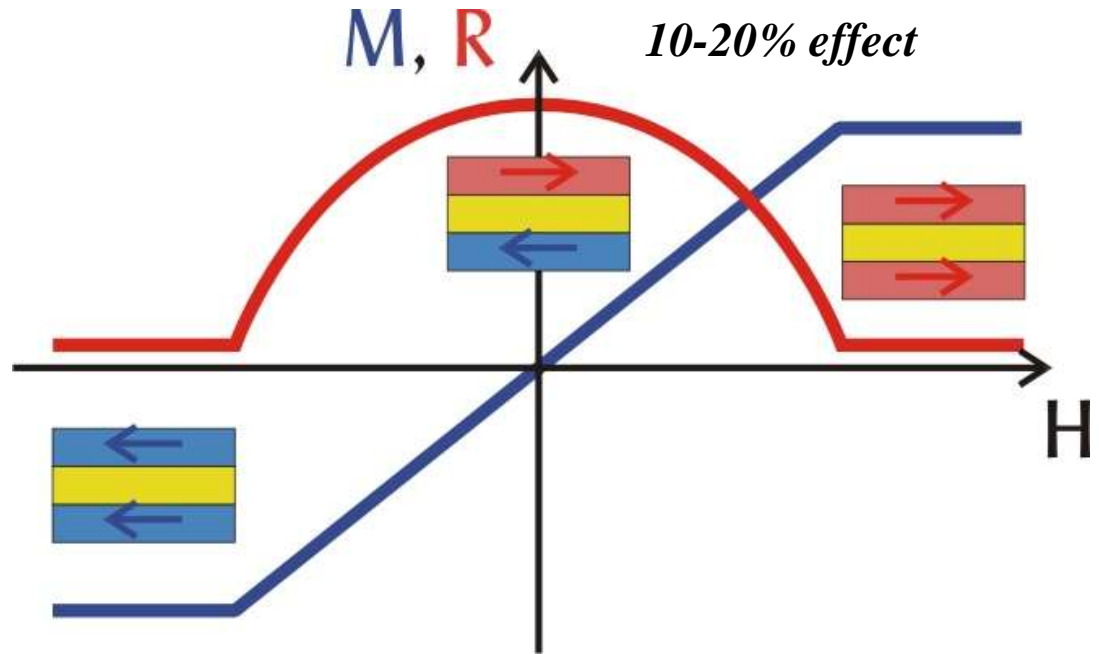
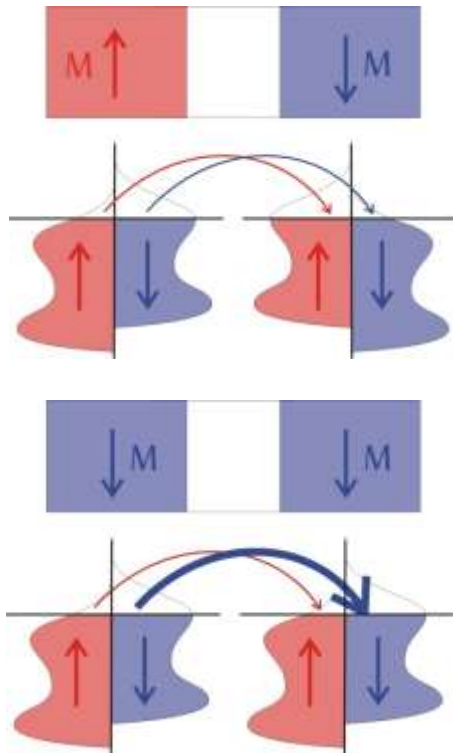
2007 Nobel prize



Albert Fert & Peter Grunberg

Giant Magneto-resistance (GMR)

Julliere's two-current model $I = I_{\downarrow} + I_{\uparrow}$

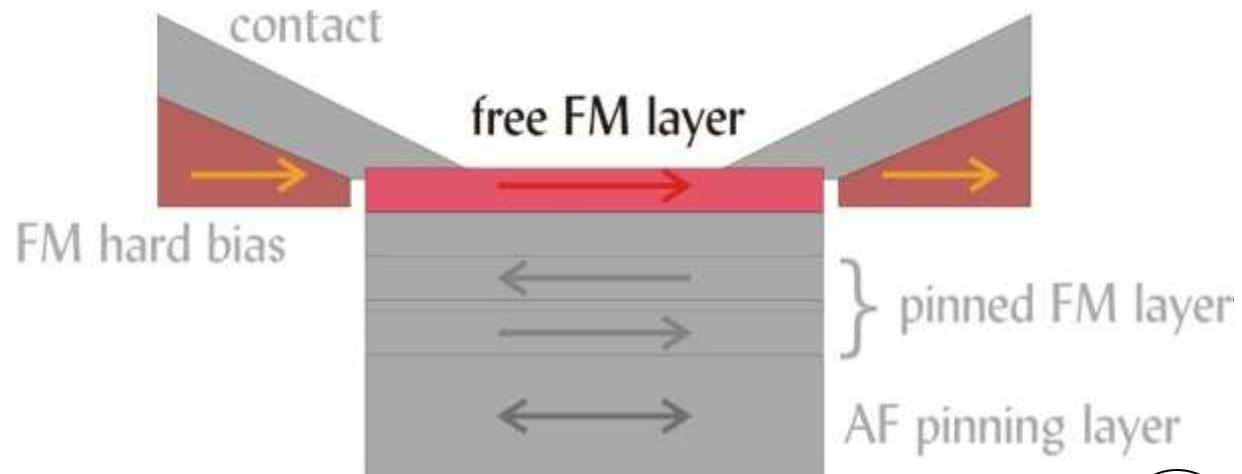


Baibich et al. *Phys. Rev. Lett.* **61** 2472 (1988)
 Binasch et al. *Phys. Rev. B* **39**, 4828 (1989)
 P. Grunberg, U.S. patent # 4,949,039

figure of merit
$$GMR = \frac{\Delta R}{R} \equiv \frac{R_{AP} - R_P}{R_P}$$

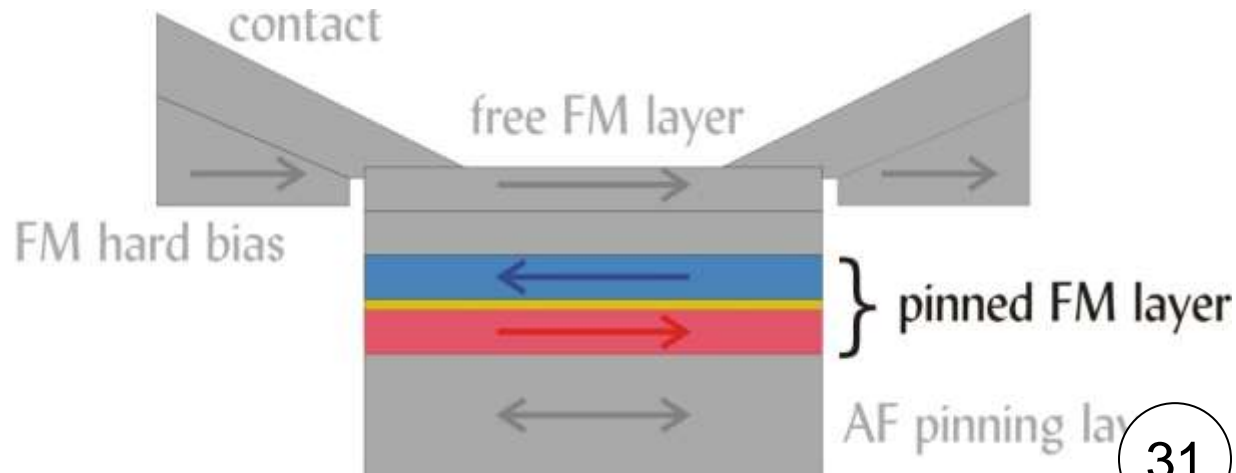
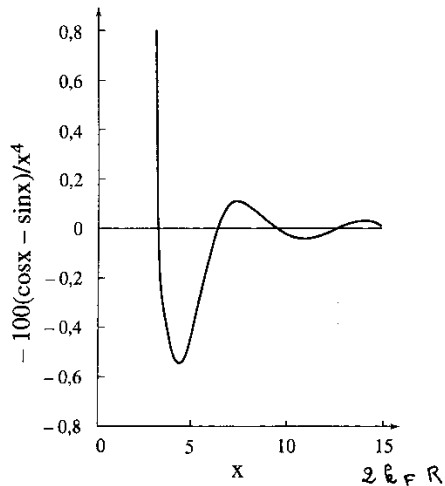
Functional layers of a GMR sensor I – the free layer

- Magnetization of the free layer rotates in the stray field of the bit transition
- Requires stable zero-field position parallel to the disk surface
- can be achieved by
 - internal (magneto-crystalline) anisotropy
 - shape anisotropy
 - bias field from hard magnet

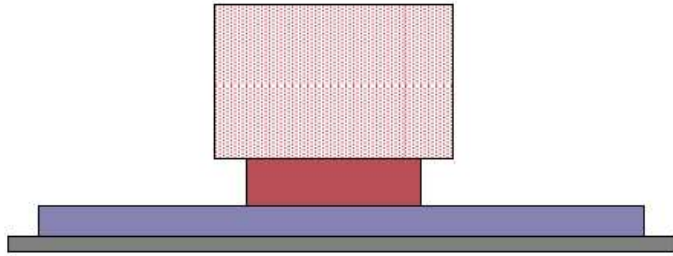


Functional layers of a GMR sensor II – the pinned layer

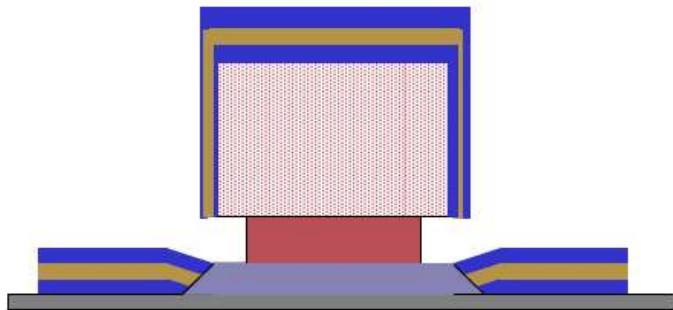
- pinned layer provides reference direction for free layer
- stray field should not disturb free layer
 - use 2 antiferromagnetically coupled magnetic layers
 - oscillating RKKY interaction also found in thin 3d-metal films separated by suitable non-magnetic spacer layer, e.g., Fe/Cr/Fe, Co/Cu/Co, CoFe/Ru/CoFe,...
- requires stable position perpendicular to the disk surface
 - in-stack bias with hard magnetic layer
 - exchange bias with antiferromagnet



- 1) Produce undercut resist structure (193nm photolithography)



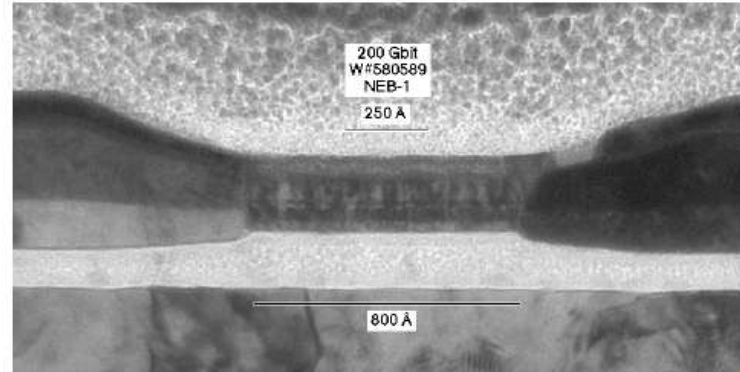
- 2) Ion Mill, then IBD HB/leads



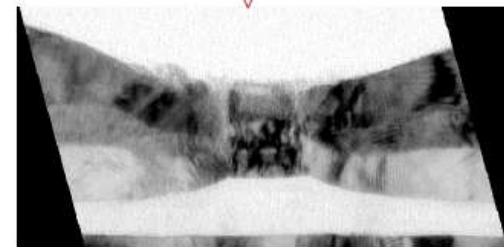
- 3) Lift-off Resist



Excellent process control is possible

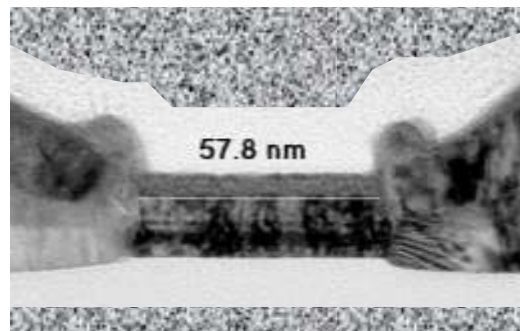


TW=80nm

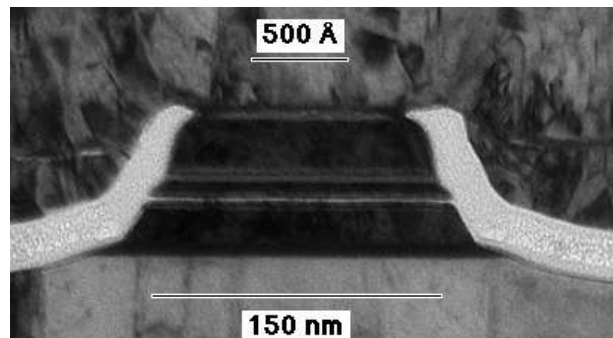


TW=13 nm !!

New sensor geometries required for continued scaling

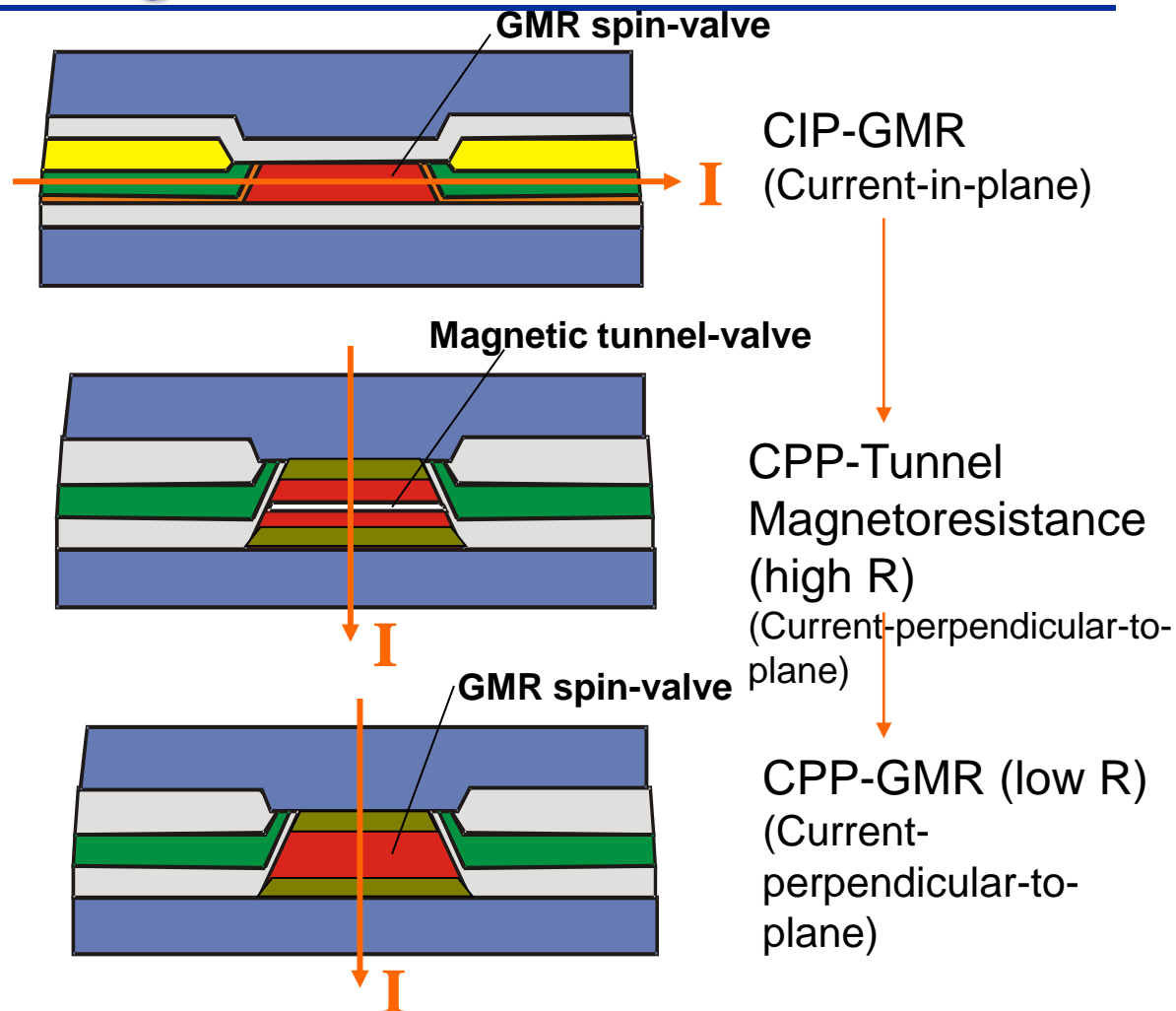


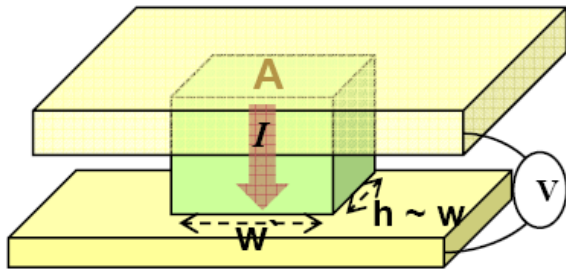
Tunnel-valve head



driven by

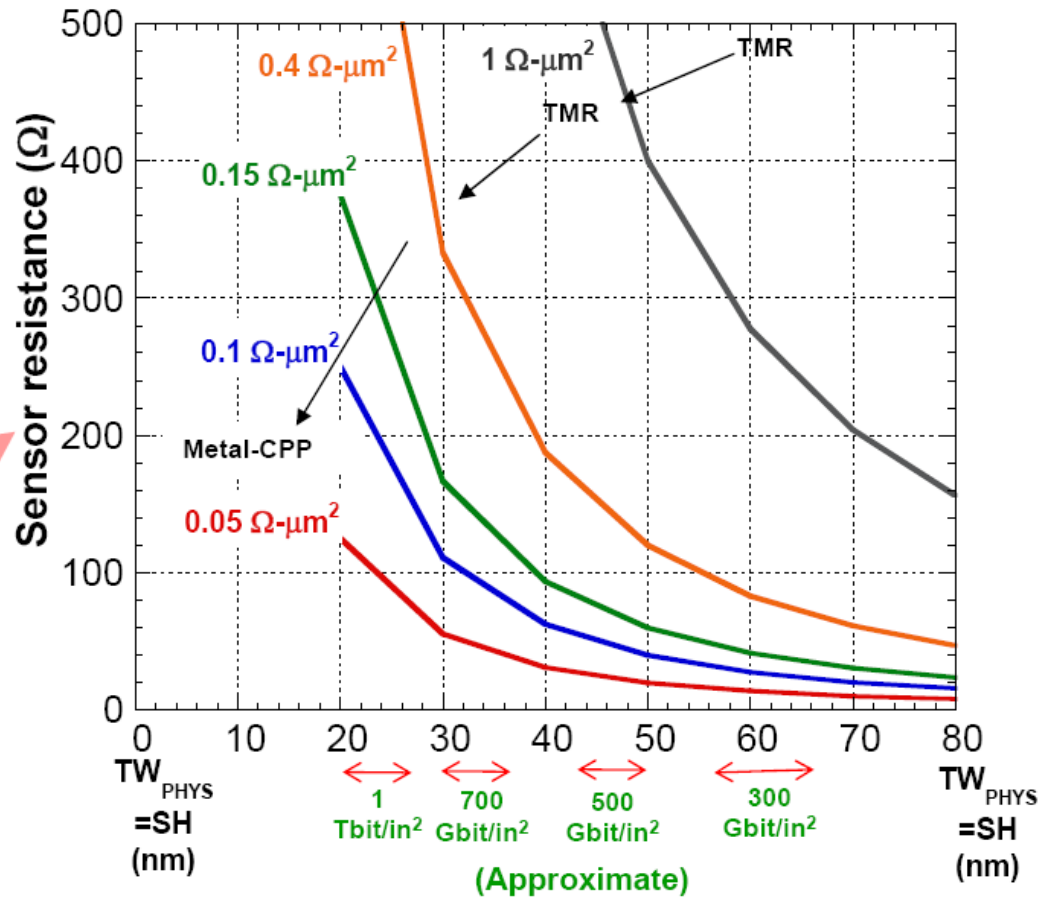
- scaling of gap
- $\Delta R/R$ improvement
- absolute value of R





Area $A = w \times h \sim w^2$
 $R_{\text{Sensor}} = R_j (\Omega\text{-}\mu\text{m}^2) / A$

R_{Sensor} increases with decreasing sensor size (higher recording density)



$R \ll \sim 500\Omega$ is desirable

Low $R =$

- Low noise
- Large bandwidth (high data rate)

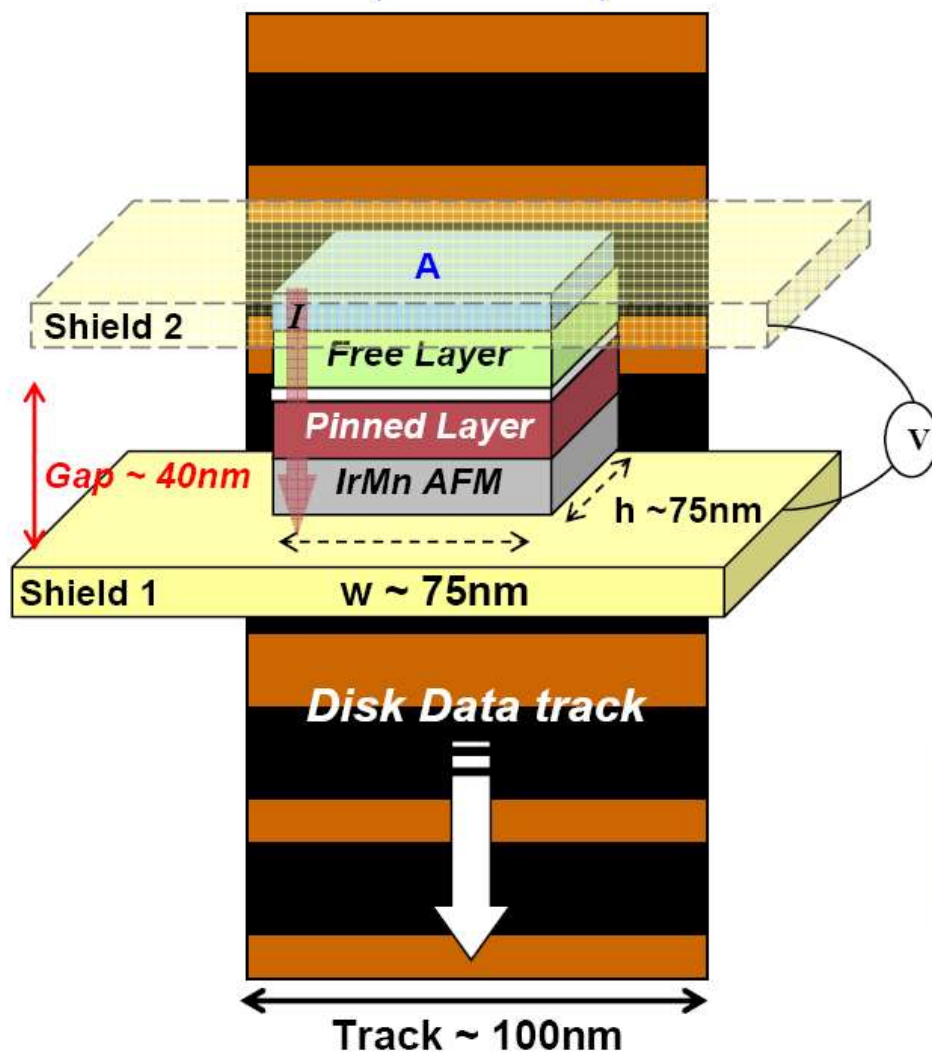
For density $\gg 300 \text{ Gb/in}^2$
 Need sensor $RA \ll 1 \Omega\text{-}\mu\text{m}^2$

All-metal CPP-GMR

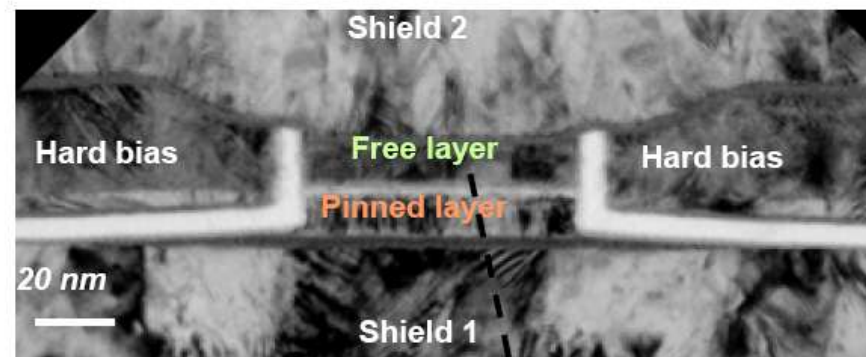
$0.02 - 0.1 \Omega\text{-}\mu\text{m}^2$

Low-resistance, robust sensor
 down to smallest dimensions

CPP read sensor (Current Perpendicular to sensor Plane)



View from disk

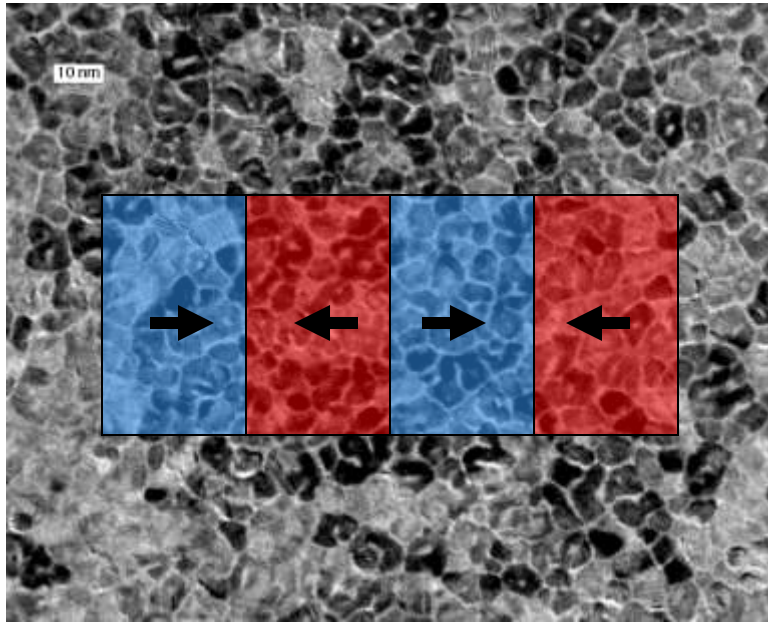


MgO tunnel barrier ~ 9Å
 Junction RxA product ~ 2 Ω-μm²
 TMR ~ 80%

Media

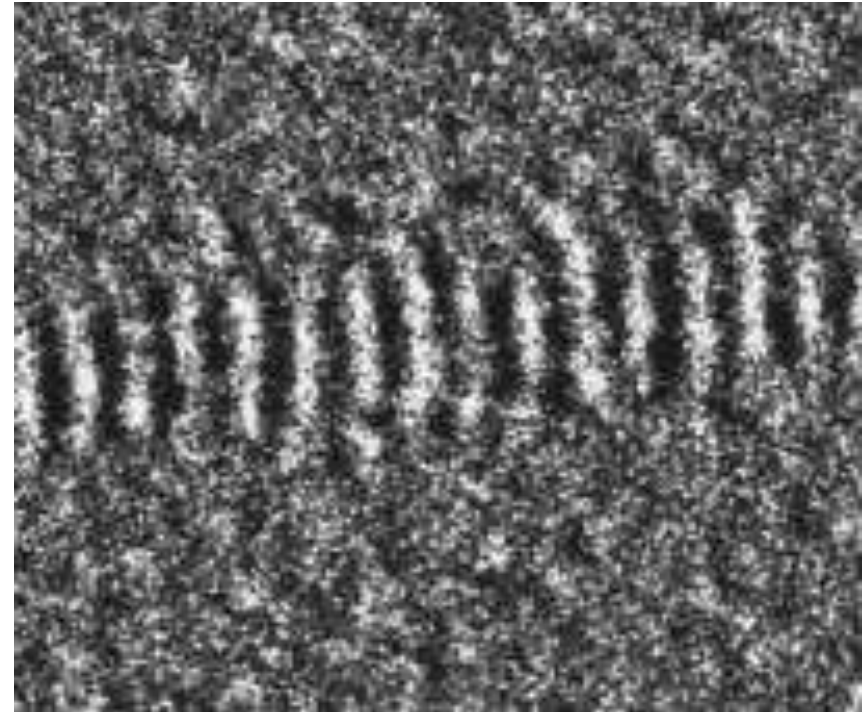


Bits & Media Microstructure



100 nm

$\langle D \rangle = 8.5 \text{ nm}$
 $\pm 2.5 \text{ nm}$

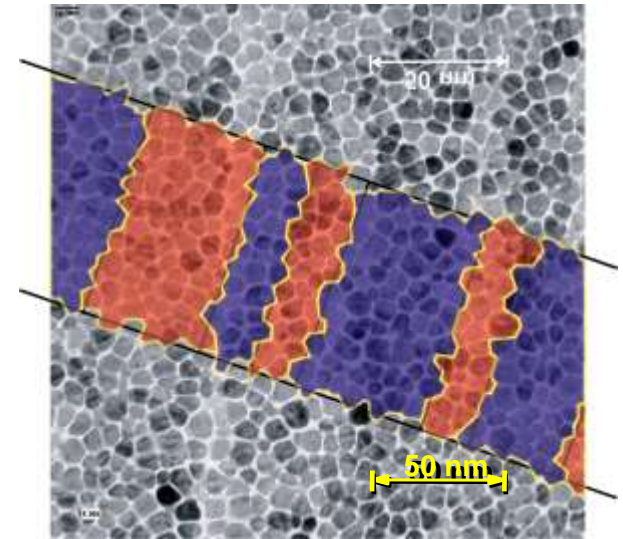


1000 nm

$\text{SNR} \propto \sqrt{N}$ N : # of grains/bit

Signal and Noise

- Signal
 - Volume and moment of magnetic material
 - Orientation of grains (relative to reader and track)
 - Complete grain switching
- Noise
 - Uncertainty in transition position
 - Width of transition
 - Granularity of medium
 - Magnetic reader (GMR) noise
 - Electronic amplifier noise (Johnson, shot etc)

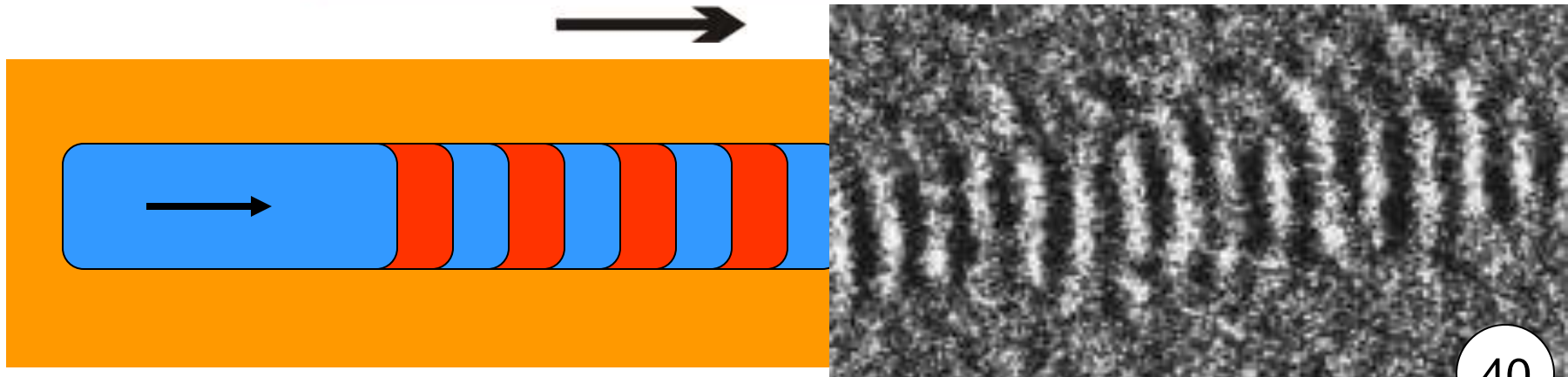
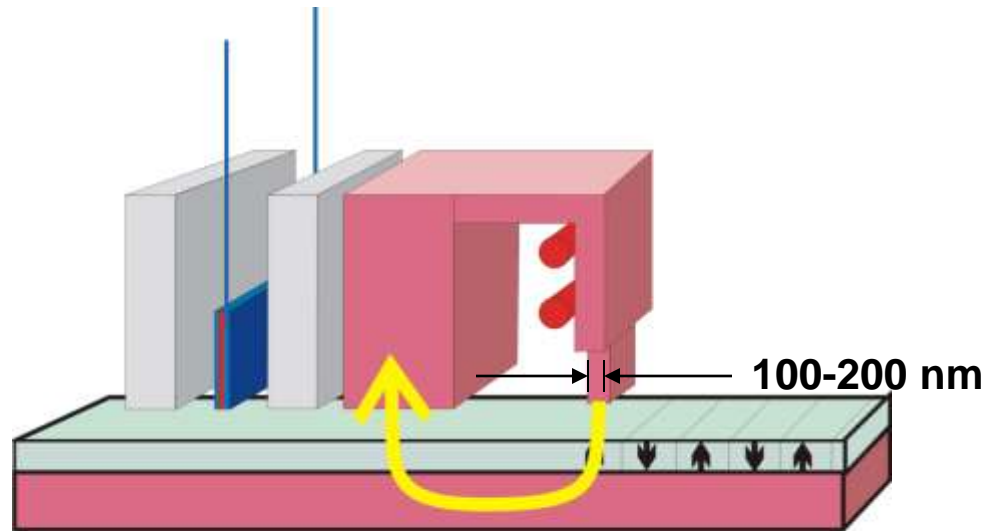


Perpendicular granular media

$$\text{SNR}_{\text{media}} \propto \sqrt{N} \quad N: \# \text{ of grains/bit}$$

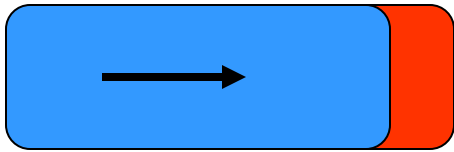
Magnetic super-resolution

Head pole is > 100 nm but bits are 15 nm?

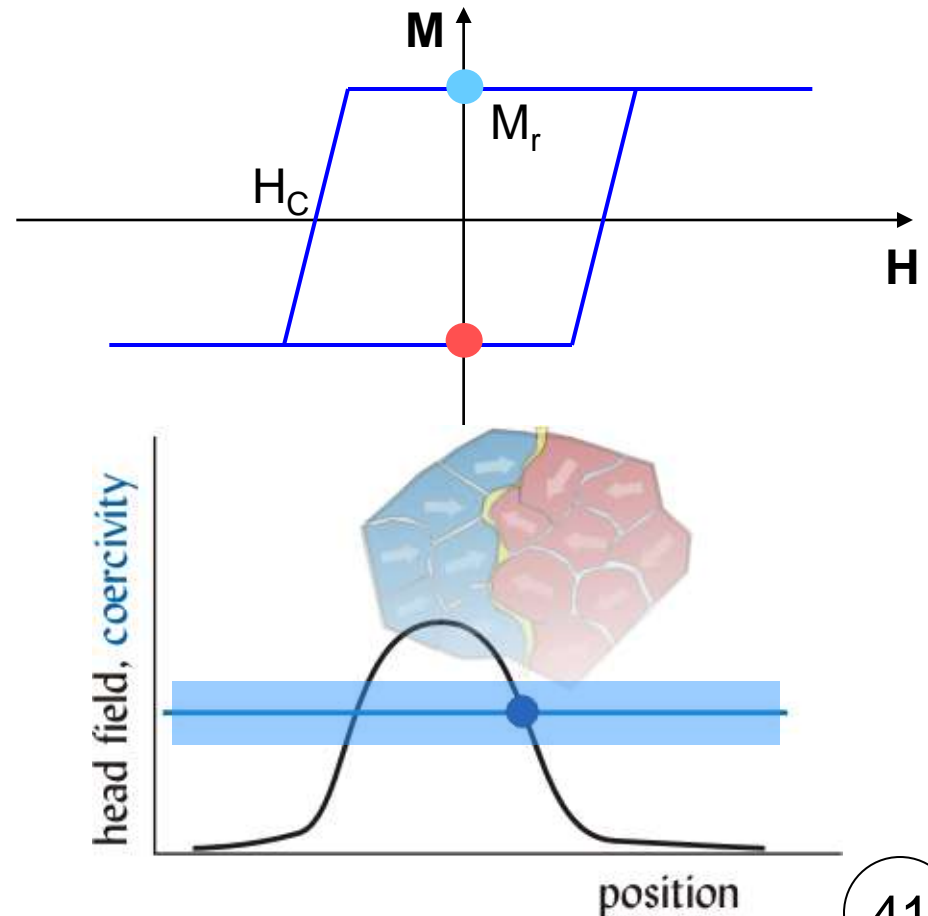
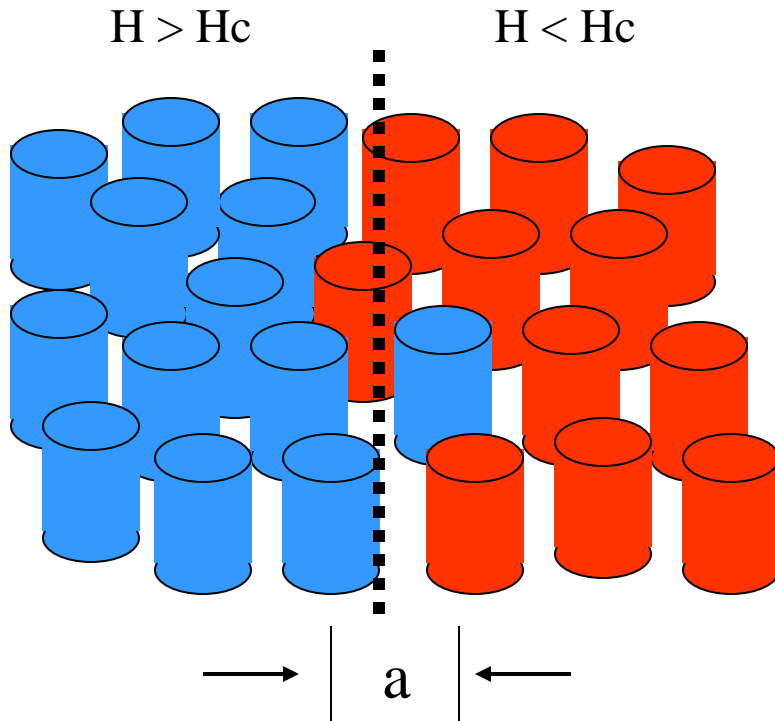


Density limit I

How sharp can you make the transition?

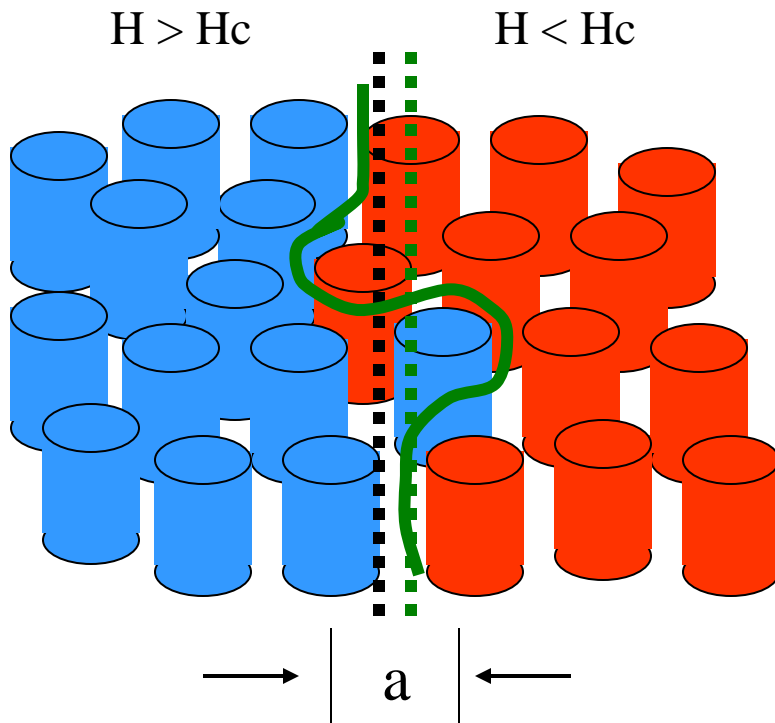
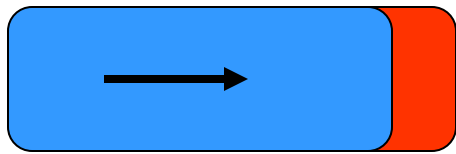


Sharpness: $dM/dx = dM/dH * dH/dx$



Density limit II

How accurately can you place the transition?

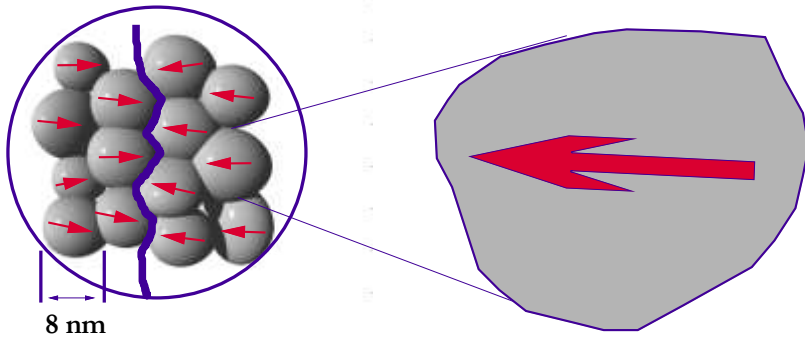


$$\sigma_x = \frac{\pi^2 a}{4} \sqrt{\frac{s}{3W}}$$

$$\sigma_x < 10\% \text{ of bit length}$$

$$5\sigma_x \text{ half the bit length}$$
$$10^{-6} \text{ probability}$$

Magnetic vs. thermal energy



Magnetic energy $E = K_U V$

$K_U V = 100 k_B T$ $\tau > \text{age of the universe}$

$K_U V = 45 k_B T$ $\tau \sim 10 \text{ years}$

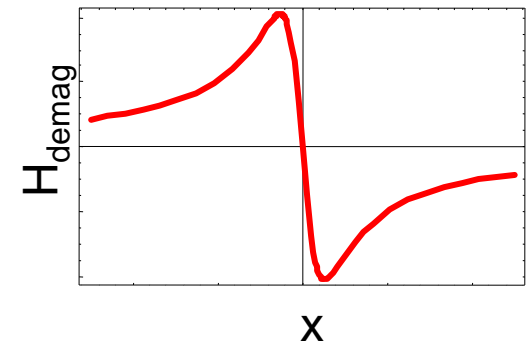
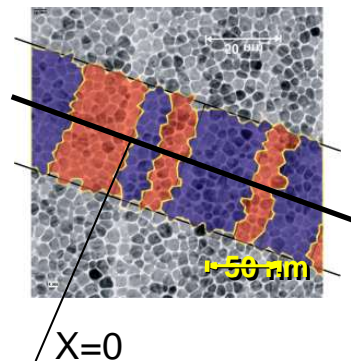
$K_U V = 25 k_B T$ $\tau \sim 7 \text{ seconds}$

In products often $K_U V / k_B T > 70$ is used due to other contributions, operation temperature range *etc.*

In longitudinal media the demag fields at a transition help drive thermal activation

$$E_B^+ = \Delta E = K_U V (1 - h)^2$$

$$h = \frac{H_{app} + H_{demag}}{H_k}$$



demag. field profile from the center of an isolated transition

Reversal of a single domain particle

- Simple coherent non-interacting rate equation model

$$\tau_{\pm}^{-1}(h) = f_0 \exp\left(-\frac{E_B^{\pm}(h)}{k_B T}\right)$$

f_0 is attempt frequency 10^9 - 10^{12} Hz

E_B is the energy barrier

k_B Boltzmann constant; T temperature

- E_B for aligned particles (neglecting the reverse process) is

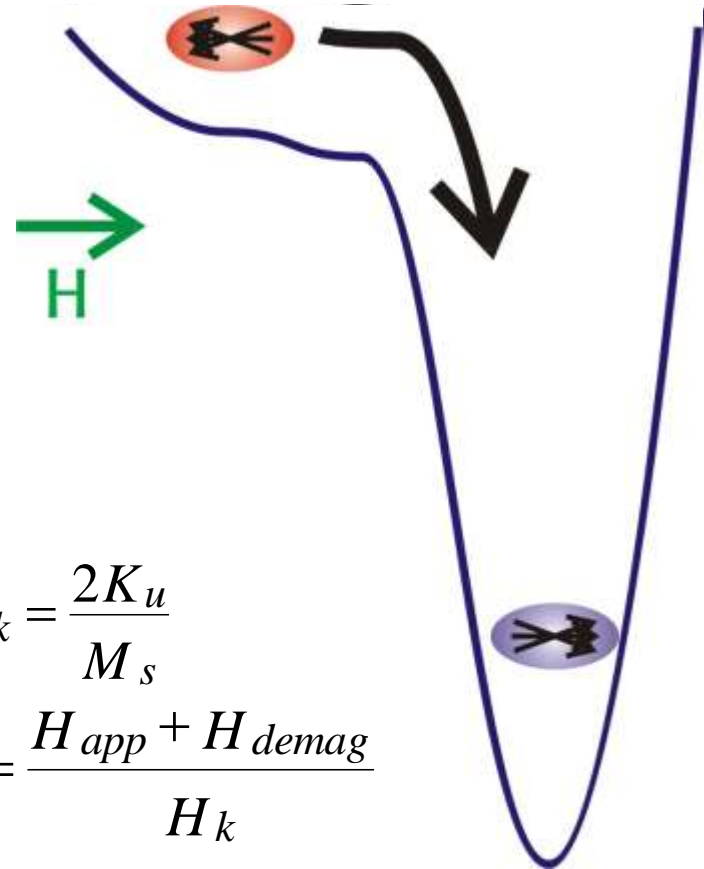
$$E_B^+ = \Delta E = K_U V (1-h)^2$$

K_U : uniaxial anisotropy ($K_1 + K_s$..)

V : volume of particle

$$H_k = \frac{2K_u}{M_s}$$

$$h = \frac{H_{app} + H_{demag}}{H_k}$$



E.C. Stoner and E.P. Wohlfarth *Phil. Trans. Roy. Soc.* **A240** (1948) 599

R. Street and J.C. Woolley *Proc. Roy. Soc.* **A62** (1949) 562

L. Neel *Compt. Rend. Acad. Sci., Paris* **228** (1949) 664

W.F. Brown *Phys. Rev.* **130** (1963) 1677

Signal decay

Thermally activated magnetization reversal has two important consequences for an ensemble of SW-particles

1 – magnetization decay

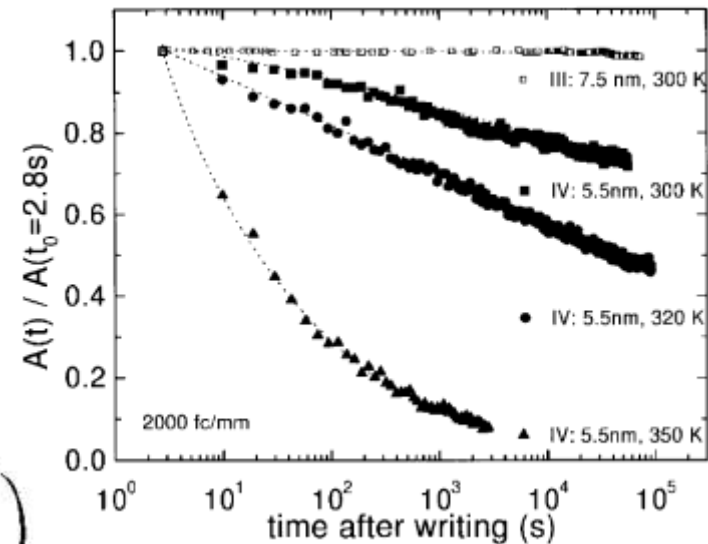
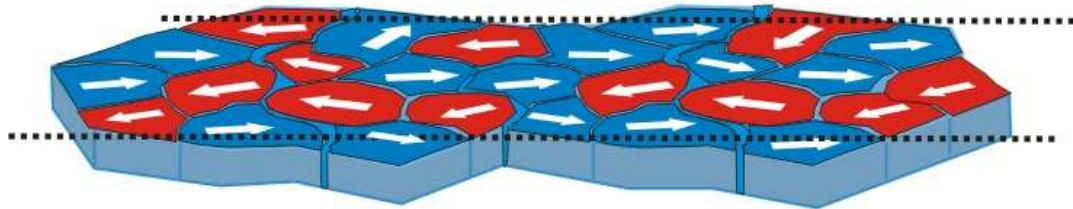
$$E_B(H) = \ln \left(\frac{t_x \cdot f_0}{|\ln x|} \right) \cdot k_B T$$

$$t_x = |\ln x| (f_0)^{-1} \exp \left(\frac{E_B(H)}{k_B T} \right)$$

x: fraction of retained magnetization after time t_x

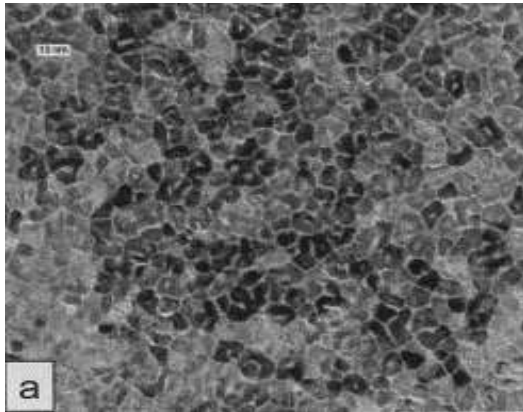
2 – time dependent coercivity

$$H_{CR}(V, t_p) = H_0 \cdot \left(1 - \left[\frac{k_B T}{K_u V} \cdot \ln \left(\frac{t_p \cdot f_0}{\ln 2} \right) \right]^n \right)$$

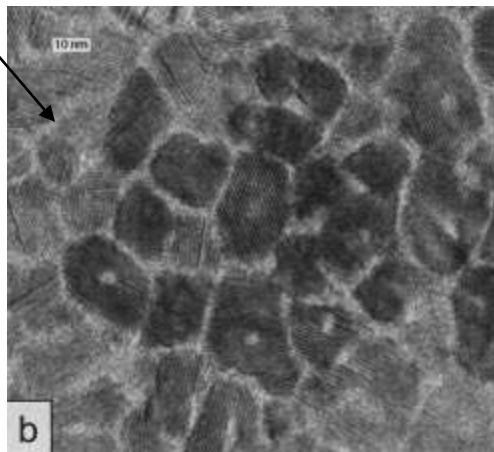


Grain size and distribution reduction

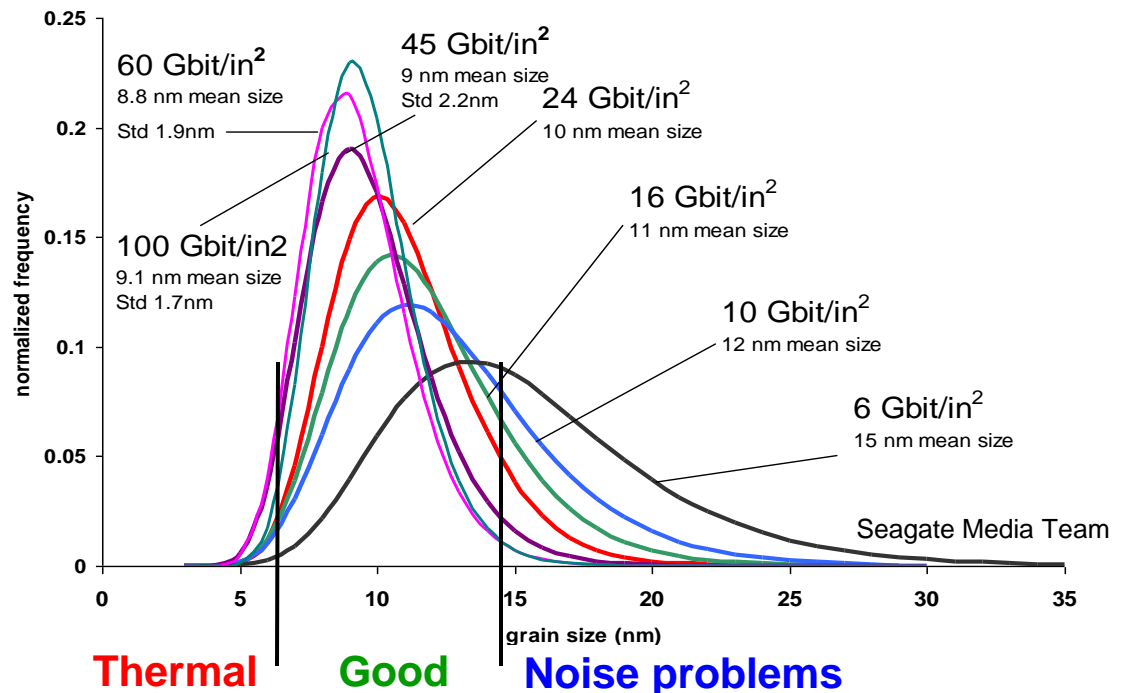
CoCrPtB - 35 Gbit/in² medium



Amorphous grain boundaries



- Smaller grains, better isolation
- But...
 - Thermal activation of small grains
 - Increased jitter from large grains



The importance of grain size & distribution

criterion for data stability:
allow max. 10% signal loss over 10 years

logarithmic time scale is deceptive

1 sec

1 day $\sim 10^5$ sec

1 year $\sim 3 \cdot 10^6$ sec

10 years $\sim 3 \cdot 10^7$ sec

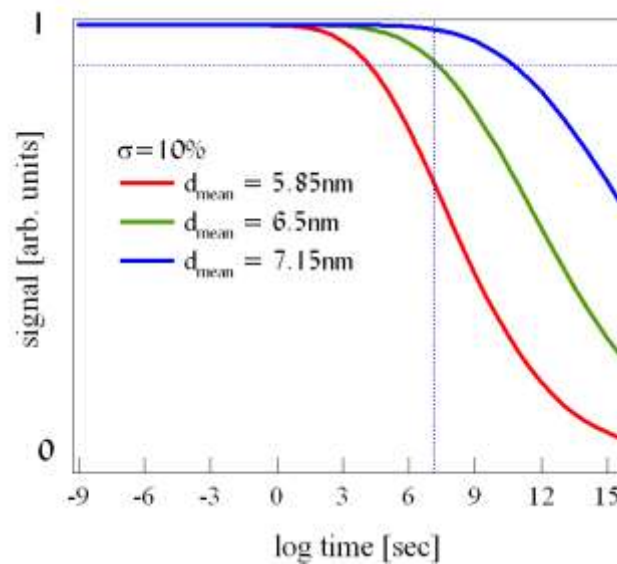
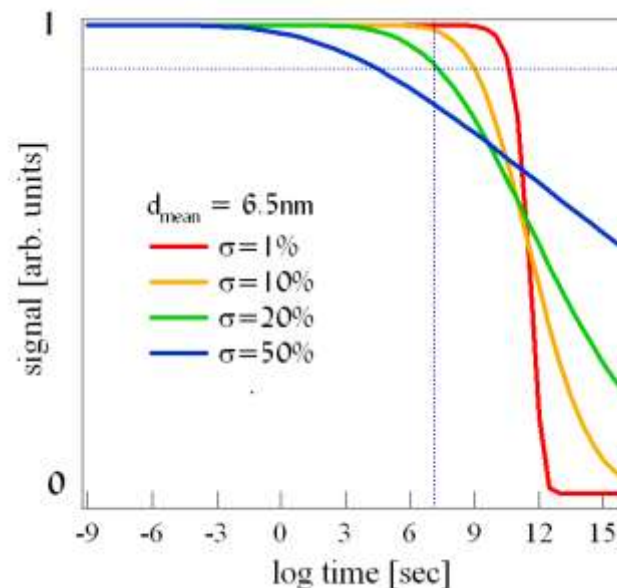
300.000 years $\sim 10^{12}$ sec

media parameter

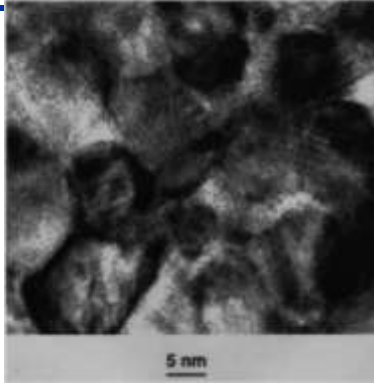
$M_S = 350 \text{ emu/cm}^3$

$K_U = 2.5 \cdot 10^6 \text{ erg/cm}^3$

$t = 20 \text{ nm}$



Distribution Narrowing

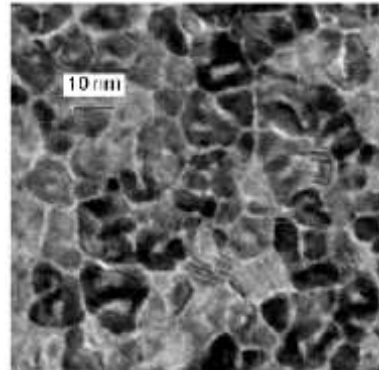


10 Gbit/in²
product media

12 nm grains

$$\sigma_{\text{area}} \cong 0.9$$

J. Li, *et al.*,
J. Appl. Phys. **85**, 4286 (1999)

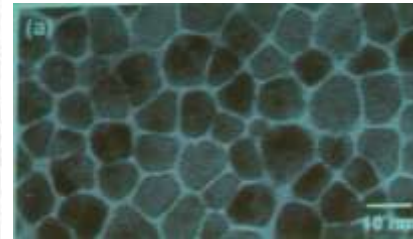


35 Gb/in²
prototype media

8.5 nm grains

$$\sigma_{\text{area}} \cong 0.6$$

M. Doerner *et al.*,
IEEE Trans. Mag. **37** (2001) 1052

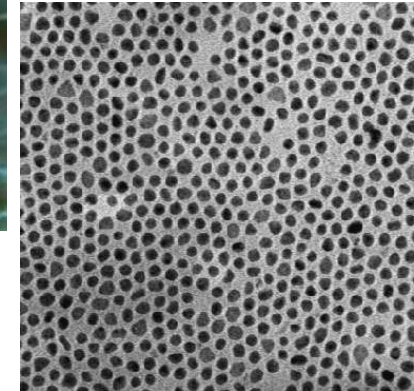


600 Gb/in²
prototype media

8.5 nm grains

$$\sigma_{\text{area}} \cong 0.2$$

Tanahashi *et al.*,
TMRC 2008



Nanoparticle arrays

4 nm particles

$$\sigma_{\text{area}} \cong 0.05$$

S. Sun *et al.*,
Science **287**,1989 (2000) 1989

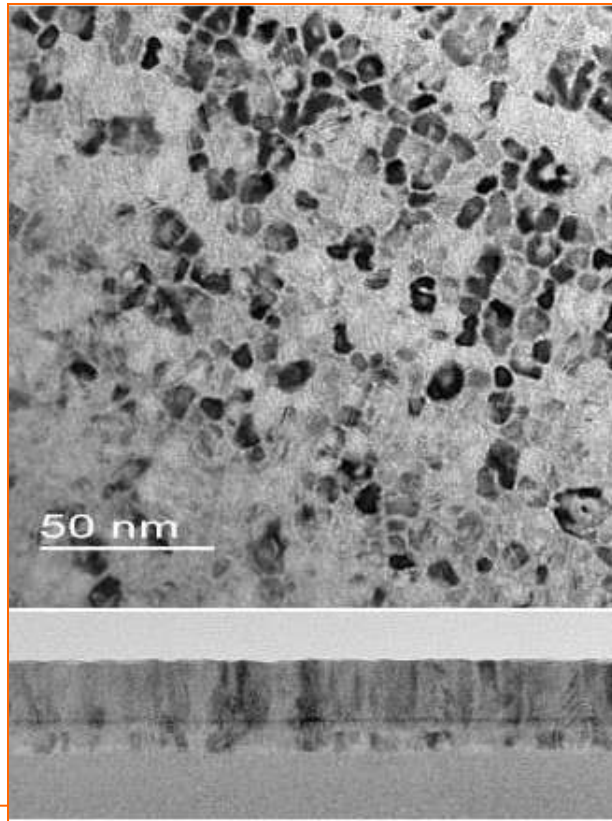
simultaneous nucleation and growth in PVD leads to log-normal distribution

– fundamental problem !

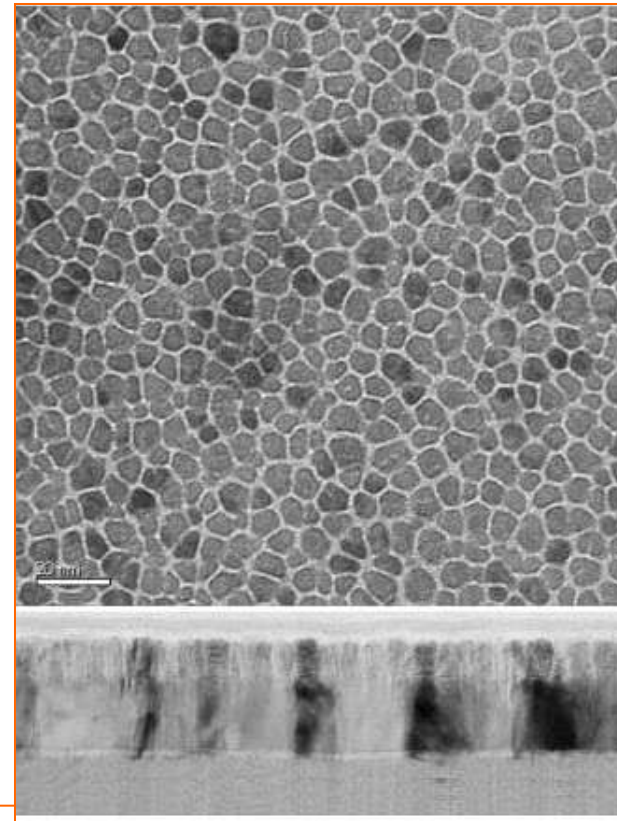
challenge: novel, mass production compatible deposition techniques

Microstructural Comparison

Longitudinal conventional

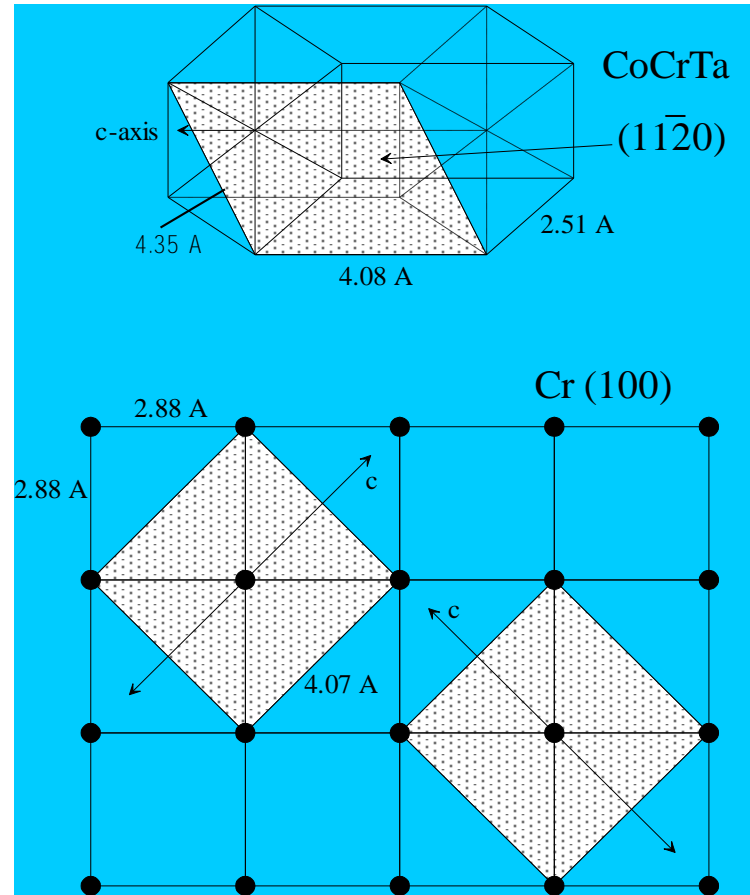
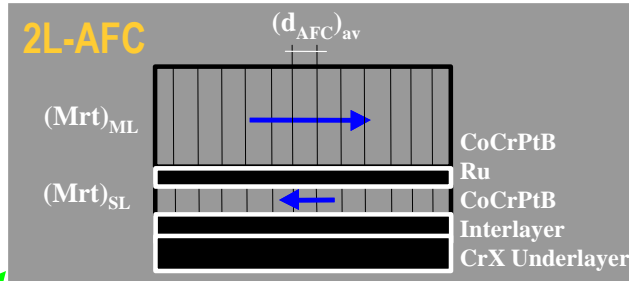


Perpendicular granular

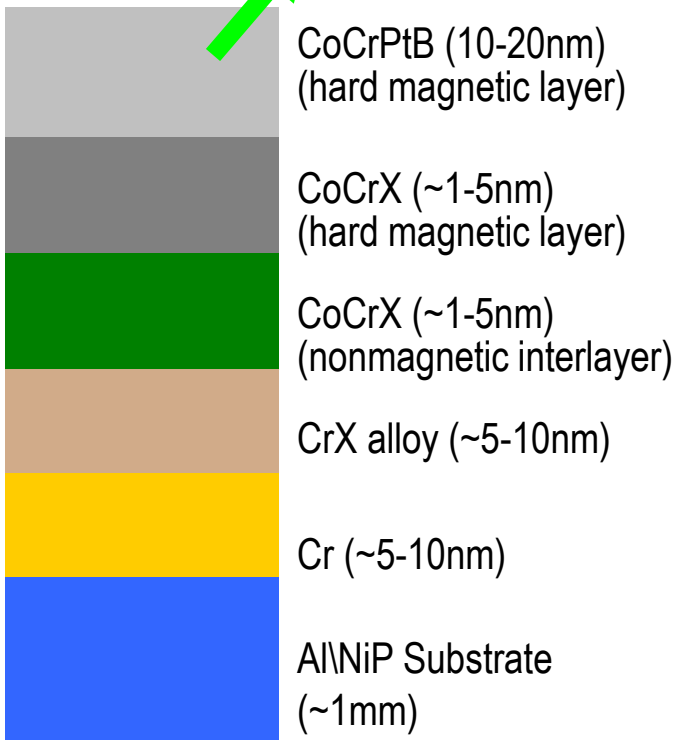


- Granular segregation for perpendicular media enables significantly sharper grain definition.

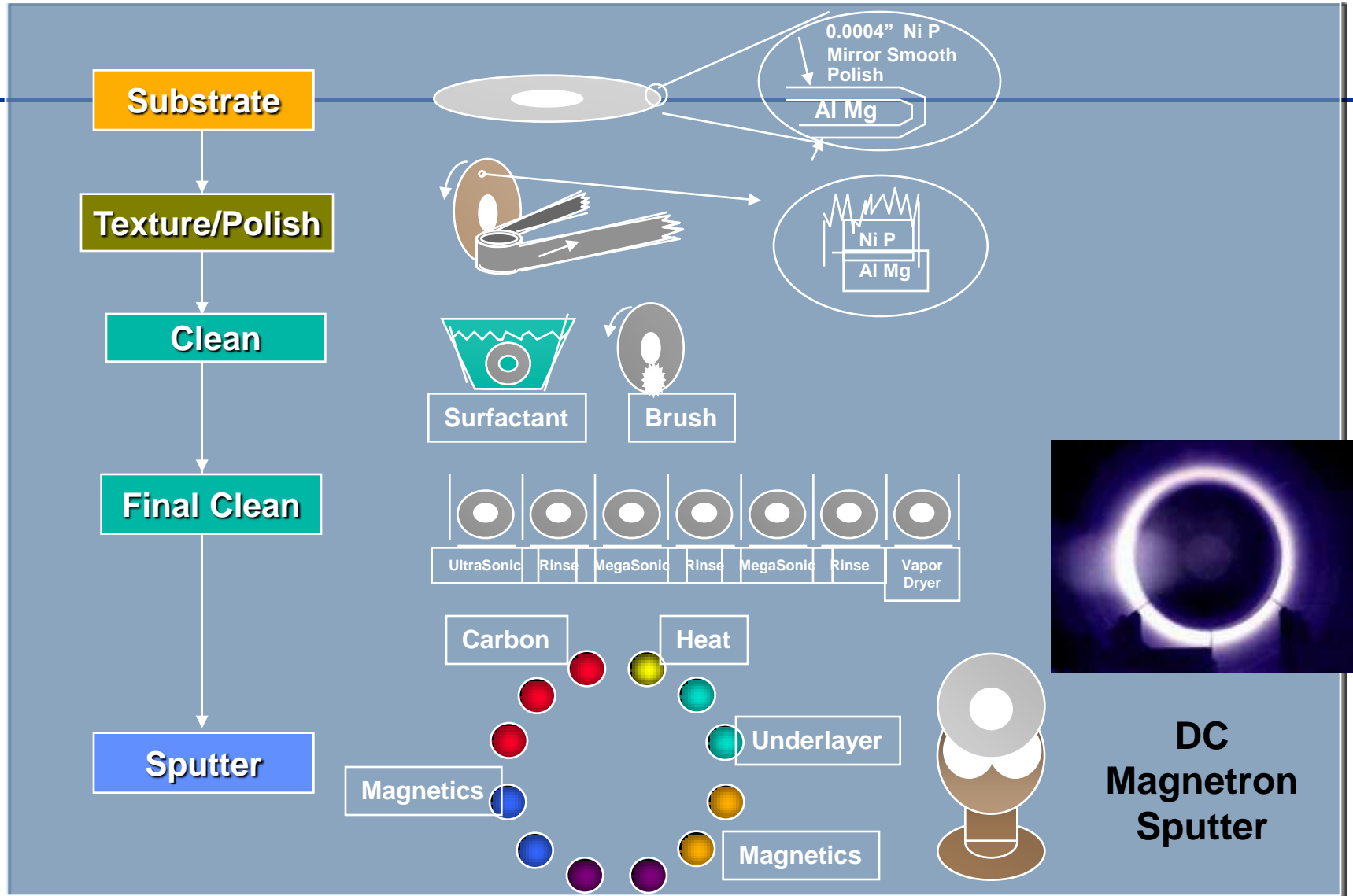
Longitudinal Media Design



$\langle 11.0 \rangle$ hcp alloys epitaxially grown on $\langle 200 \rangle$ Cr/CrX template

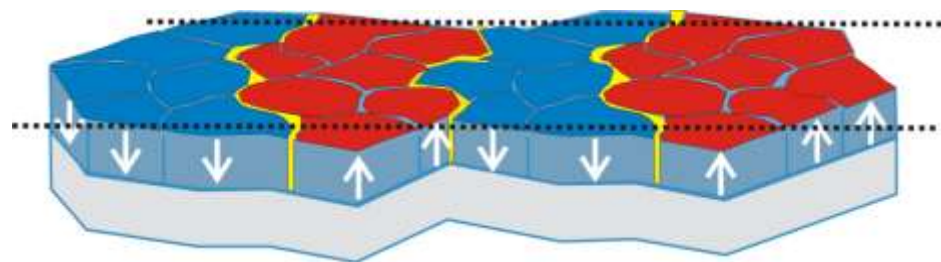
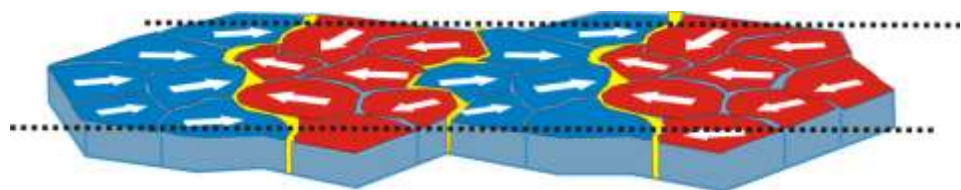


Media Process Flow



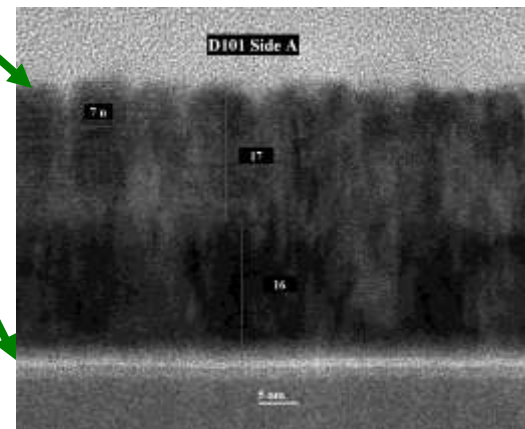
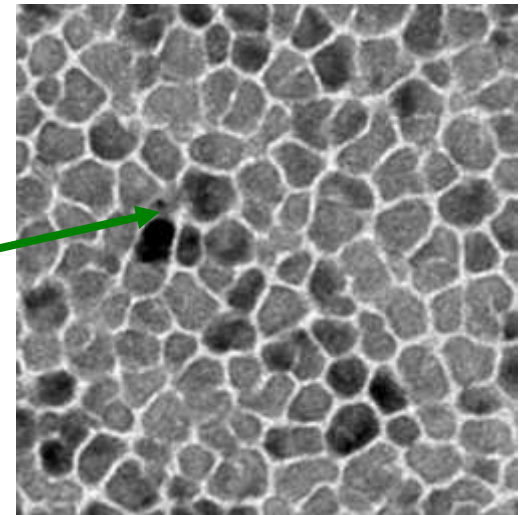
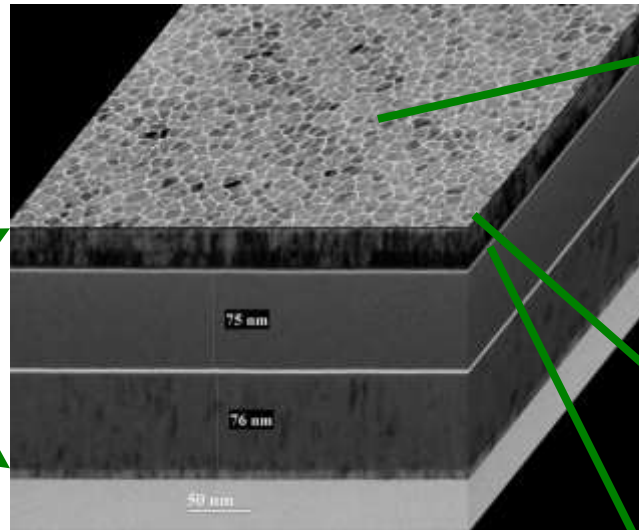
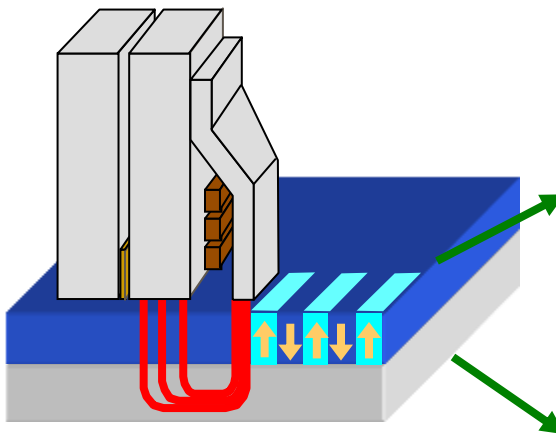
Media differences LMR \leftrightarrow PMR

- position in write gap in combination with soft magnetic underlayer (SUL) provides higher write field, allows higher K_U , H_{SW} media
- magnetostatics of high density recording destabilizes longitudinal bits but stabilizes perpendicular bits
- perpendicular media have near perfect magnetic orientation
- tunability of exchange coupling and magnetostatics (composite media)
- SUL requirements
 - high M_S to match write head material
 - high permeability >50



Perpendicular media

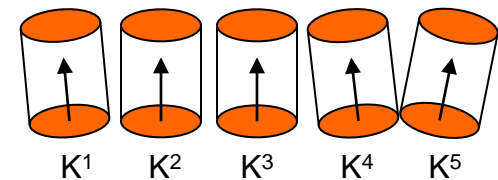
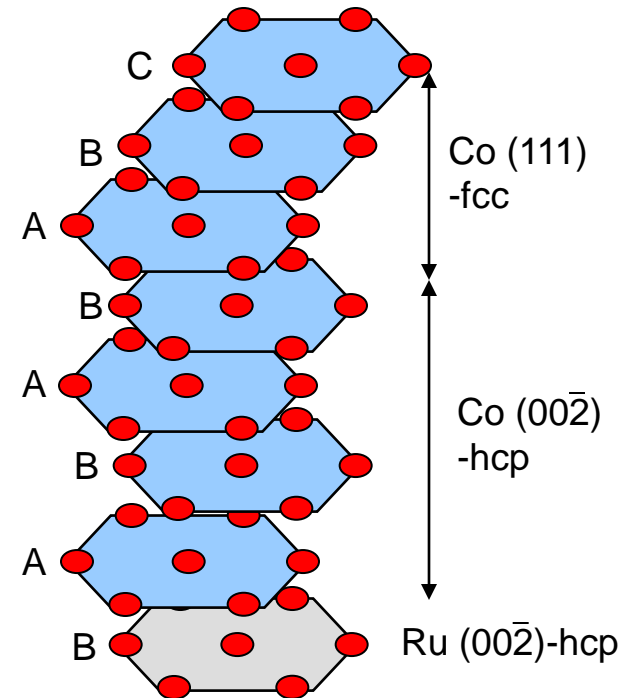
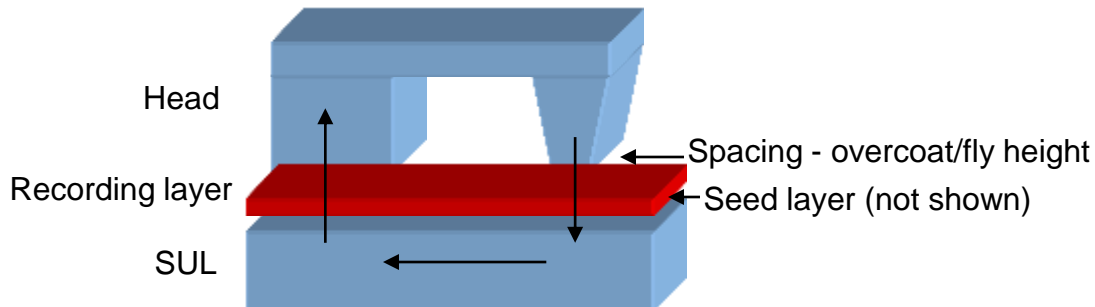
CoPtCr-SiO_x media



**Single layer media with oxide segregant
were used for 1st PMR product generations,
135 ~300 Gbit/in²**

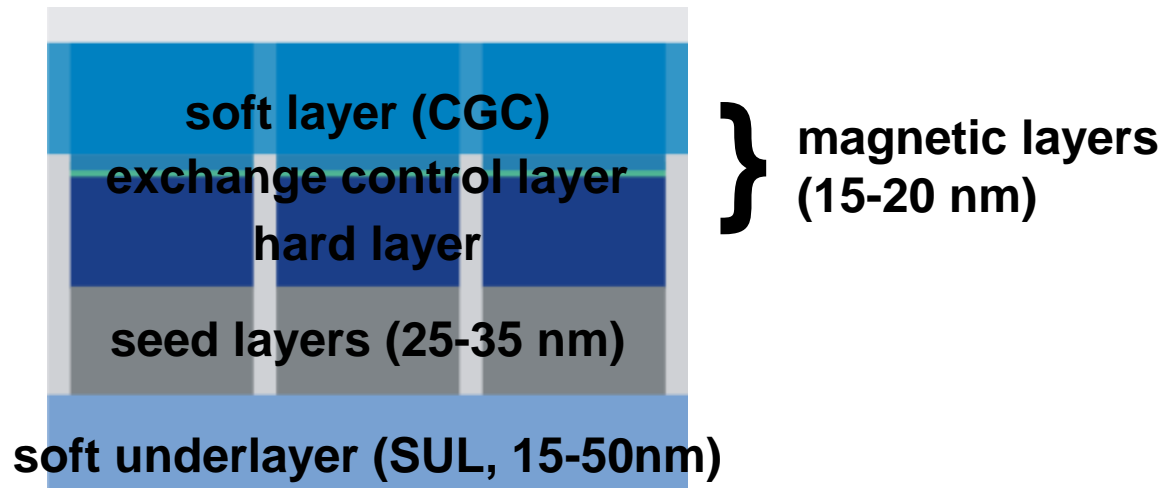
CoCrPt-oxide perpendicular media

- Challenges
 - grow grains with hcp c-axis perpendicular to the plane without stacking faults and with small dispersion of easy axes angles
 - minimize spacing loss between SUL and recording layer
 - significant constraint on seed and underlayer structure

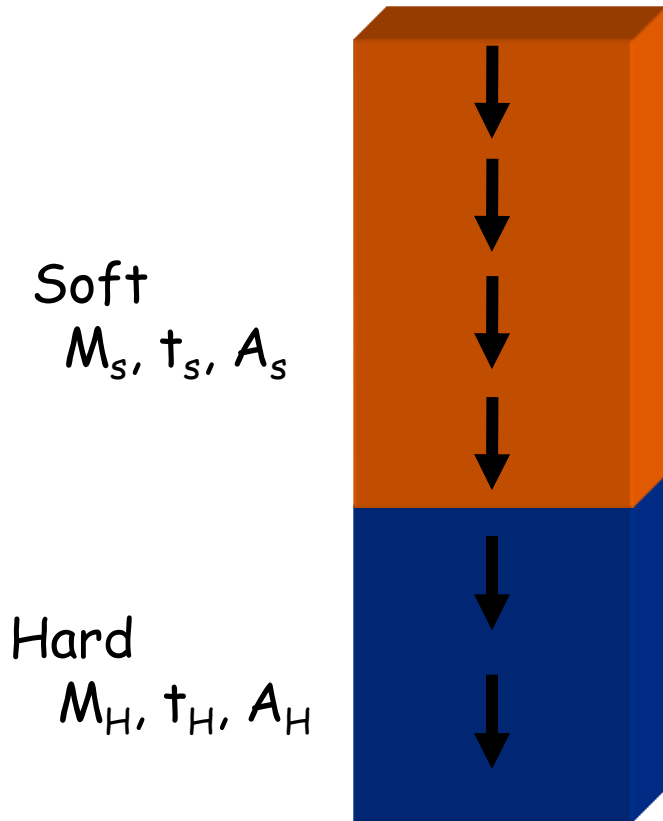


Novel media ideas – CGC & ECC

- a laterally more exchange coupled layer, typically near the top of the layer structure, allows controlled and uniform grain-to-grain exchange, reducing the switching field distribution – this type of media is called Continuous Granular Composite (CGC) media
- splitting each grain into a hard and soft region with controlled exchange coupling between the regions allows to reduce the required switching field without reducing the energy barrier – this type of media is called Exchange-Coupled-Composite (ECC) media (first published by R.H. Victora, IEEE Trans. Magn. **41** (2005) 537)
- Applying a field rotates the soft region and so changes the angle of the total effective field acting on the hard region ($H_{\text{app}} + H_{\text{ex}}$)



Exchange spring structures



H

$$H_N \approx \frac{\pi^2 A_s}{2 M_s t_s^2}$$

Domain wall compression

$$H_C \rightarrow \sigma_S(H) = \sigma_H$$

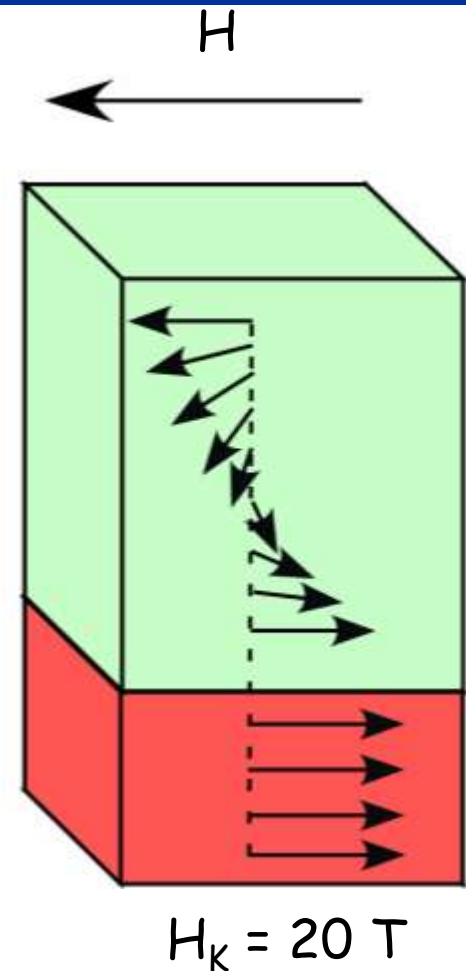
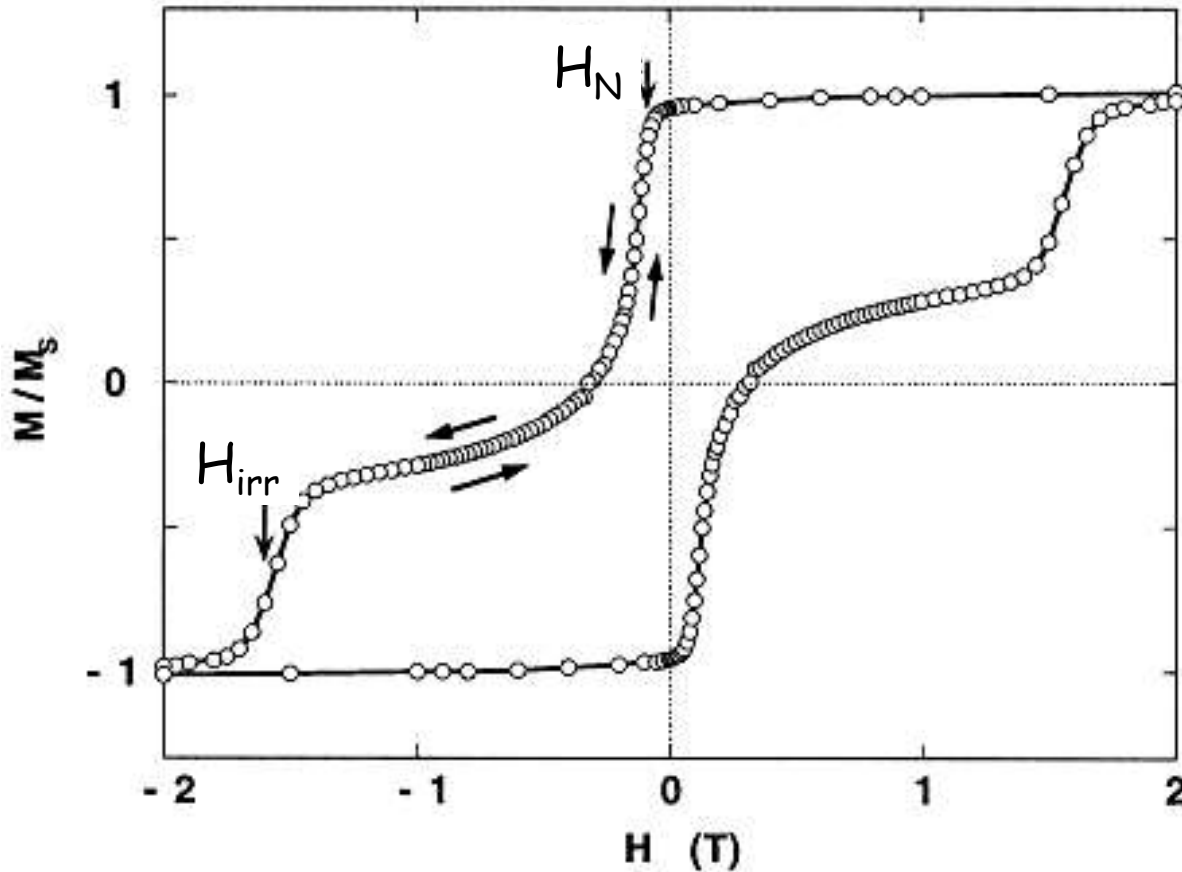
- Permanent magnets
Spin transport devices
Perpendicular & patterned media
- lower H_C faster than $K_U V$
 - Improved angle dependence

Goto *et al.*
J. Appl. Phys. **36**, 2951 (1965).

E. Fullerton, J. Magn. Magn. Mat. **200**, 392 (1999)

Exchange spring structures

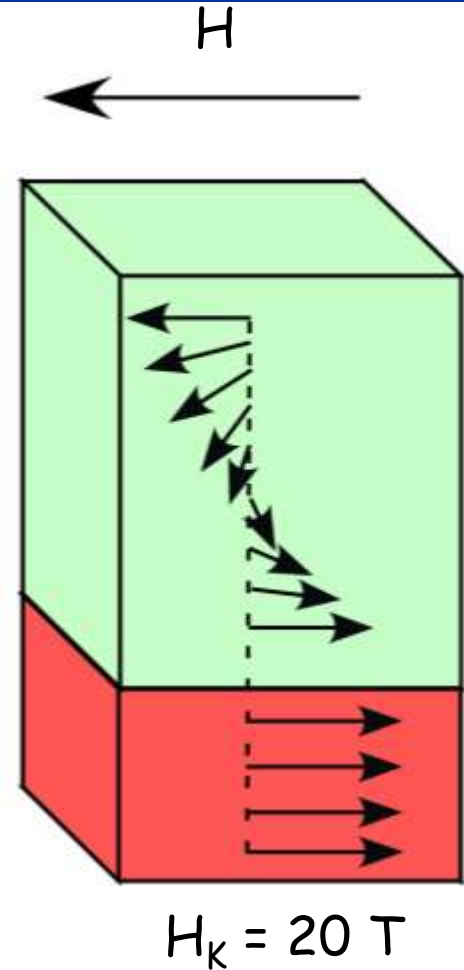
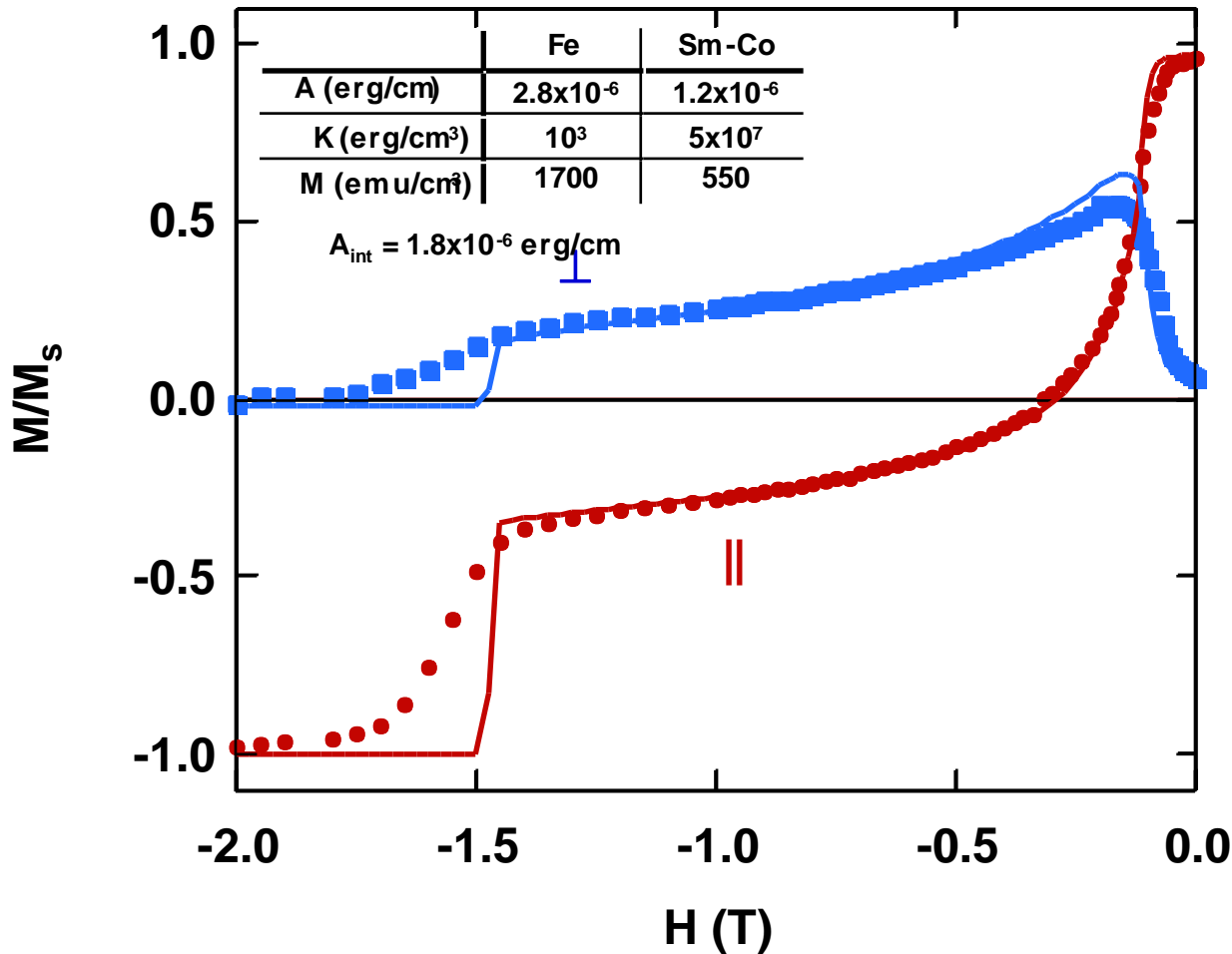
Sm-Co(200Å)/Fe(200Å) T=25K



E. Fullerton *et al.*, PRB **58**, 12193 (1998).

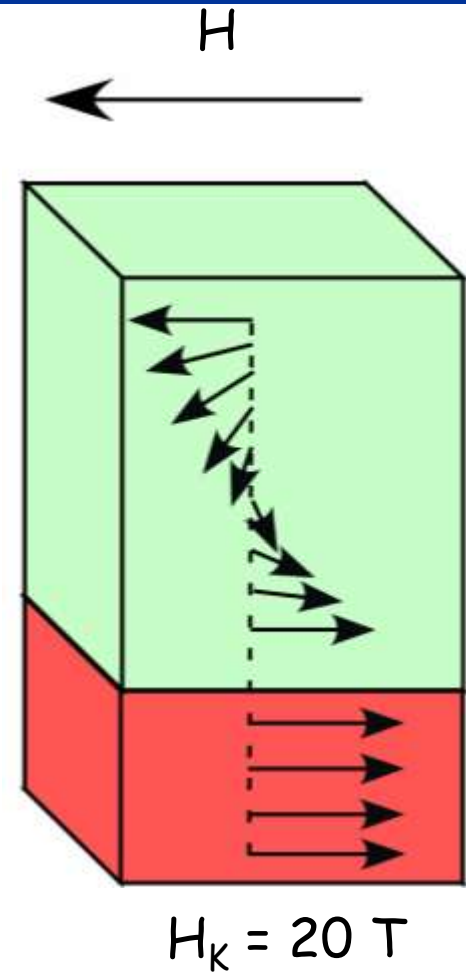
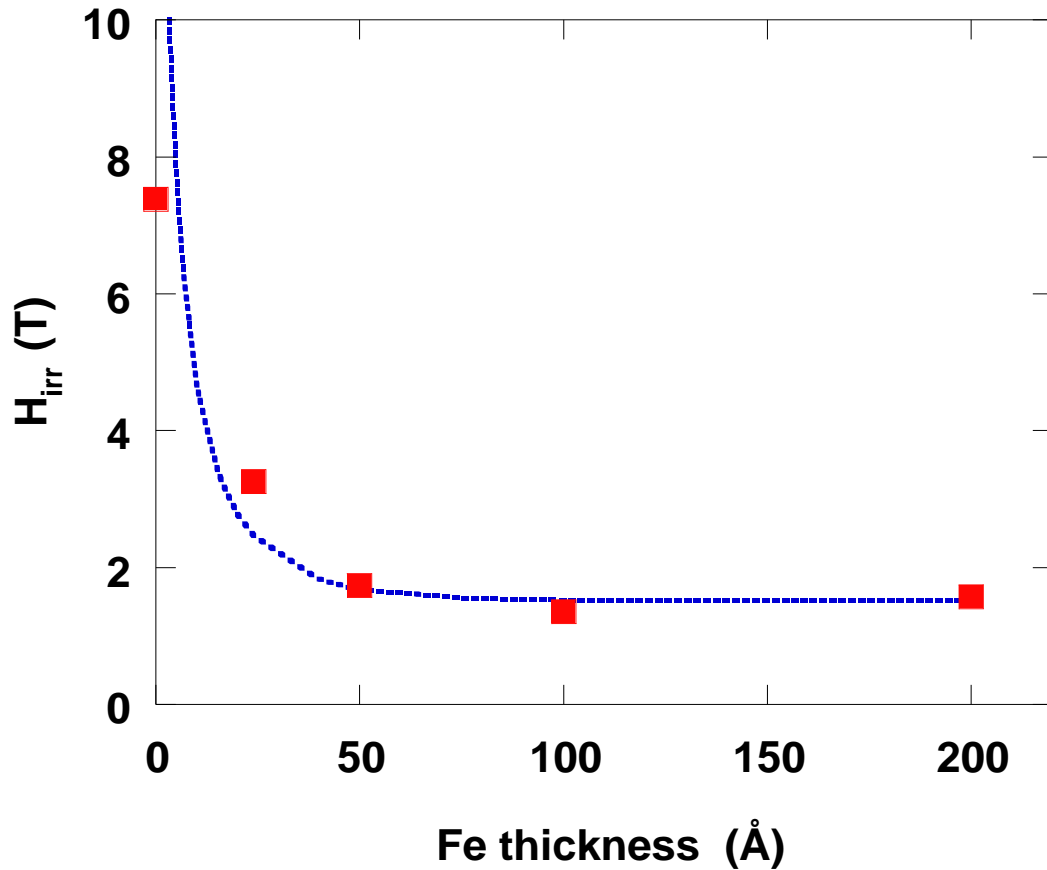
Exchange spring structures

Sm-Co(200Å)/Fe(200Å) T=25K



Exchange spring structures

Sm-Co(200Å)/Fe(t) T=25K



Exchange spring advantages

H_C decreases much faster than the energy barrier

H_C depends on the domain wall energy of the hard layer

$$H_C \propto \sqrt{KA}$$

$$\sigma H_K \rightarrow \sigma \sqrt{H_K}$$

Soft layer provides a torque so reduced angular dependence of H_C

Unusual and potentially useful dynamics

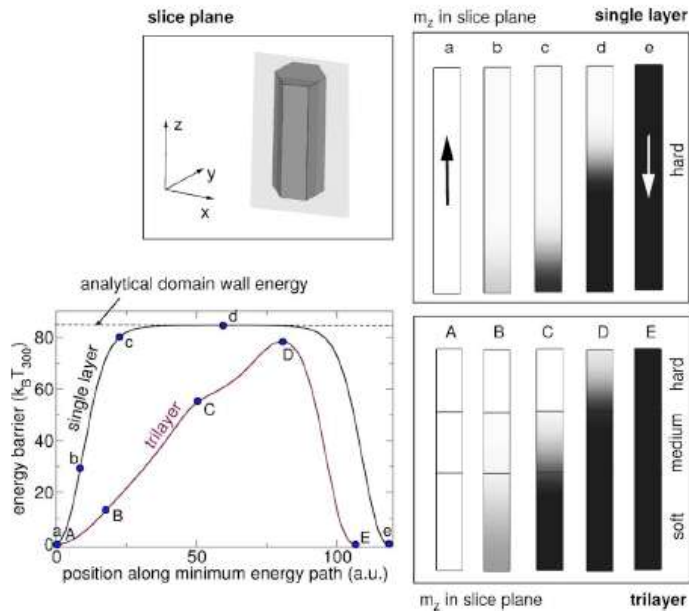
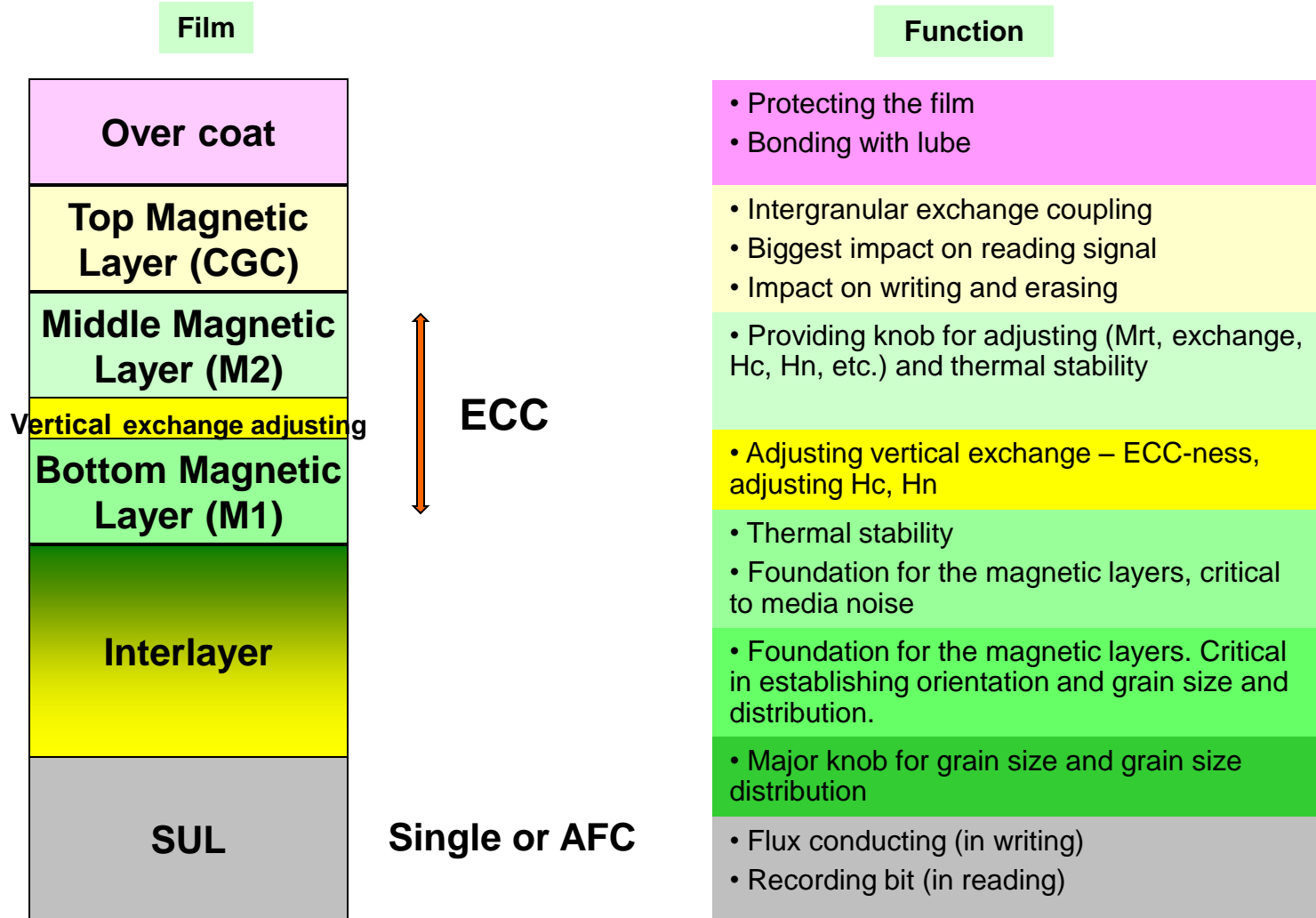


FIG. 3. Energy barrier and thermally activated switching process for a single phase media and the trilayer of Fig. 1. The hardest layer of the trilayer is 7 nm. The grain diameter is 5 nm. The z component of the magnetization during thermally activated switching is color coded.

Basic Perpendicular Media Structure

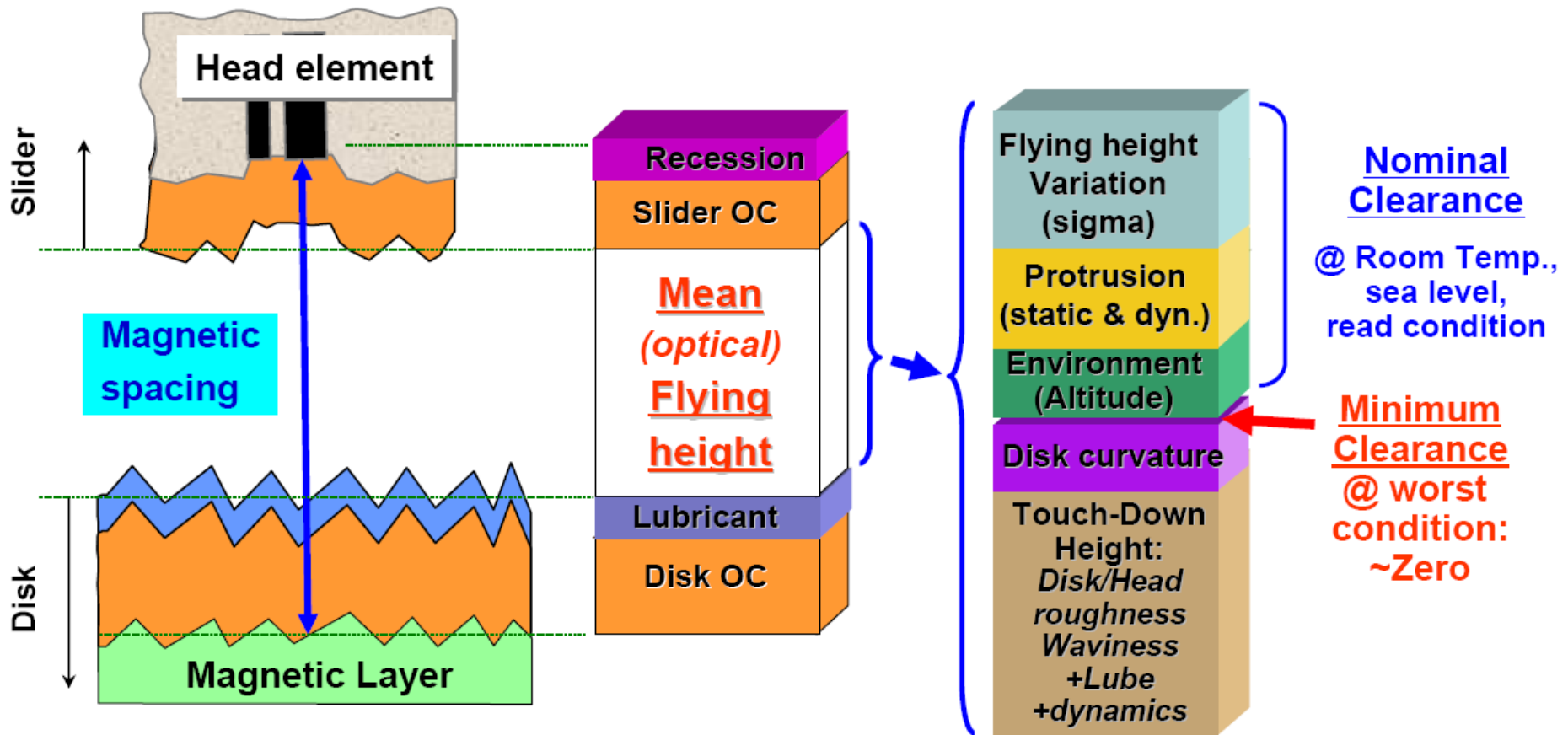


Head-Disk-Interface (HDI)

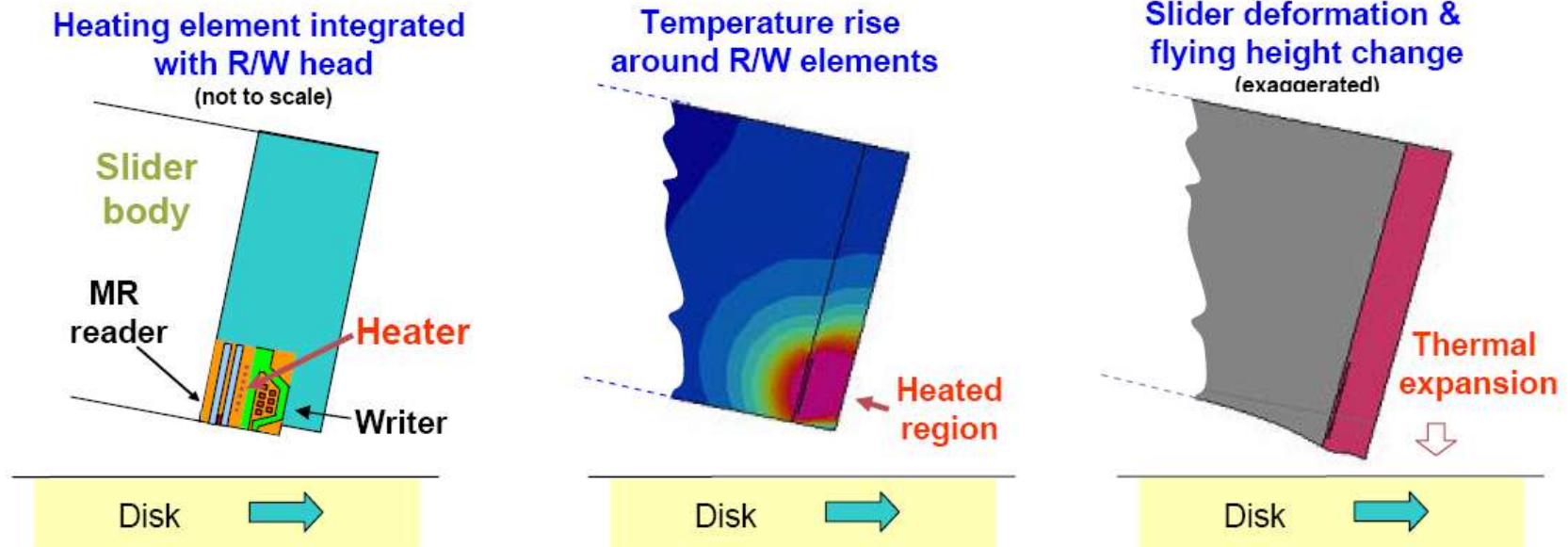


HDI at Ultra Low Flying Height

- For 70 Gbits/in² Areal Density magnetic spacing ~ 18 nm
- For 1 Tbits/in² Areal Density magnetic spacing < 7 nm



- TFC (Thermal Flying-height Control) - *recent introduction ~2005*
 - **Magnetic Spacing** is one of strongest levers for areal density
 - → Control flying height with small **thermal actuator (heater)** built into head
 - Only active during read or write → better reliability
 - Compensates head protrusion (deformation) due to writing, temperature change, etc.
 - Absorbs fly-height differences between heads, brings each head to lowest possible safe flying height.
 - **requires 6-pad slider and 6-leads connecting to redesigned preamp/write-driver chip**



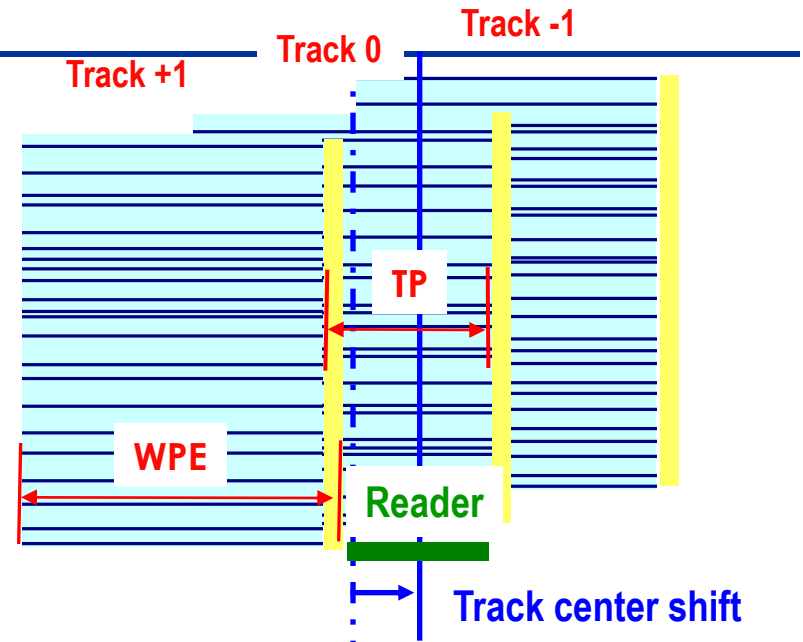
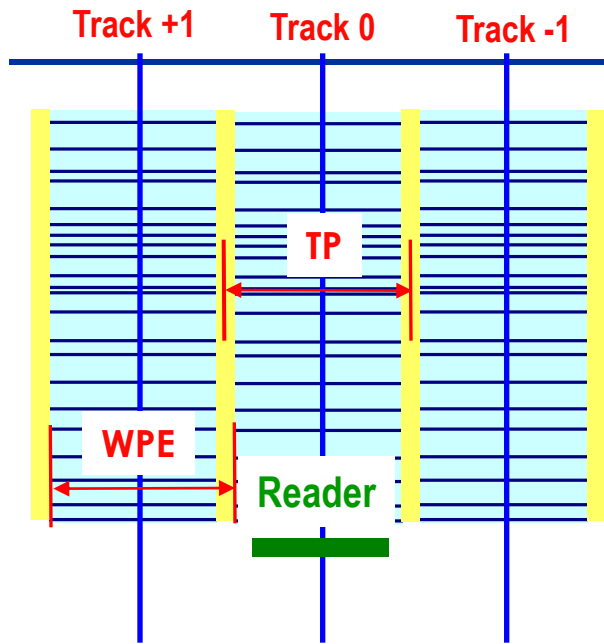
Limits of “conventional” magnetic recording



Extending PMR

- **Need PMR extension to 1.5 Tbps or higher**
 - Higher linear density – no clear path (SFD reduction, grain size reduction)
 - Higher track density – doable
- **Steps to improve track density**
 - Reduction of both writer and reader dimension – conventional PMR
 - Head writability limitation – controlled by $4\pi Ms$ of writer material
 - Thermal stability limitation of media H_c
 - **Reduction of only reader dimension – S(hingle)MR**
 - Use wide head to write higher track density
 - Reader dimension limitation - controlled by line-width capability in semiconductor
 - 2D SMR
 - No need to reduce both the reader and writer dimension
 - Implementing ISI (inter symbol interference) in step 1
 - Full 2D decoding of read back signal in step 2
- **Future Techniques to cover 1.5 Tbps**
 - HAMR, BPM, HAMR + BPM,

How SMR works



Conventional:

- Random access of each data track
- Nearly no overlapping between tracks
- Track pitch is controlled by writer (WPE) and reader dimensions
- Adjacent track erase could come from both side

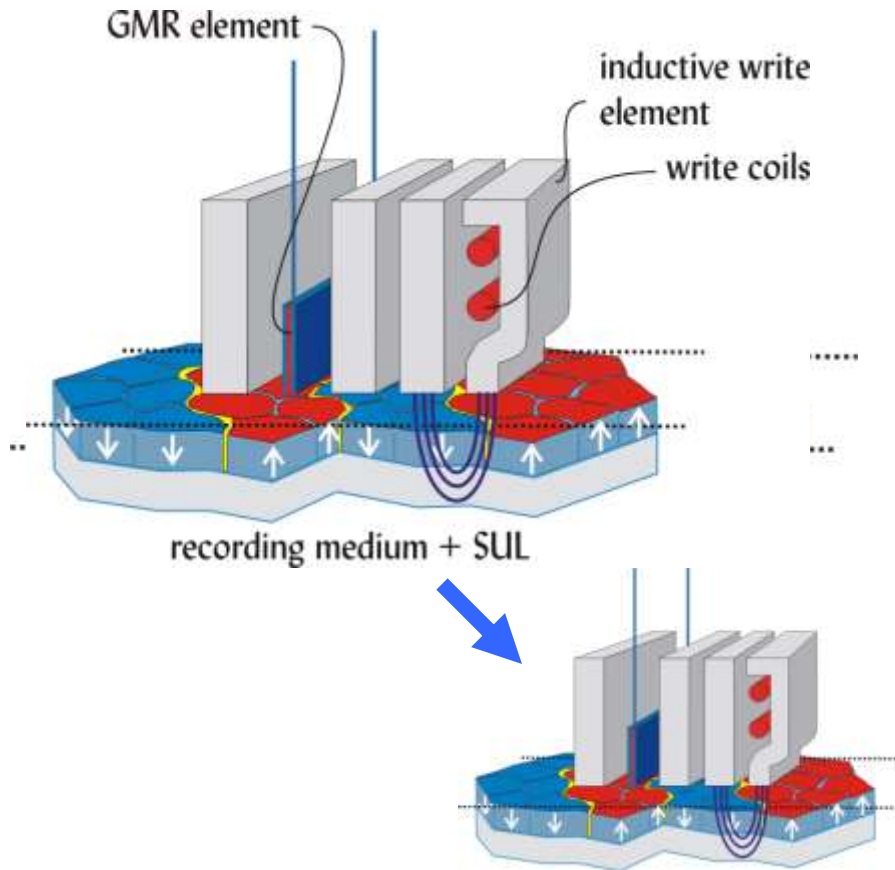
Bandit (Shingle):

- Data track written in sequential order
- Could have severe overlap between tracks
- Track pitch is controlled primarily by reader dimension
- Adjacent track erase only comes from one side

Advantage & drawbacks of SMR

- Head and media writability requirement is less critical
- For the same head/media
 - Typically see 10-15% gain in SMR at MD and with reasonable reader and writer margin
 - The SMR gain is higher at ID or OD
 - SMR track pitch is nearly flat from ID->MD->OD
 - Conventional PMR track density is lower at ID and OD
 - The SMR gain is higher if WPE >> reader dimension
- SMR has less requirement for erasure
- Performance hit
 - No more random access for write
 - Erase and write a band of data
- Format efficiency loss

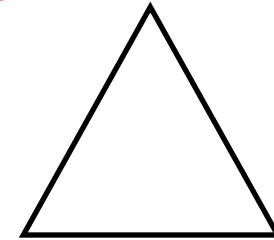
Limits to 'conventional' scaling in magnetic recording



$$\text{SNR}_p \propto 10 \cdot \log_{10}(N)$$

$$\cong 30 \text{ dB for } N=1000$$

Signal-to-Noise Ratio



**thermal
stability**

writeability

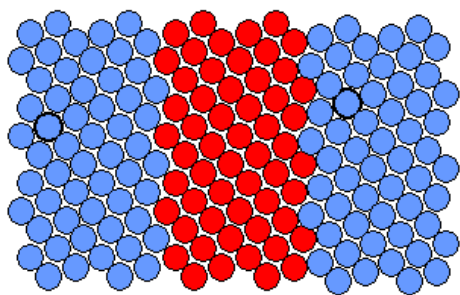
$$\text{stability} \sim \frac{K_u V^*}{k_B T}$$

$$B_{S, \max} = 2.4 \text{ T}$$

The achievable areal density using 'conventional' scaling is limited by trade-off between **SNR**, **thermal stability** and **writeability**

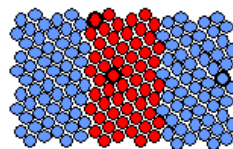
Superparamagnetic Effect

Superparamagnetic Limit

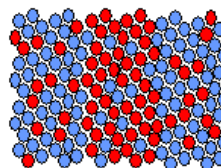


To preserve SNR, number of grains in a bit must be constant

$SNR \sim \log_{10}(N)$
Therefore higher densities require smaller grains



The smaller bits have a higher probability of flipping and the data is unstable

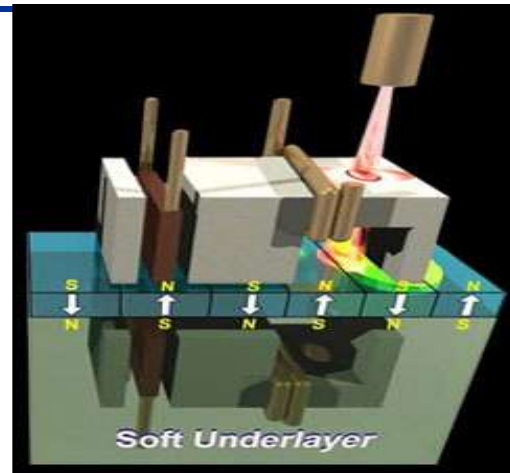


High areal density means small volume

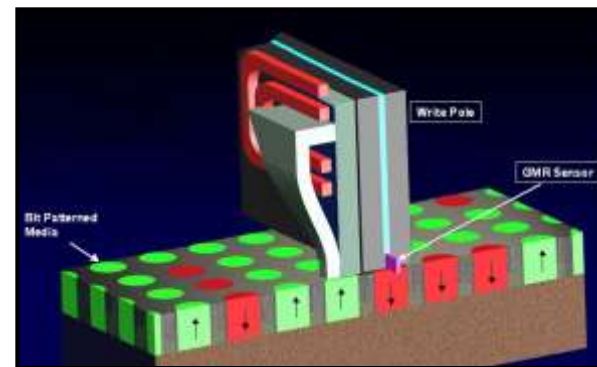
$$\tau = f_0^{-1} \exp\left(\frac{K_u V}{k_B T}\right)$$

$\frac{K_u V}{k_B T} = 40 - 60$ is considered acceptable

HAMR: Increase **K**



BPM: Increase **V**

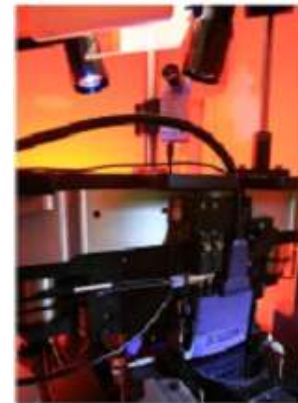


Patterned Media

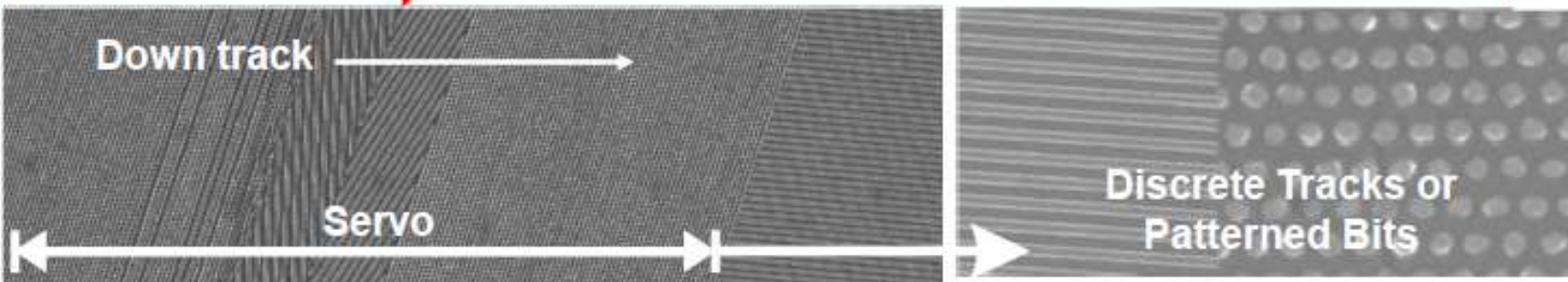
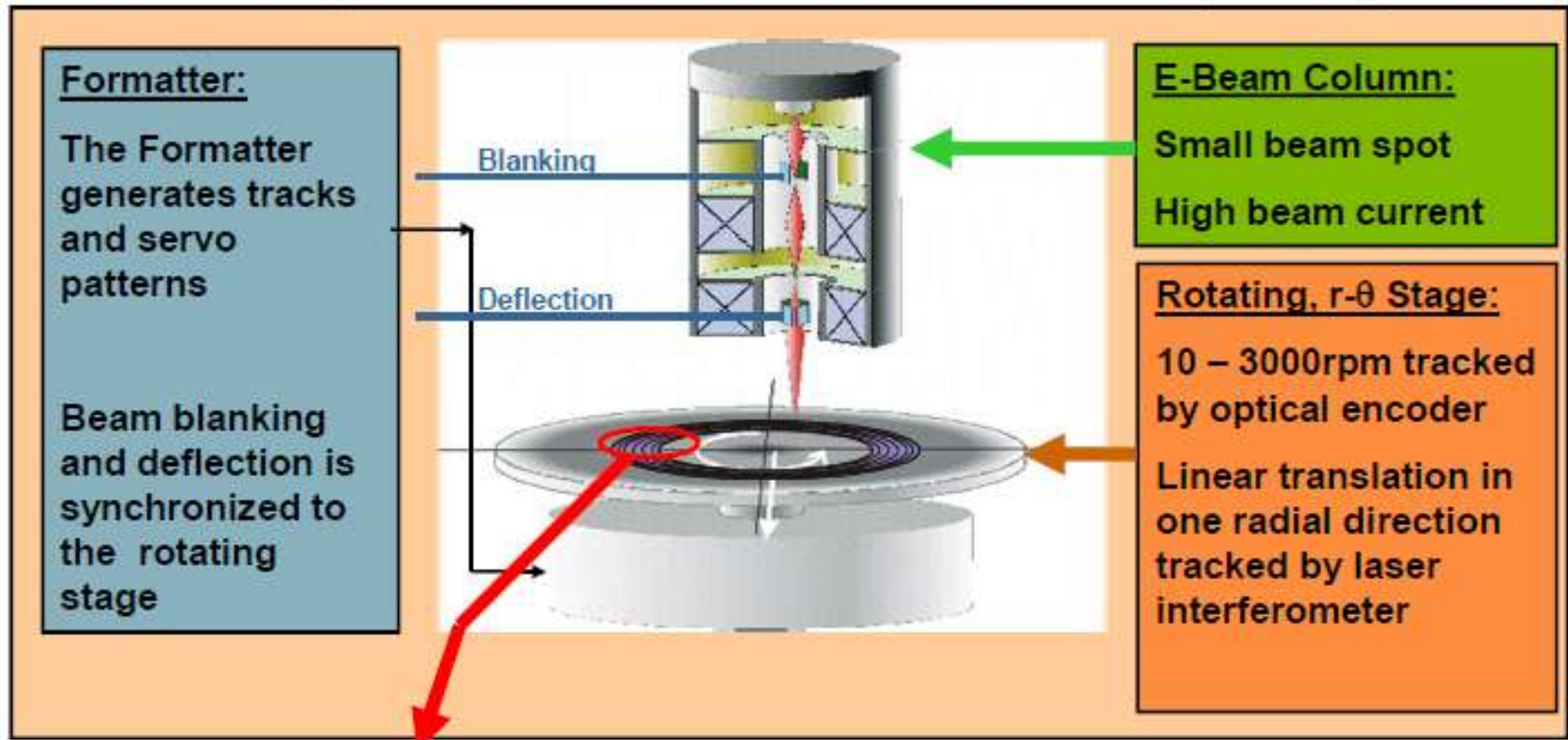


Patterned Media Fabrication

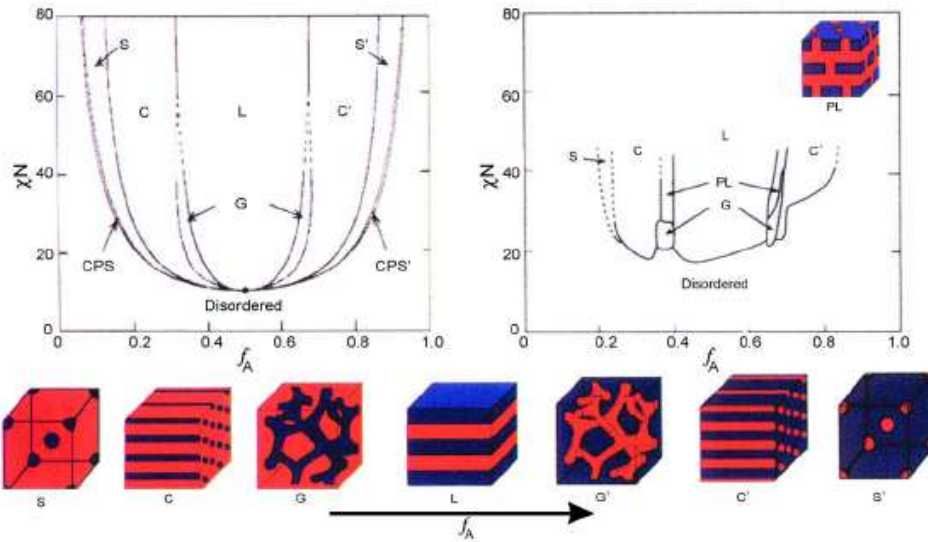
1. **Mastering**
 - Rotary-stage e-beam lithography **(MUST)**
2. **Template fabrication**
 - Directed self-assembly (DSA) of block copolymers
 - Double patterning **(alternative)**
 - Template replication
3. **Nanoimprint lithography (NIL)**
 - UV cure
 - Template cleaning
4. **Magnetic dot formation**
 - Ion beam etch
 - Ion implantation
5. **Metrology**
 - Critical dimension & sigma control
 - Defect control



Mastering: Rotary-Stage E-Beam Writer



Block Copolymer Self-Assembly: Pattern Resolution Set by **Materials**

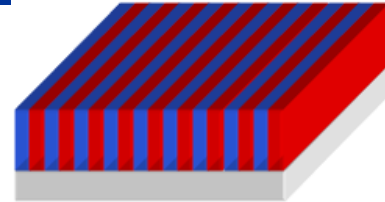


* F.S. Bates, G.H. Fredrickson, *Phys. Today* 1999



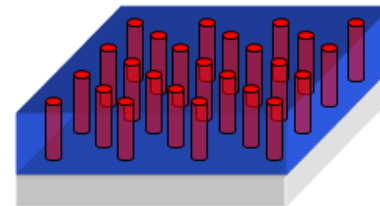
$$L_0 \propto N_{\min}^{1/2}$$

$$\chi N_{\min} = 10.5$$



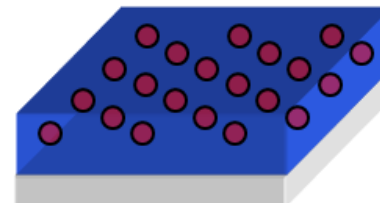
Lamella

- 1-D (2X lithography → 2D)
- Orientation control
- Flexible for skew
- Low- χ block copolymers (double-patterning)



Cylinder

- 2-D
- Orientation control
- Inflexible for skew (HCP)
- High- χ block copolymers



Sphere

- 2-D
- Inflexible for skew (HCP)
- High- χ block copolymers

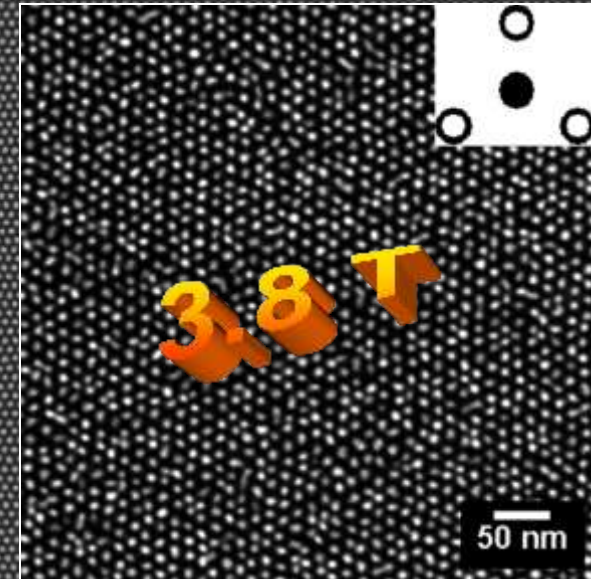
Spherical PS-*b*-PDMS: Up to ~5 Tdpsi (6nm hp)

□ 4X-16X AD multiplication using spherical PS-*b*-PDMS

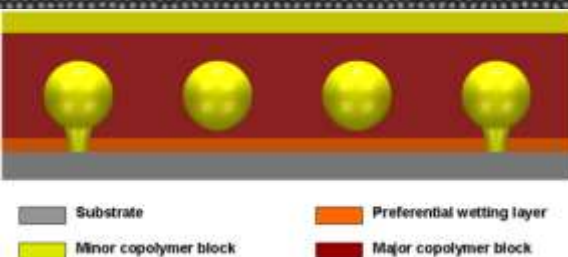
(S. Xiao *et al. Adv. Mater.* 2009)

□ Advantages over PS-*b*-PMMA

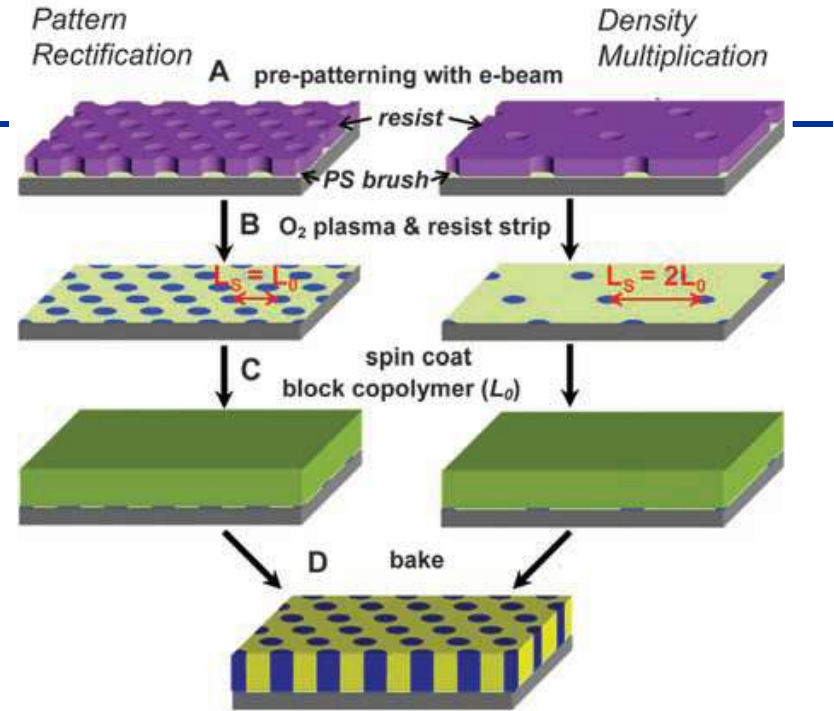
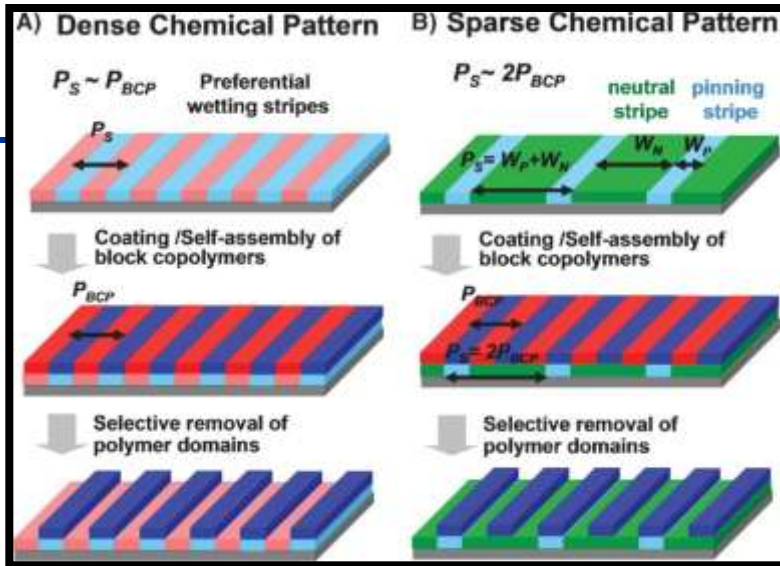
- Better AD extendibility (~5 T vs. ~1 T)
- General approach to various BCPs due to the elimination of the need of orientation control



Solvent anneal



DSA for Density Multiplication



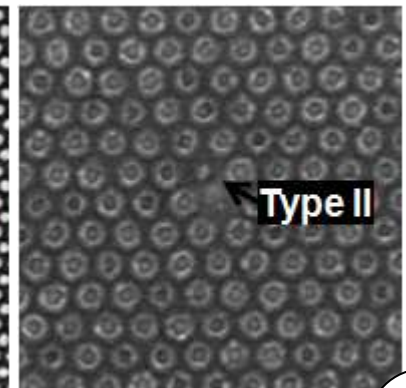
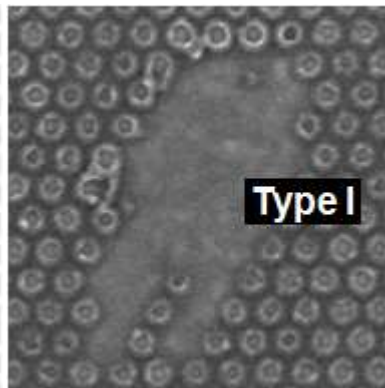
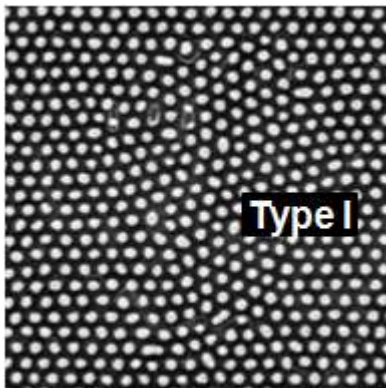
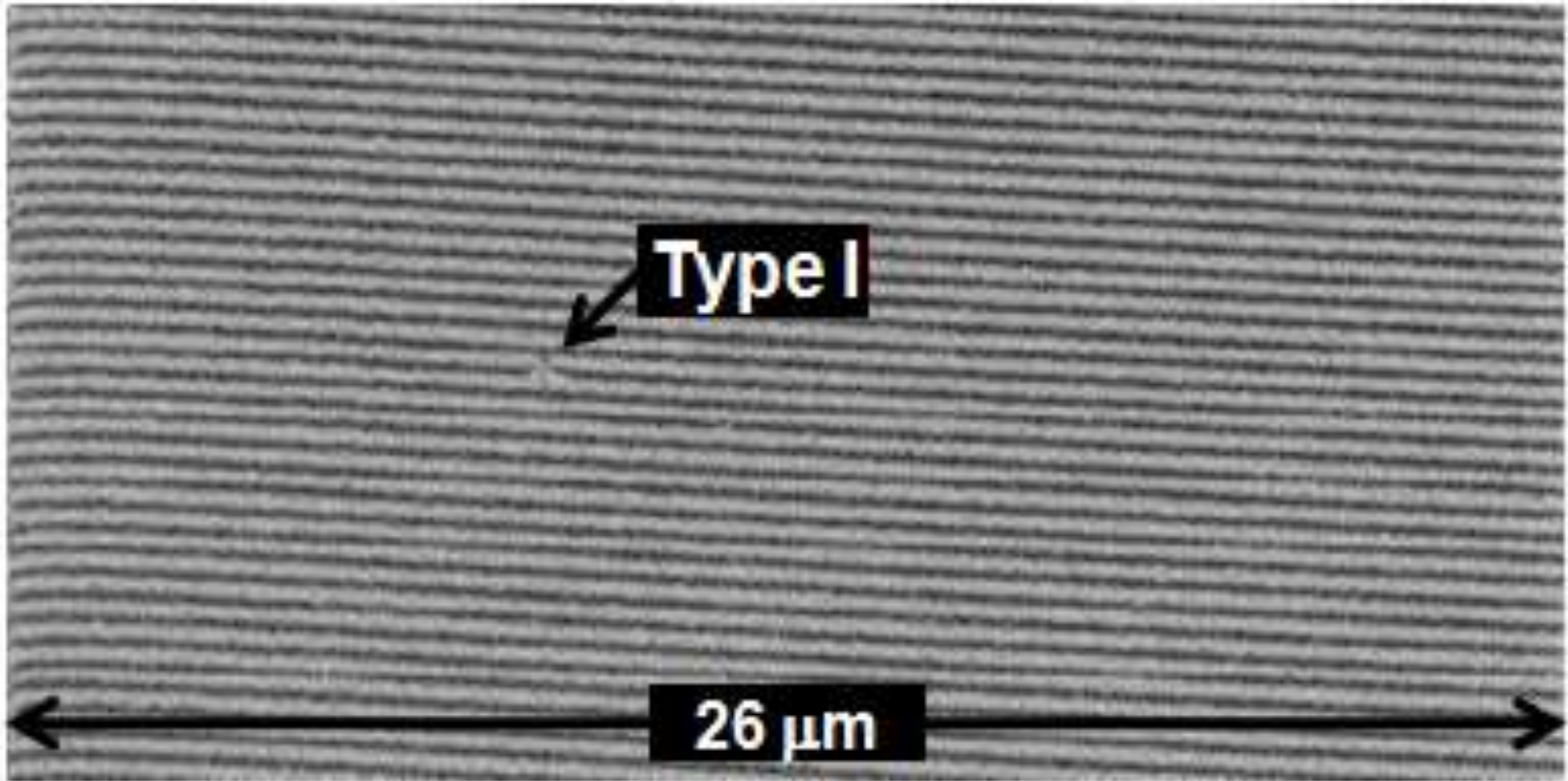
DSA + EBL → density multiplication

□ Lamella system: J. Y. Cheng *et al.*, *Adv. Mater.* 2008 (IBM)

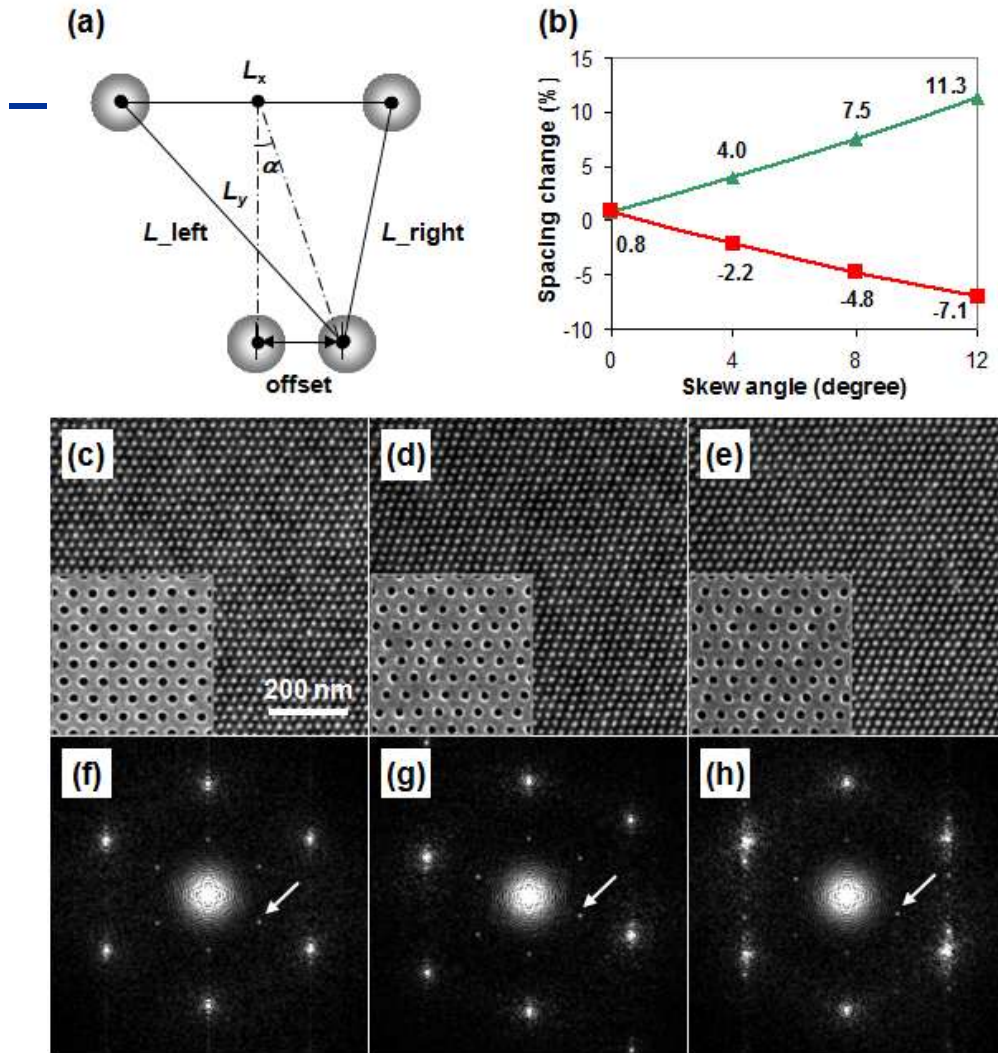
□ Cylinder system: R. Ruiz/P. Nealey *et al.*, *Science* 2008 (HGST & University of Wisconsin)

□ Sphere system: S. Xiao *et al.*, *Adv. Mater.* 2009 (Seagate Technology & University of Massachusetts)

Challenge: Defect Control



Challenge: Skew (Deviation from HCP)

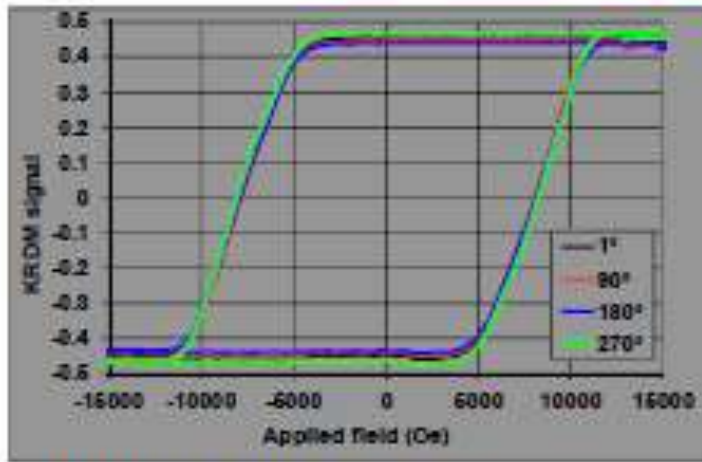


“The actuator arm and suspension of the rotary actuator are collinear making the movement of the slider follow an arc and not a straight line.”

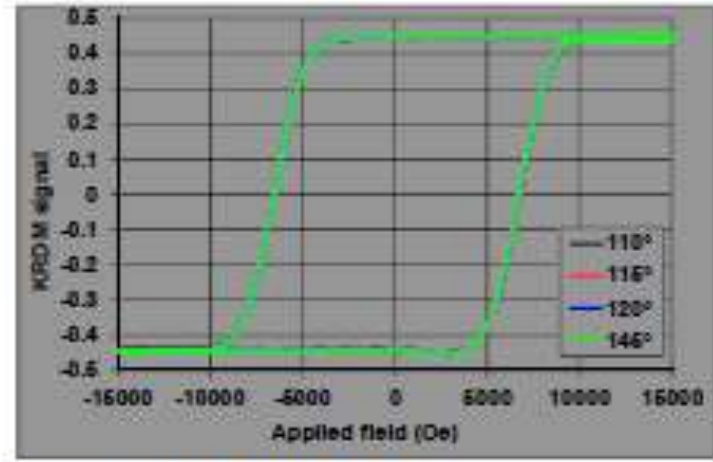
-Hard Disk Drive: Mechatronics And Control By Abdullah Al Mamun et al.

*S. Xiao et al., *Nanotechnol.* 2011

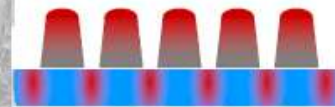
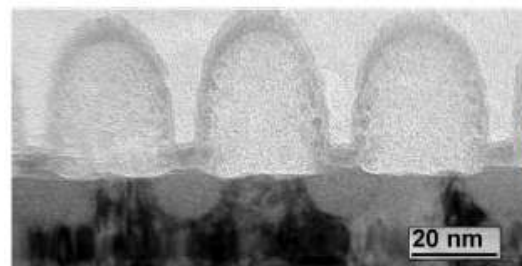
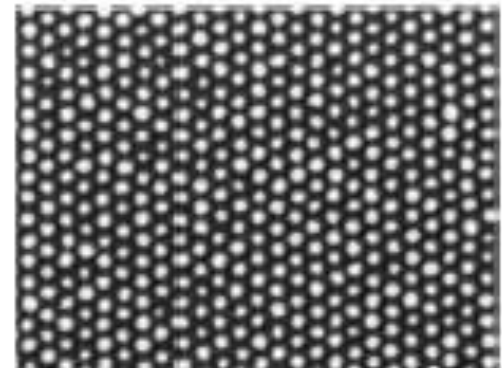
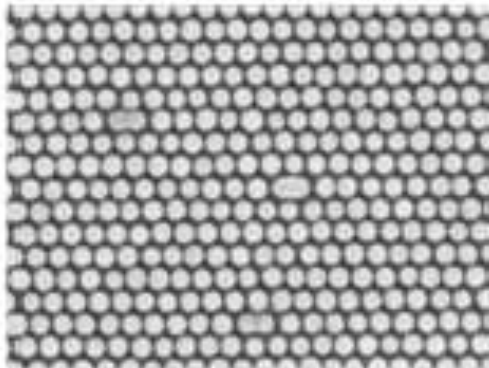
Ion Implantation



Ion implanted media @ 500G

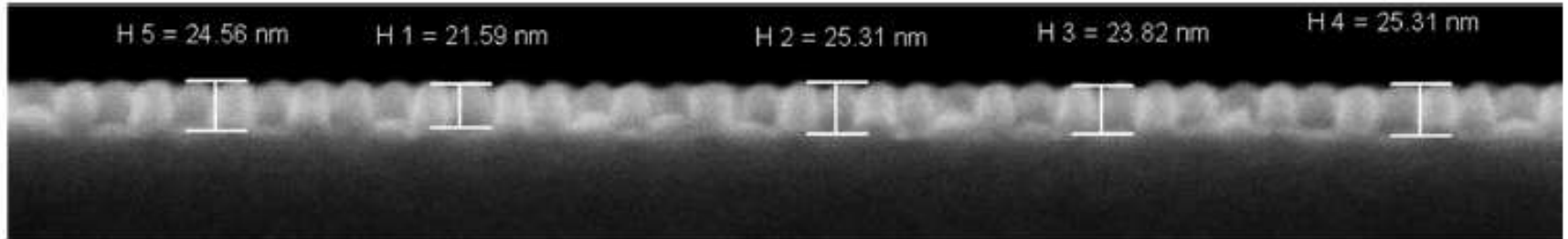


Ion implanted media @ 1T

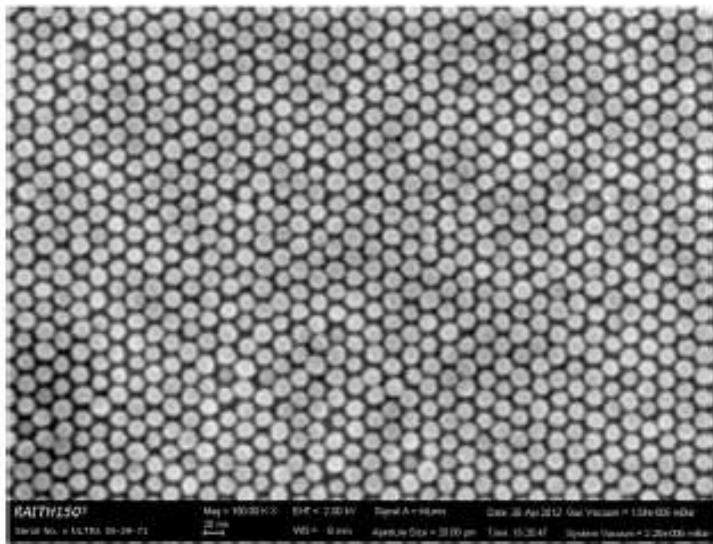


1.5 Tdpsi Media (11 nm hp)

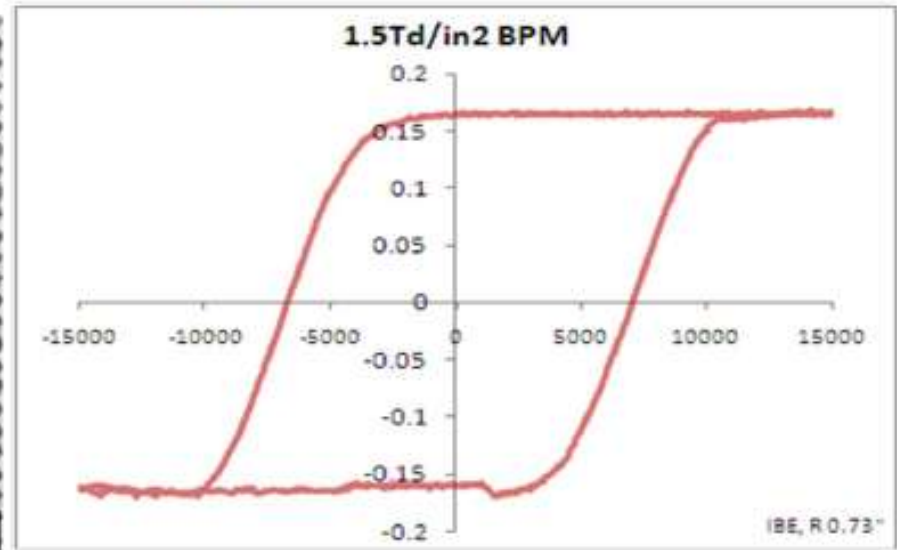
Template (cross-section)



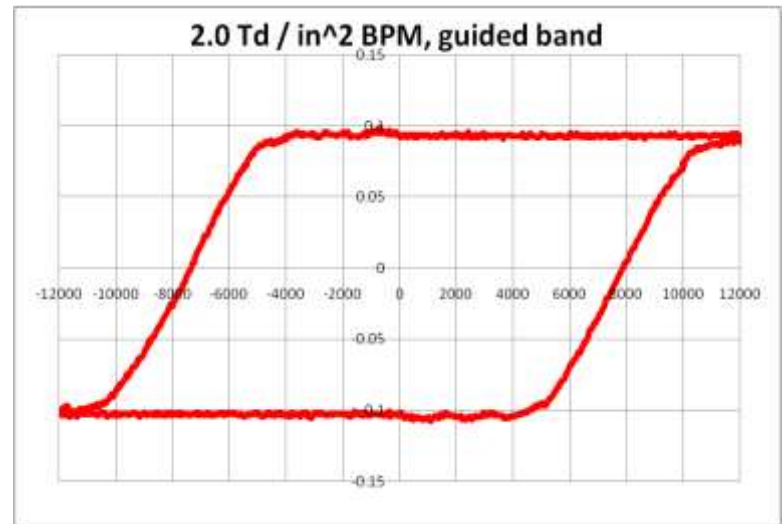
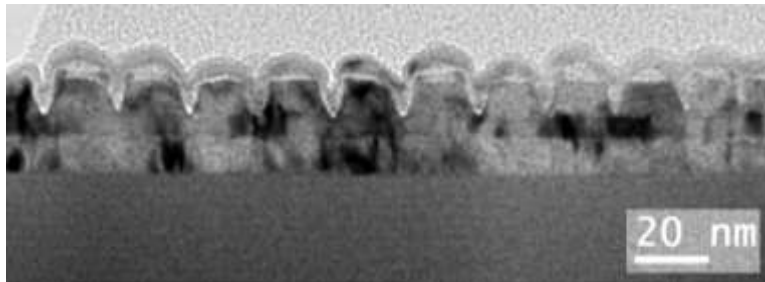
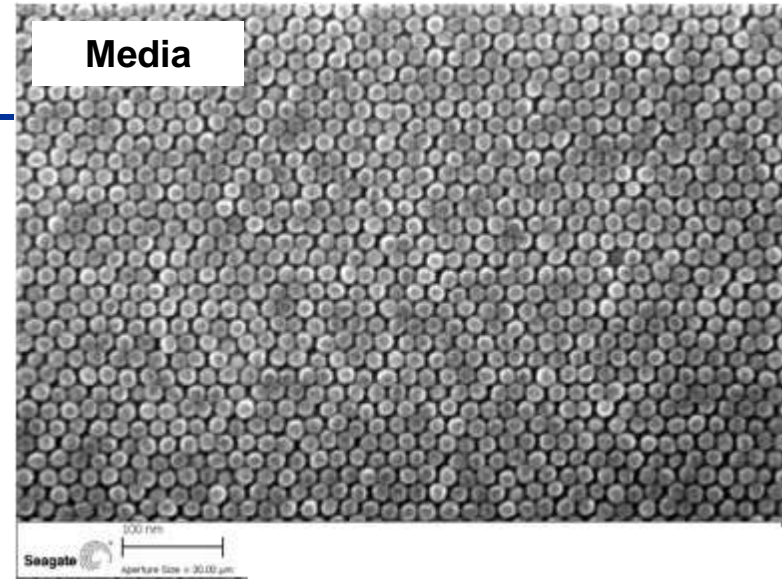
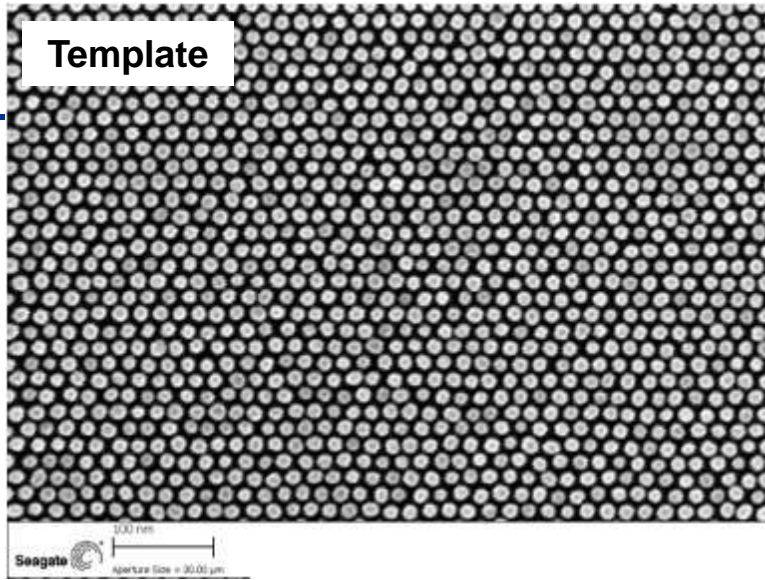
Fabricated Media



Magnetic data



2 Tdpsi Media (9.6 nm hp)



Loc	R (")	Hc Ave	Hn Ave	Is Ave	Ir Ave	KuV /kT	SFD (%)	Int. field
G	0.73	7644	5250	0.10	0.09	92.6	8.0	2041

Summary

-
- **BPM fabrication involves multiple lithography techniques, i.e. e-beam, nanoimprint, DSA, double patterning etc.**
 - **Major challenge in BPM lithography is master template creation, which requires combination of rotary-stage e-beam/DSA/double patterning.**
 - **DSA using block copolymers for BPM application (highest resolution) needs new block copolymer materials, having both high resolution (i.e. extendible to 5-10 Tdpsi or 8-12 nm full pitch) and good pattern transfer capability (i.e. Si-containing).**
 - **HCP systems (i.e. sphere PS-*b*-PDMS) may support BPM technology demo at 2-5 Tdpsi, with innovative skew solutions, while rectangle systems are more appealing in terms of skew.**
 - **As for magnetic island formation, IBE produced good 1T/1.5T/2T BPM media, and ion implantation is also promising.**

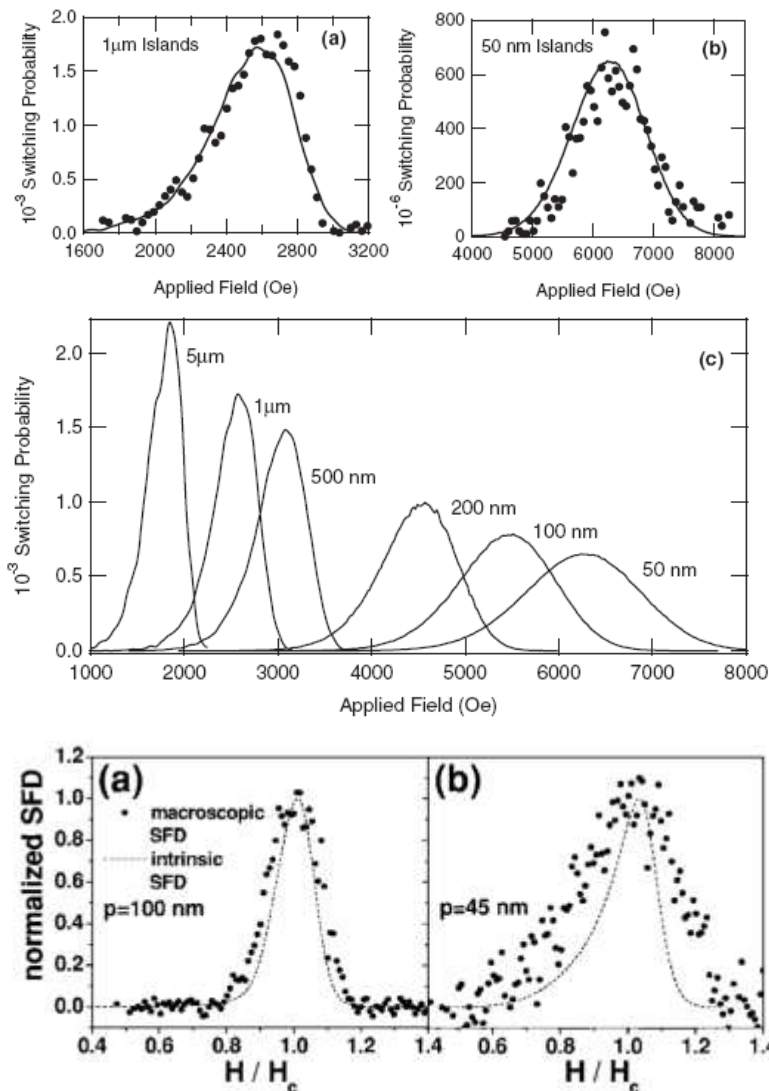
Switching Field Distributions (Literature)

SFD distribution in bit patterned media is size dependent and has various sources¹

- process damage
- magnetic properties
- dipolar fields

In Co/Pd multilayers on pre-patterned substrates the intrinsic and dipolar contributions to SFD have been quantified by comparing SFDs determined from remanent magnetization curves and the $\Delta H(M, DM)$ -method^{2, 3, 4}

Best published results are $\sigma_{K_{int}} = 5-7\%$



¹ T. Thomson et al., Phys. Rev. Lett. 96 (2006) 257204

² O. Hellwig et al., Appl. Phys. Lett. 90 (2007) 162516

³ A. Berger et al., IEEE Trans Mag 41 (2005) p3178

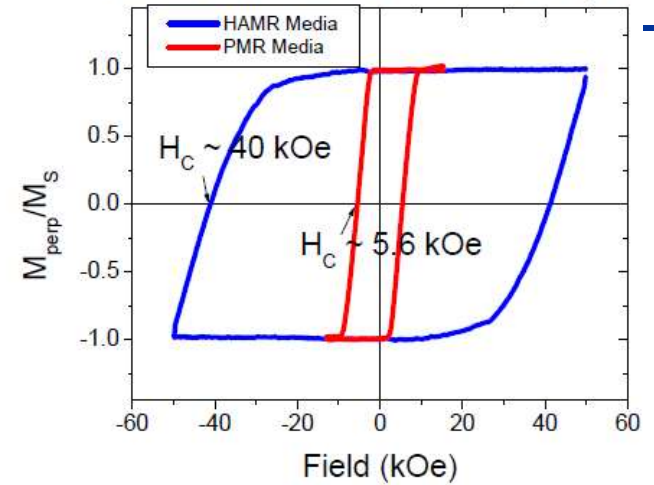
⁴ D. Weller, A Dobin et al., Intermag 2008

Heat Assisted Magnetic Recording



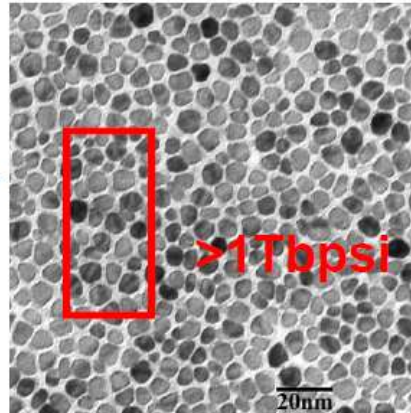
Heat Assisted Magnetic Recording (HAMR)

HAMR vs PMR Media Loops



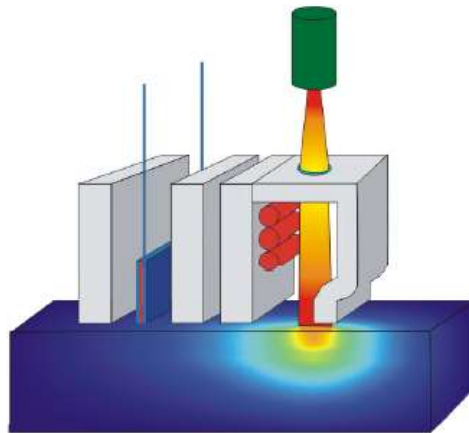
Increase Areal Density

increase density by smaller grains



make smaller grain stable

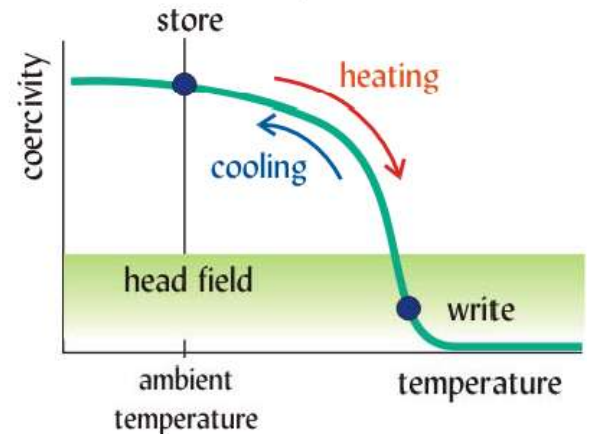
by increasing anisotropy



need localized heat source (<50nm)

integrated head with near field transducer

heat media to write



Heat Assisted Magnetic Recording

• Primary Benefits Demonstrated

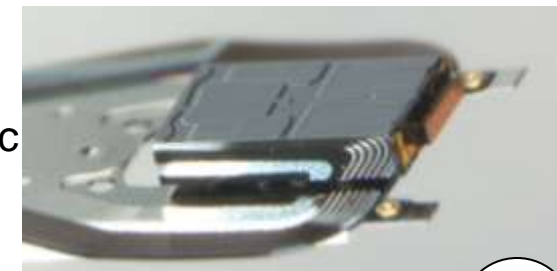
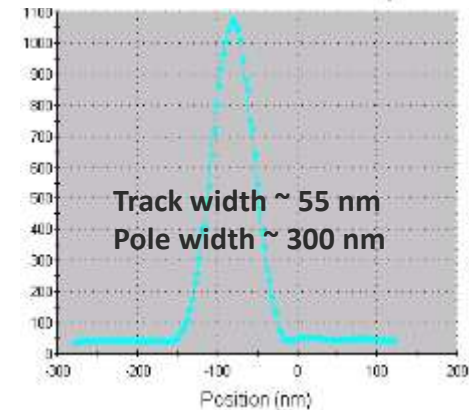
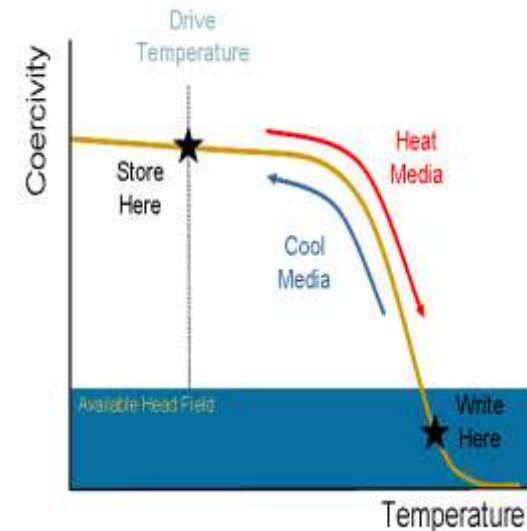
- Ability to fabricate and record on high Hk media (>50kOe)
- Effective write field gradient demonstrated at > 3x perpendicular
- Write width determined by thermal spot not magnetic width

• Recent Highlights

- New FePt media have shown performance benefits with near field transducer heads
- HAMR areal density attainment is greater than 1 Tb/in²
- Integrated HGAs now flowing
- HAMR drives are reading and writing user data

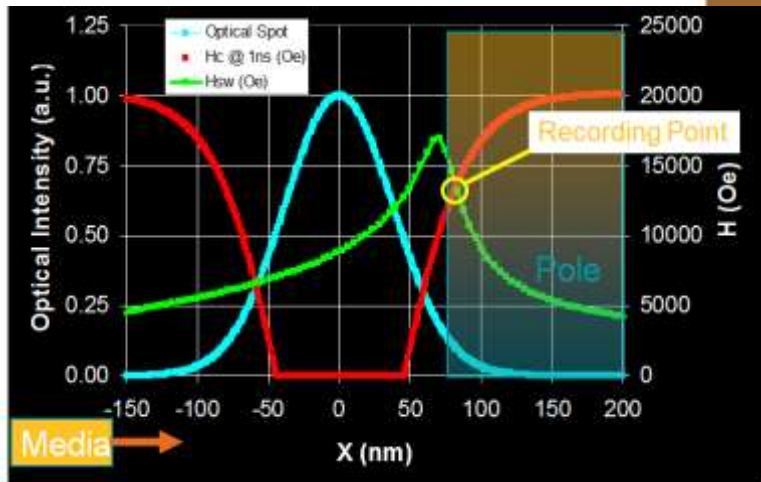
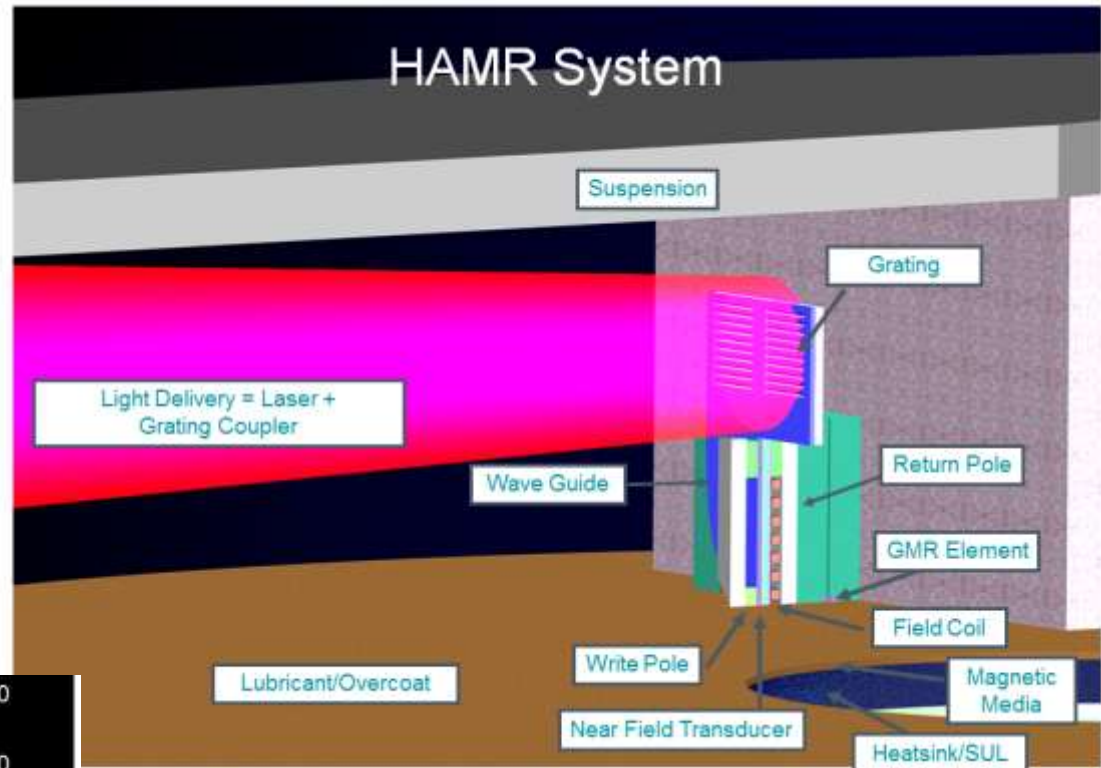
• Challenges

- Reliability with new thermal stresses in head, HDI and laser
- NFT design for AD, reliability and yield in an integrated head
- HMS and accurate clearance setting with thermal induced dynamic protrusion and media roughness



An example of HAMR System

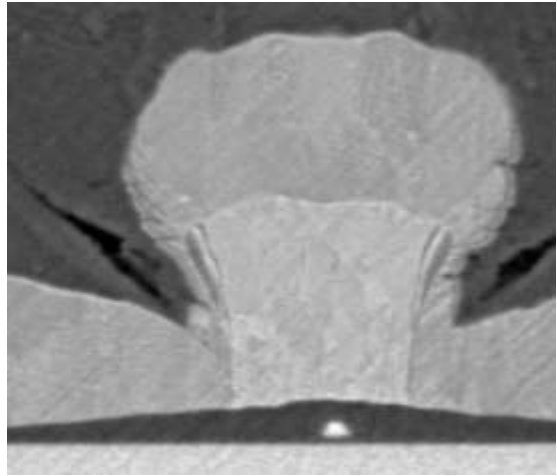
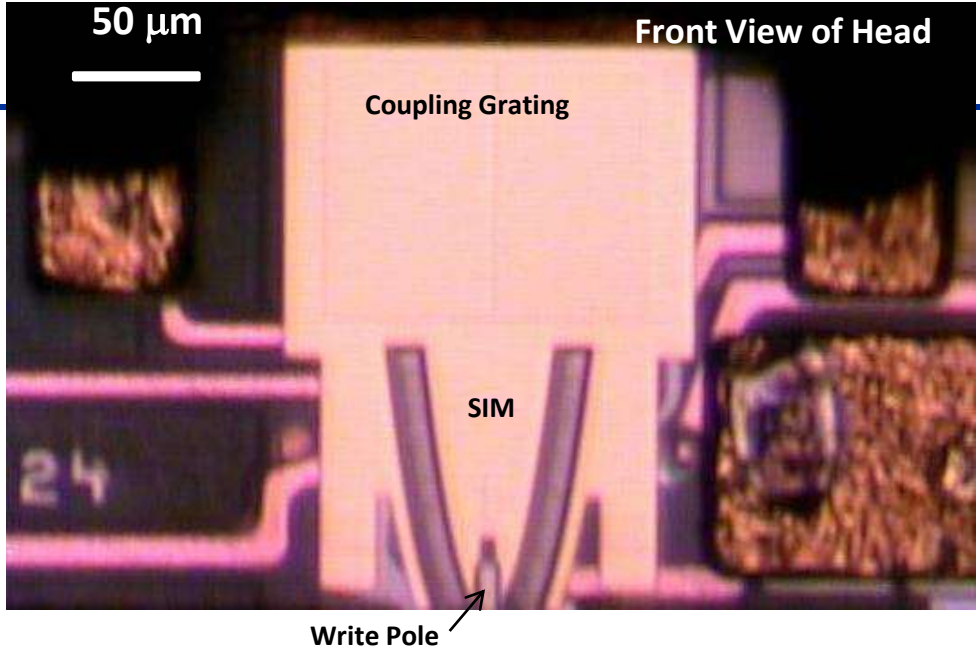
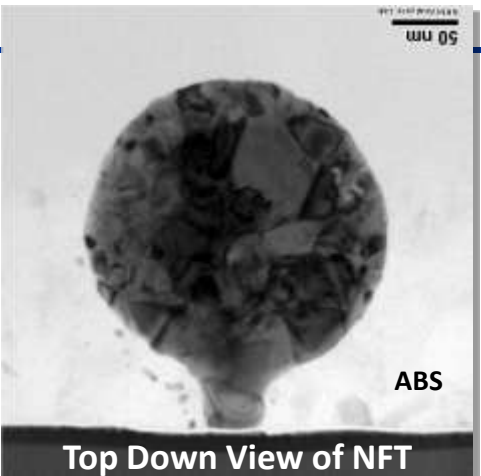
- Pole 75 nm from center of optical spot
- Write gradient (thermal and magnetic field) is not optimum
- Recording point is under the pole => Light Blocked?



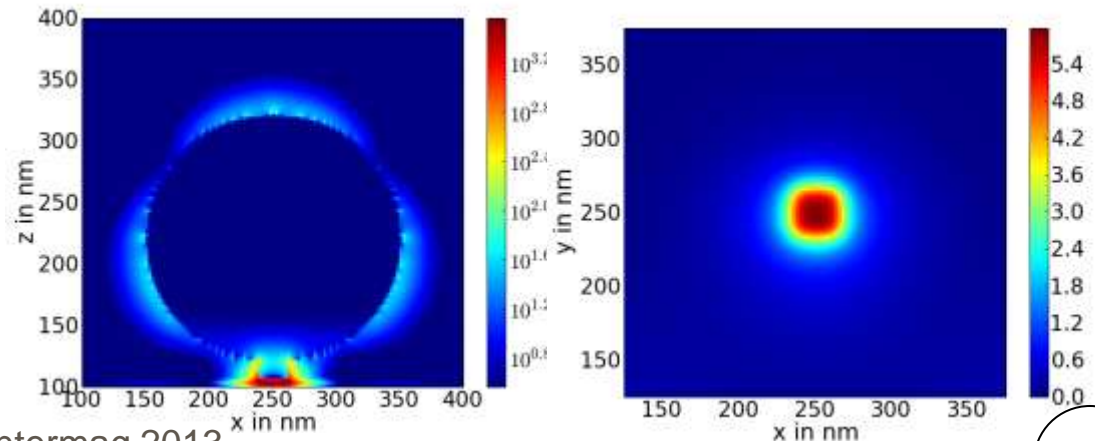
How to optimize recording point:

- Magnetic field (pole position, writer design, write current)
- Thermal spot (optical spot, power, media thermal properties)
- Media magnetic properties (Hc, Curie temperature)

Seagate HAMR Integrated (Writer & Reader) Head with NFT



Modeling showing the plasmonic resonance and confined E field

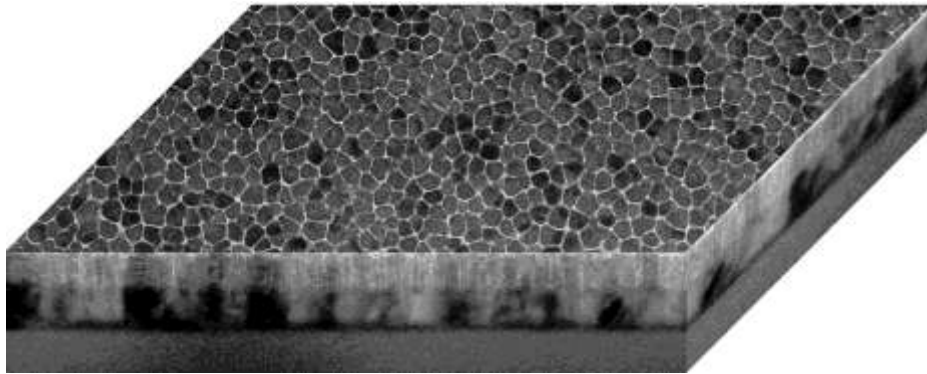


Kaizhong Gao

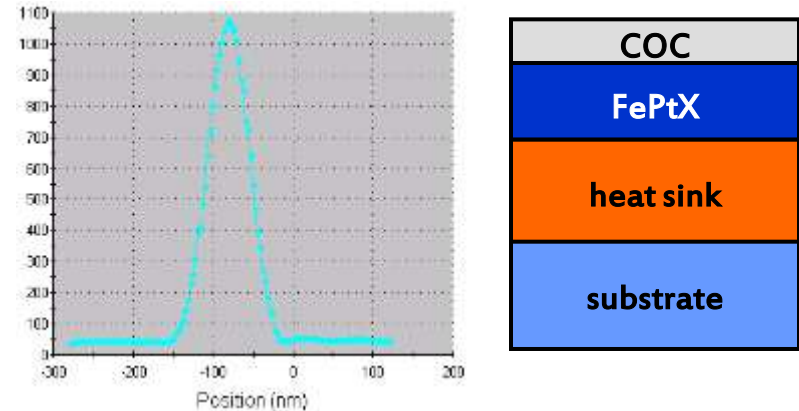
Intermag 2013

HAMR Media Design

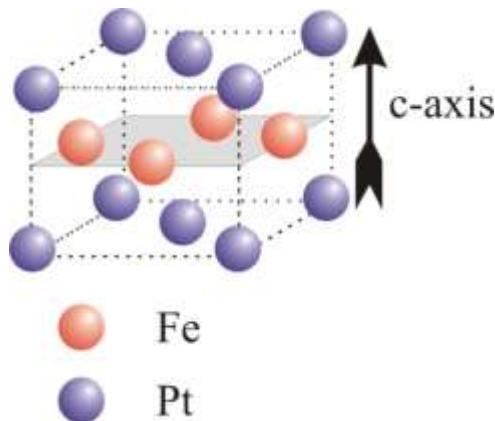
Good Microstructure



Well Defined Thermal Profile



Good Texture and Ordering

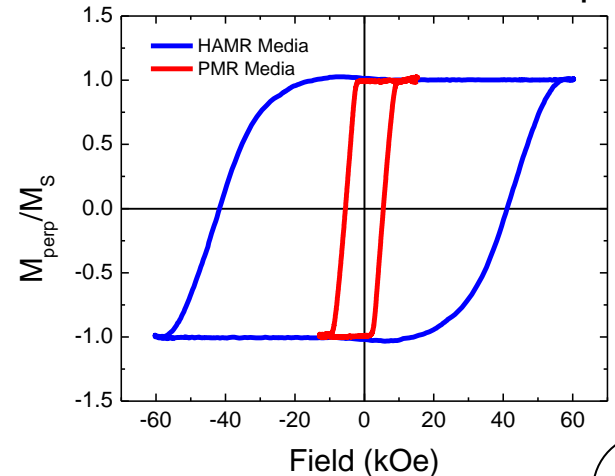


FePt L₁₀ material used for HAMR media offer

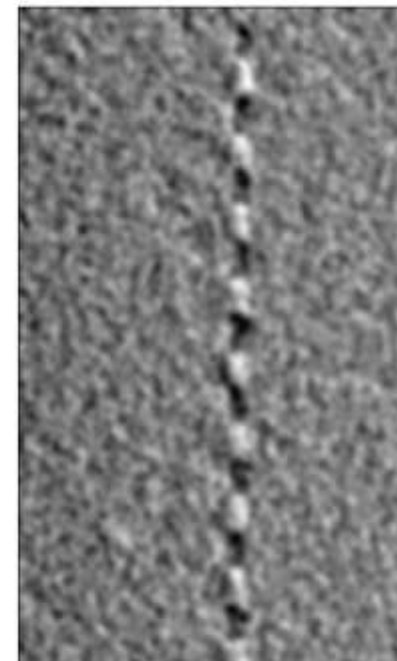
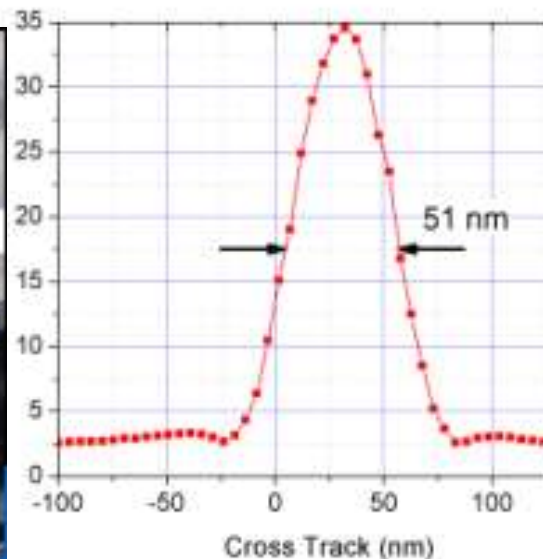
- higher anisotropy
⇒ larger stability
- larger dH_K/dT
- lower T_C than CoCrPt alloys used in PMR

Magnetic Property & Distribution

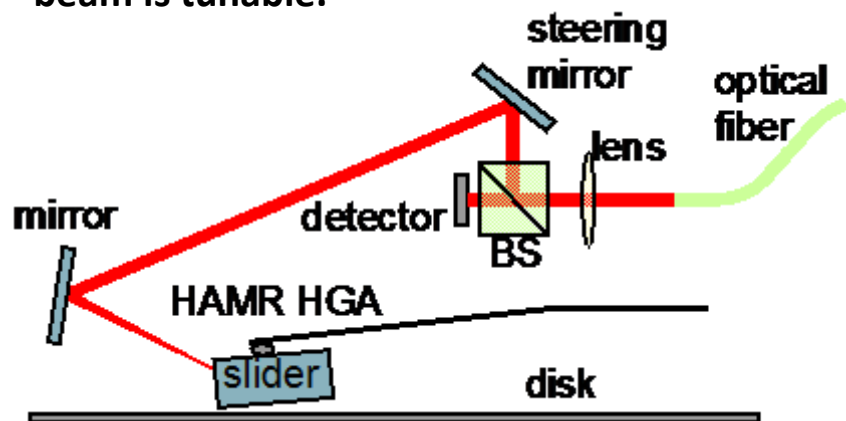
HAMR vs. PMR Media Loops



HAMR Spinstand Tester



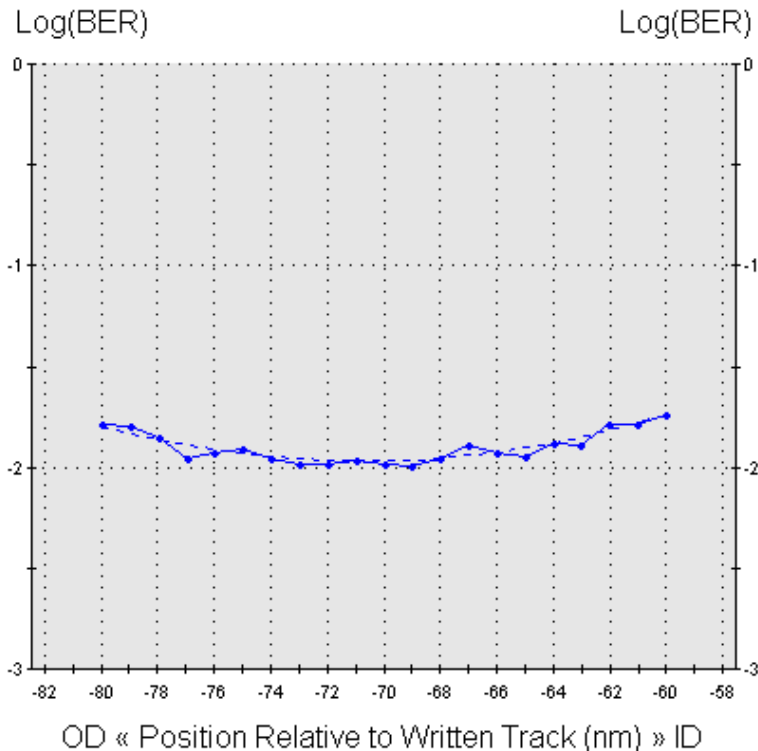
Both incident position and angle of laser beam is tunable.



- ADC: 242 Gbps (15.5 dB ACSNm)
- LD: 706 kBPI (BL: 36 nm)
- TD: 343 kTPI
- HMS: ~ 15 nm

W. Challener *et al*, Nature Photonics 3, 220 - 224 (2009)

Seagate HAMR Demo: 1.007 Tbps (1975 kBPI x 510 kTPI)



OTC = 0 nm
RWD = -70.72 nm
Log(BER) = -1.99
Squeeze = 0 %TP
OTC Threshold = -2
Curve Fit = Quadratic

LD = 1975.0 KBPI
TD = 510.0 KTPI
AD = 1007.3 Gb/in²

Data Rate = 833.9 Mb/s
RPM = 4200; Sectors = 16
Radius = 24.384 mm; Skew = 0.00°
TD = 510.0 KTPI; TP = 49.8 nm
Iw = 61.0 mA bp; Bias = 0.350 mA
Code: SID formatted

Key Milestone: High BPI and TPI

Kaizhong Gao

Intermag 2013

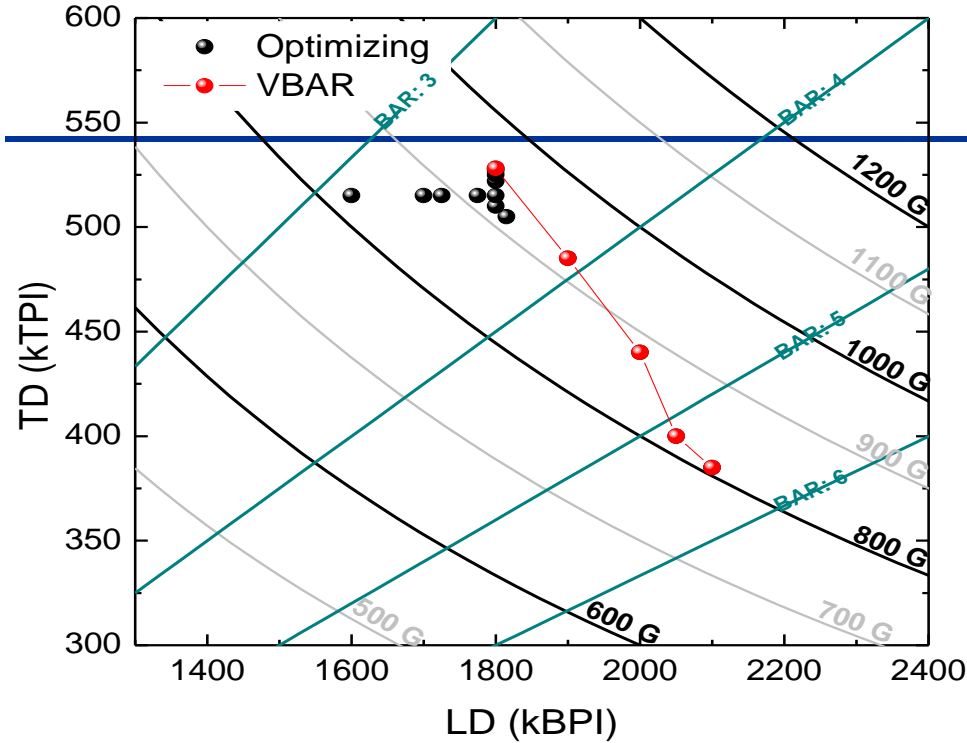
Demo Criteria

- Adjacent tracks written both sides with same conditions as data track
- On-track BER = $10^{-2.0}$ with no correction/iterations

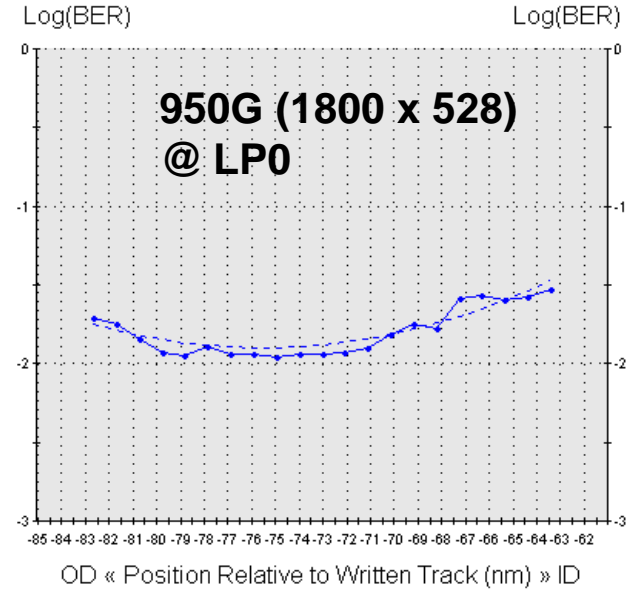
Procedure:

1. Write data track and then SQZ tracks (1 write/side) at a given TP
2. Measure bathtub, record minimum raw BER of bathtub
3. Reduce TP until the BER of data track reaches -2.0
4. Record AD at this TP and this linear density
5. Repeat 1 through 4 for various linear densities and report the highest AD combination and the corresponding linear and track densities.

Laser Power Dependence of VBAR



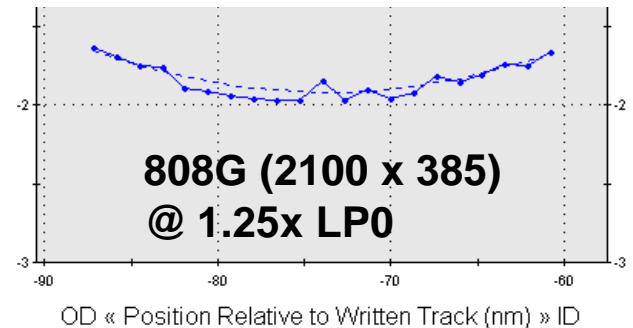
- Optimizing from 824 to 950Gbps.
- VBAR: dominant tuning parameter is Laser Power.
- 1st time to achieve 2100 kBPI @ 808Gbps in HAMR.
- Results are from another head (NOT from the 1Tbps demo head).



OTC = 0 nm
 RWO = -75.55 nm
 Log(BER) = -1.96
 Squeeze = 0 %TP
 OTC Threshold = -2
 Curve Fit = Quadratic

LD = 1800.0 KBPI
 TD = 528.0 KTPI
 AD = 950.4 Gb/ir²

Data Rate = 760.0 Mb/s
 RPM = 4200; Sectors = 16
 Radius = 24.384 mm; Skew = 0.00°
 TD = 528.0 KTPI; TP = 48.1 nm
 Iw = 61.0 mA bp; Bias = 0.320 mA
 Code: SID formatted



OTC = 0 nm
 RWO = -73.74 nm
 Log(BER) = -1.97
 Squeeze = 0 %TP
 OTC Threshold = -2
 Curve Fit = Quadratic

LD = 2099.9 KBPI
 TD = 385.0 KTPI
 AD = 808.5 Gb/ir²

Data Rate = 886.7 Mb/s
 RPM = 4200; Sectors = 16
 Radius = 24.384 mm; Skew = 0.00°
 TD = 385.0 KTPI; TP = 66.0 nm
 Iw = 64.0 mA bp; Bias = 0.100 mA
 Code: SID formatted

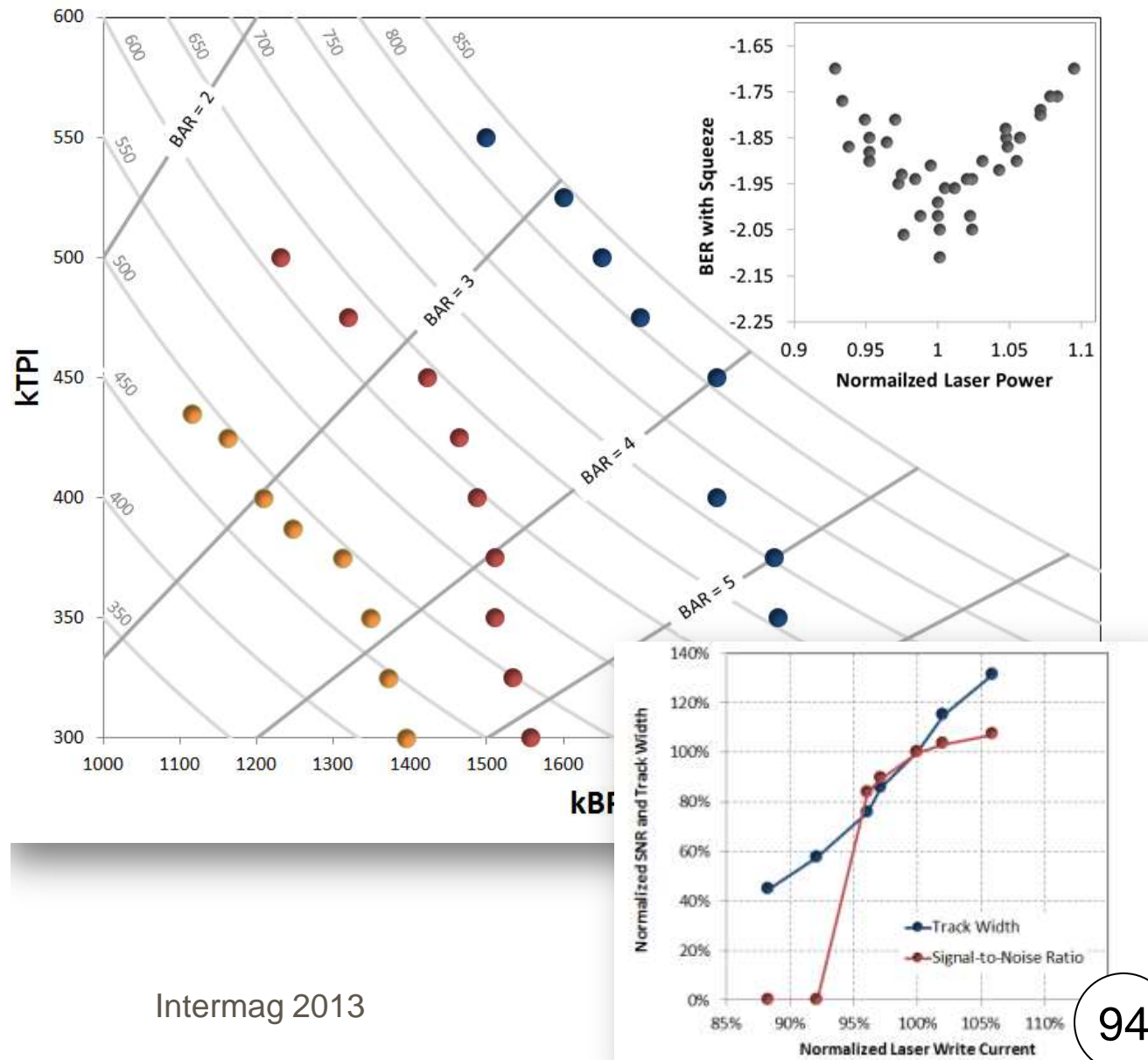
Areal Density Optimization

This plot shows three different heads (red, blue and orange) with varying degrees of areal density capability

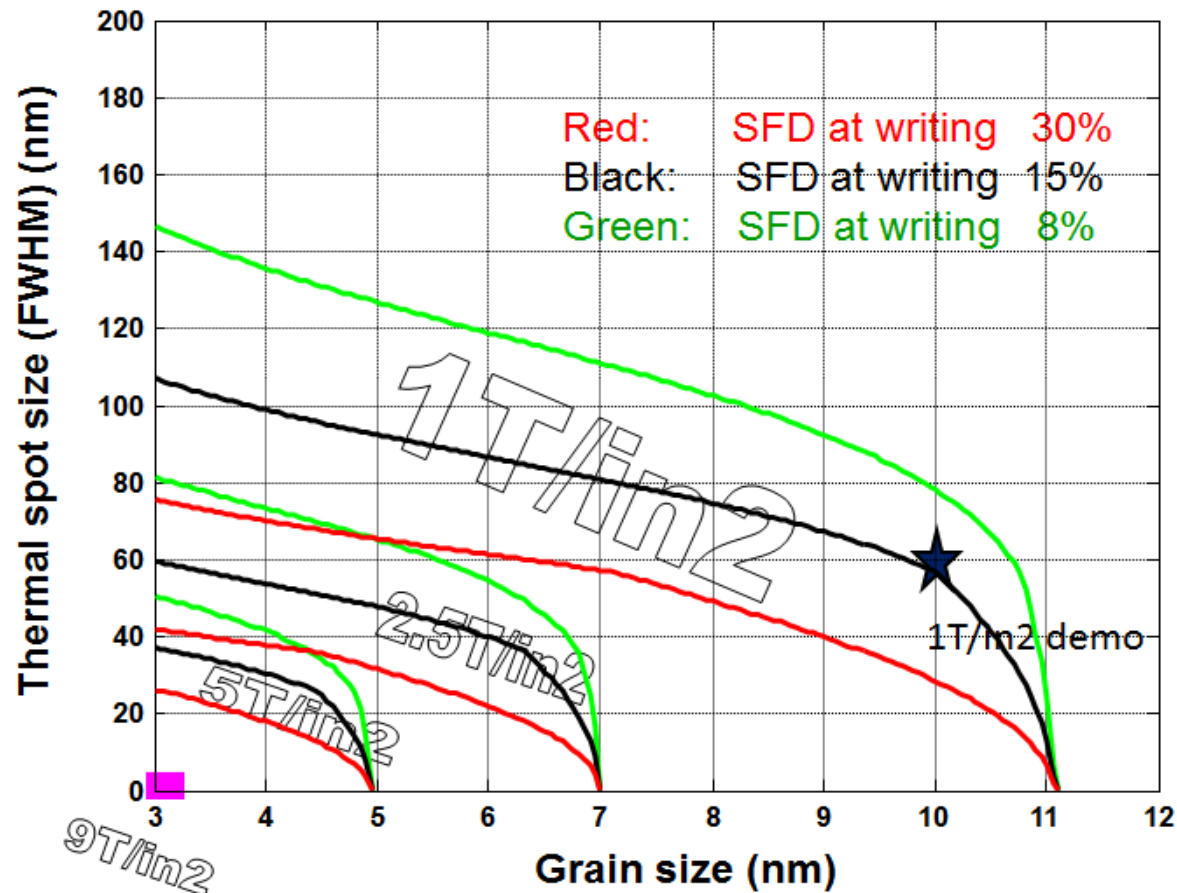
Each point used the same demo criteria, i.e. On-track BER = -2 with two adjacent tracks with 0% squeeze

By changing the laser power and re-optimizing the remaining parameters, the same head is capable of multiple areal densities

Once the system has been optimized for a particular laser power, the inset of the plot shows the sensitivity of BER to laser power. If the laser power is reduced the on-track BER drops due to a loss in SNR. If the laser power is increased, the adjacent tracks begin to erase the data



HAMR Scaling and Technology Requirement Charts



Jitter over bit length is 16%,
 Magnetization stability energy over thermal energy is above 80,
 Recording bit aspect ratio is 5,
 Read width is 60% of track width.

The smallest grain size 3nm on the figure is determined by the assumption of a maximum achievable anisotropy value

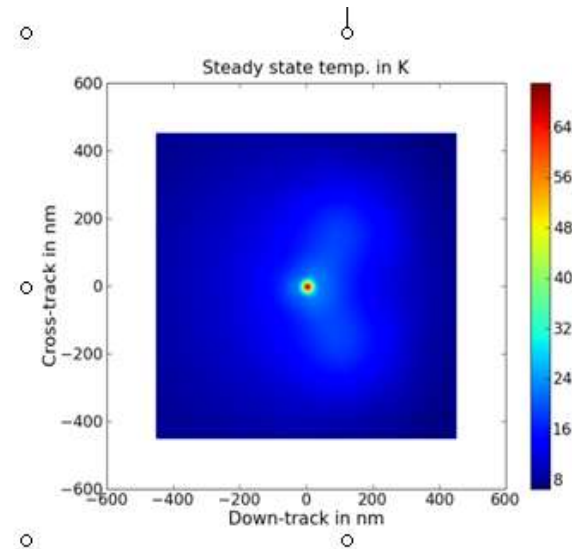
$$K = 0.7 \cdot 10^8 \text{ erg / cm}$$

Combined NFT/Thermal/Micro-magnetic Simulation of HAMR 2.9T/in² Demo

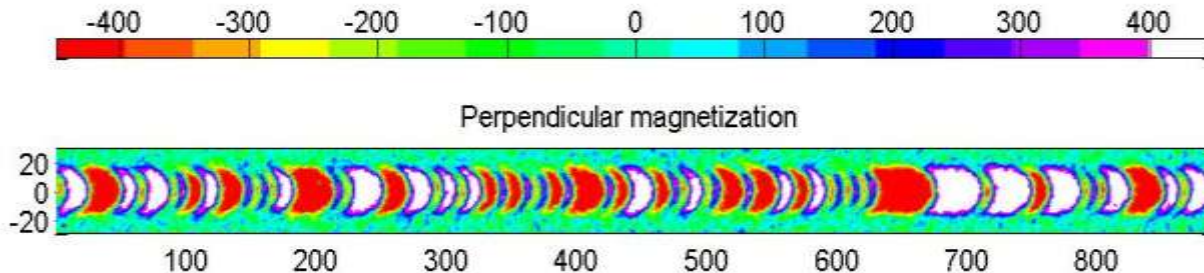
Combined optical, thermal and micro-magnetic simulation for 2.9T/in²

Media

T_c	675 K	$\sigma_{H_{ex}}/ H_{ex} $	0.05
M_s (300K)	450 emu/cc	Packing fraction	1 (ratio)
H_k (300K)	90 kOe	Vol_sigma	0.15 (ratio)
$\sigma_{H_k}/ H_k $	0.05	Tc_sigma	0.01
k_{ang}	1 degree	$\langle d_g \rangle$	4nm
$\langle H_{ex} \rangle$	10 kOe	Speed	14.4 m/s
HMSw	7.5nm	t_{media}	10 nm
SUL	10	KFCI	variable



peg width = 10 nm, peg thickness = 10 nm HMS = 7.5 nm
FWHM_DT=36.2nm, FWHM_CT=35.8nm

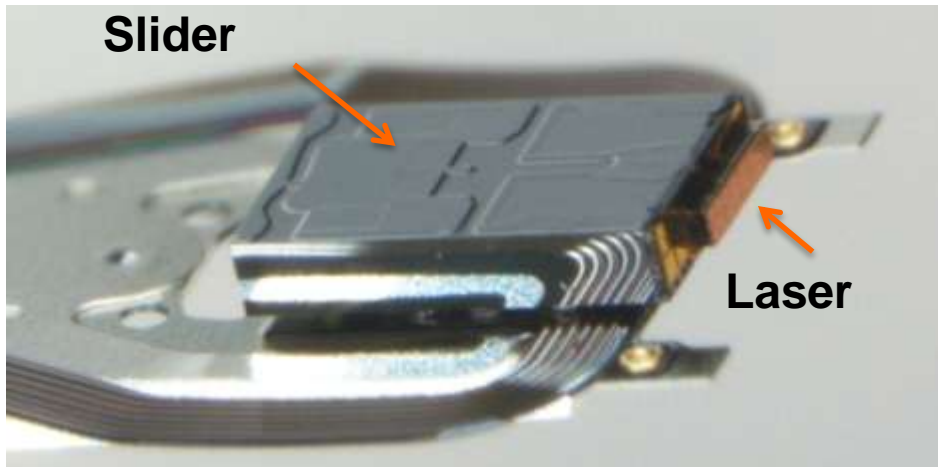


4000 kfc
track width 35nm
2.9Tpsi

A HAMR Drive

To the right is a photo of an actual HAMR drive. You can tell it is a HAMR drive because it has the laser warning sticker stuck on the front

Below is a picture of an integrated HAMR head including the laser (not the same head used in the drive)



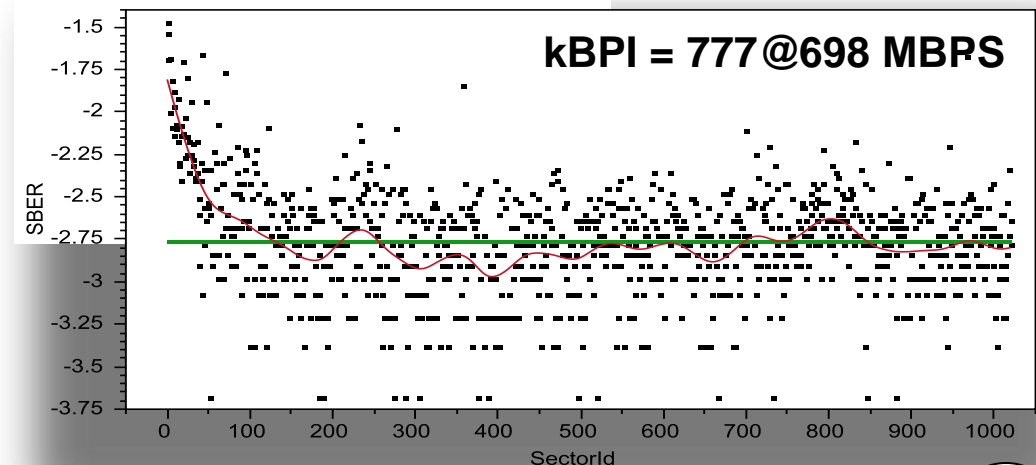
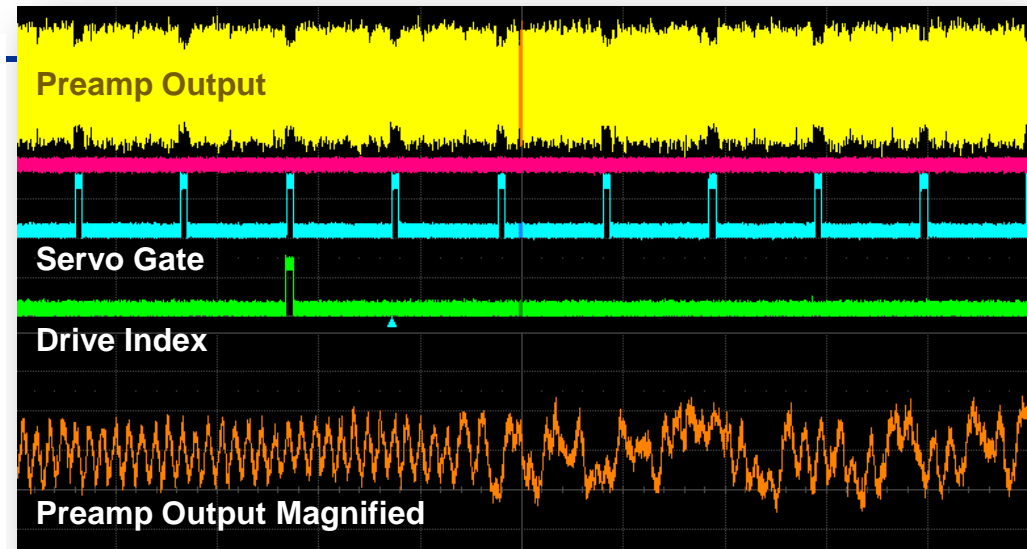
Scope Capture of HAMR Drive Data

This top figure is a scope capture from a fully functional HAMR drive after writing a full revolution of continuous sectors

The yellow trace shows the signal from the head which has been magnified. The sector preamble and sync mark are clearly visible in the magnified trace

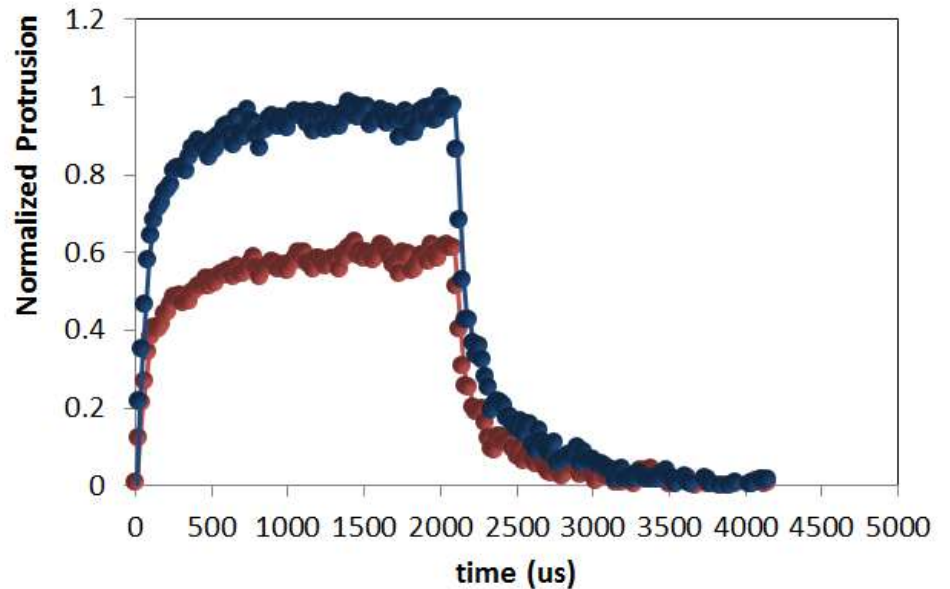
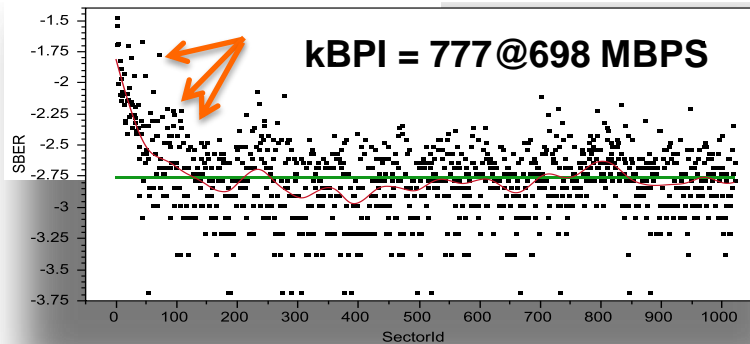
The other two traces are the servo gate and drive index

The figure on the bottom shows the sector raw BER for 1011 continuous sectors.

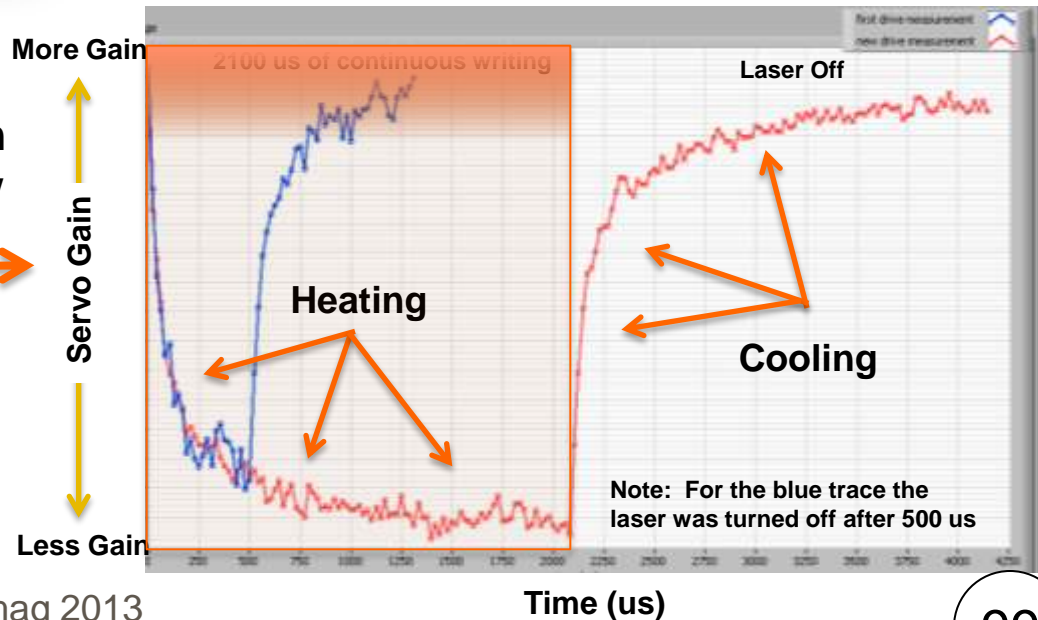
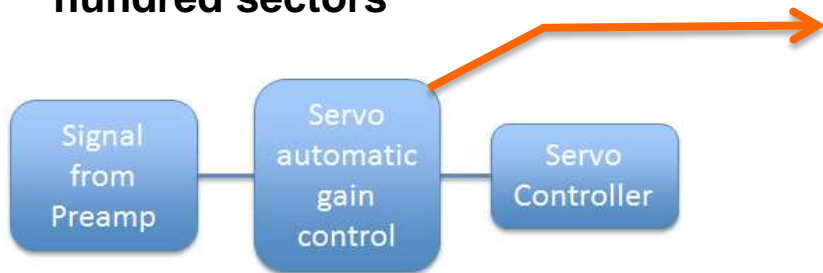


Full Track BER

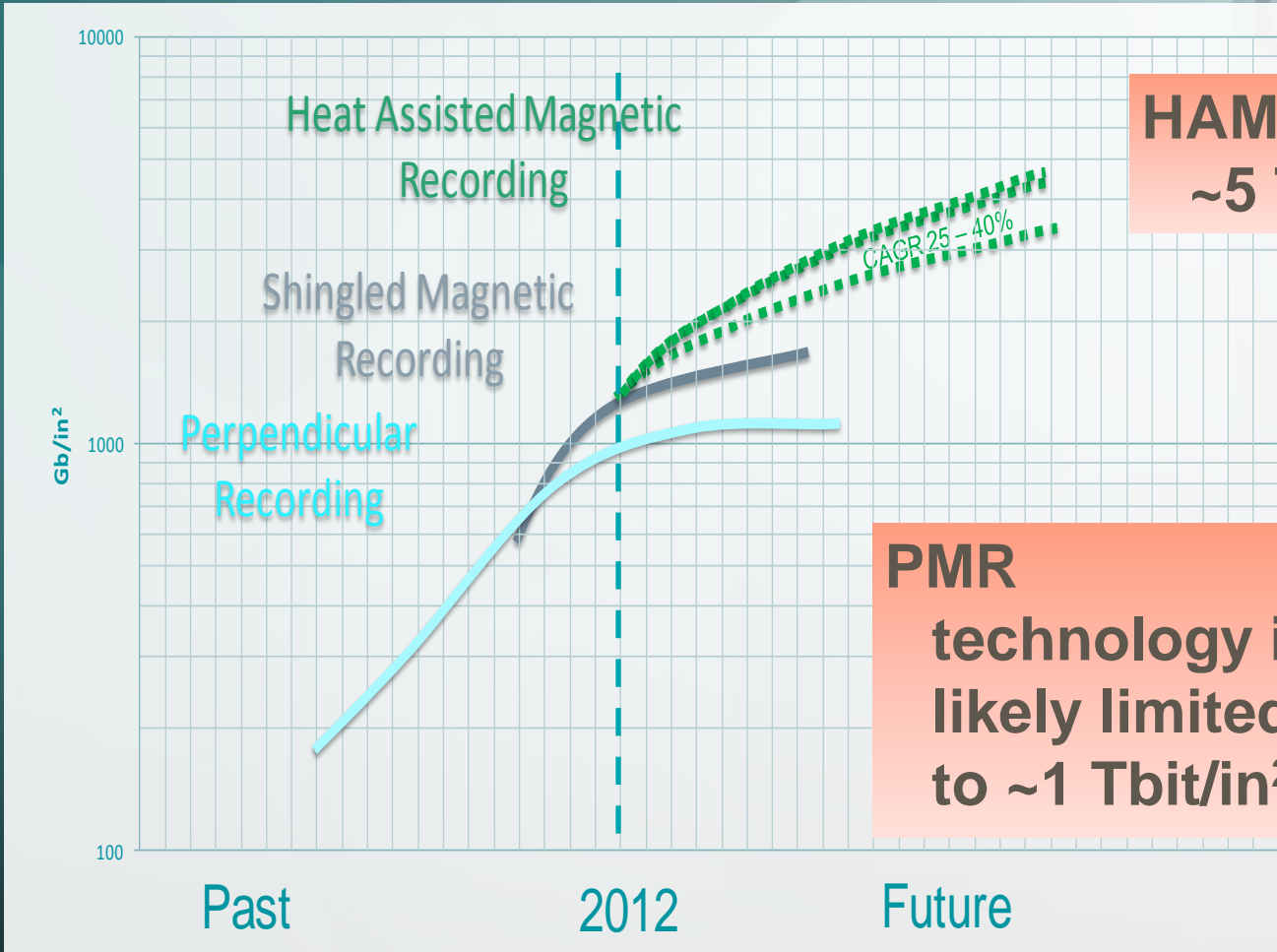
It takes 50 sectors for the BER to reach equilibrium.



The heads reach thermal equilibrium after ~1000us which is roughly a few hundred sectors



Areal Density Demonstrations



**HAMR to push to
~5 Tbit/in²**

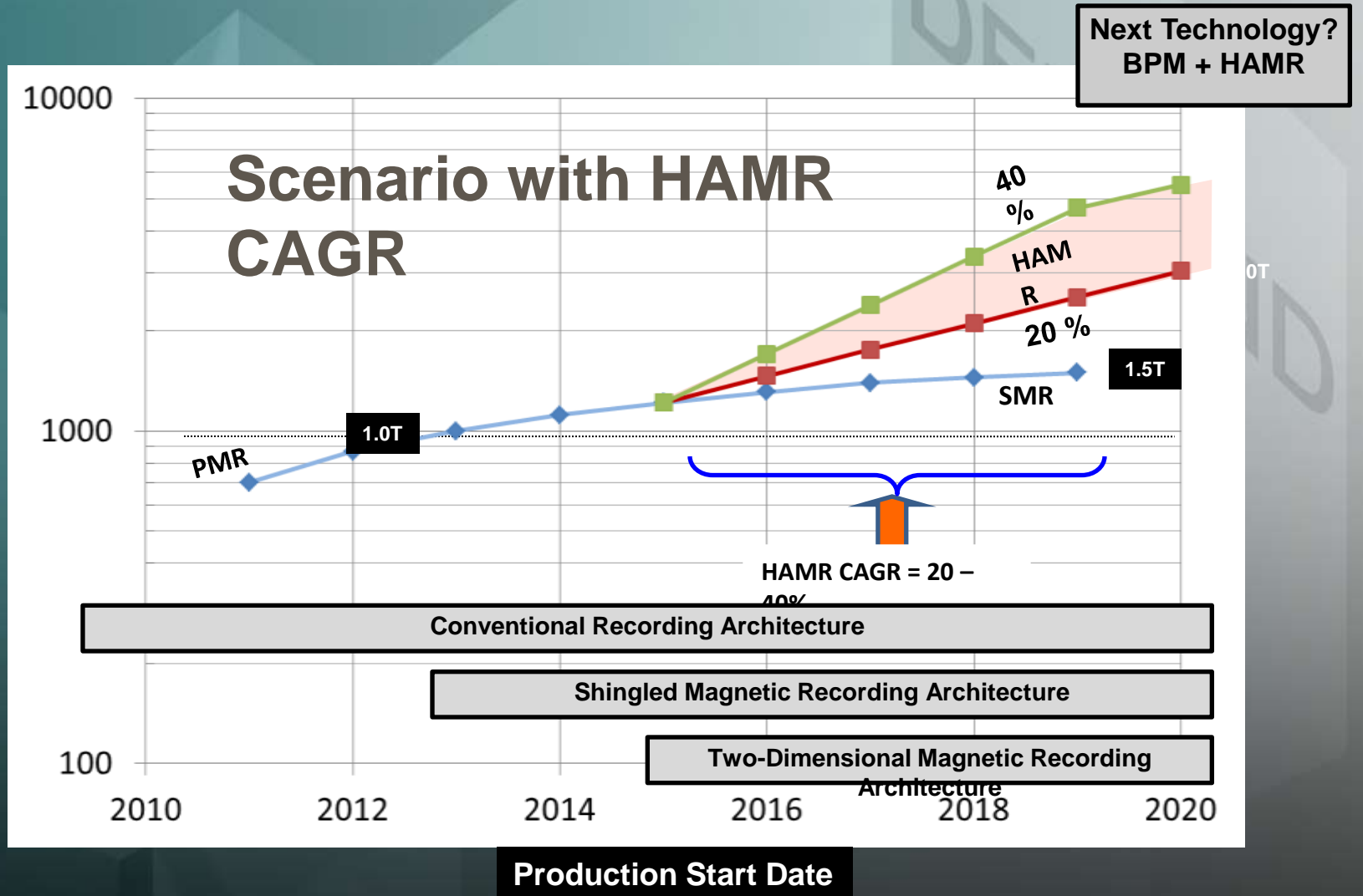
**PMR
technology is
likely limited
to ~1 Tbit/in²**

Technology transitions PMR => SMR => HAMR

Assumptions

- **PMR areal density growth rate is slowing to < 10% CAGR**
- **SMR will increase areal density by ~ 40%**
- **SMR and TDMR architectures will be used to increase capacity in selected markets**
- **Channel gains will continue at 3% CAGR**
- **HAMR production starts in 2015 with a 20 – 40% CAGR**
- **At current investment levels/technology progress, we can not put MAMR or BPM on the product roadmap before 2020.**
- **As HAMR approaches its limit, ~ 5 Tbps, or if HAMR progress is delayed, alternative technology activities will be increased.**
- **Technology investments will be committed to ensure continued drive capacity growth.**

Areal Density Growth Roadmap



Early Stage HAMR Challenges (10 Years Work)

- Optical confinement required development of plasmonic near field transducer to provide needed spot size (sub-50nm).
- FePt media as a new recording layer require significant development effort.
- Perpendicular recording set a moving target and extend areal density of HDD at rapid speed beyond longitudinal recording.

Current Challenges (within next few years)

➤ Media Distributions*

- Distributions much larger than PMR
- Benefit of large effective gradient in HAMR

➤ Electronic Noise

- Lower Mrt and high HMS

➤ Reliability*

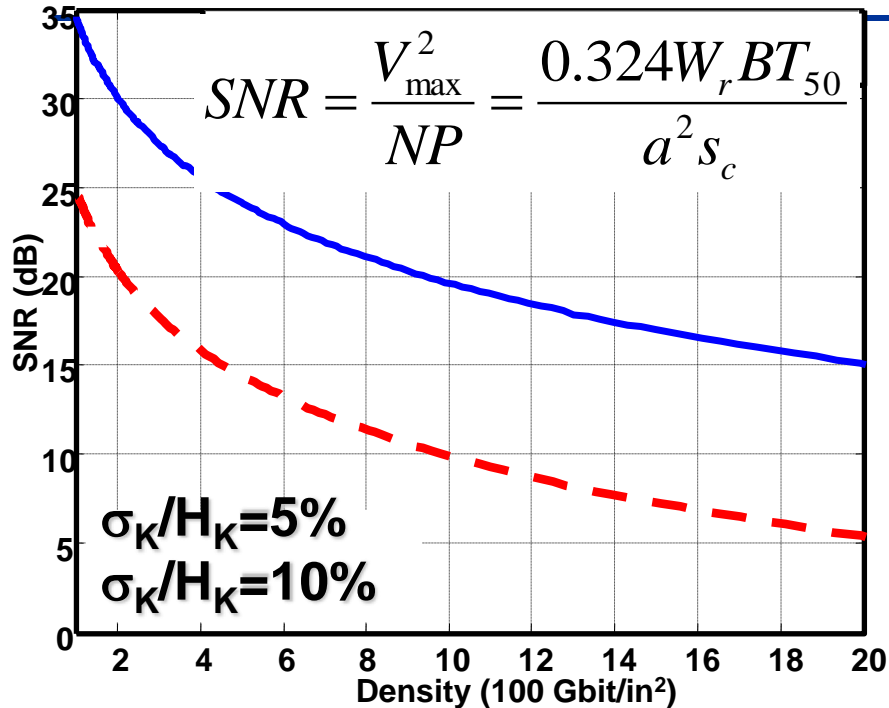
- Head, media, HDI due to thermal stress

➤ Head Media Spacing

- Larger than the current PMR
- Media roughness, coating thickness, thermo-mechanical
- Clearance management

➤ Efficient light delivery path has added complexity as compare to perpendicular recording

HAMR Recording, Impact of SFD



- Movie for compare to 10% vs. 30% H_K distribution taken out.

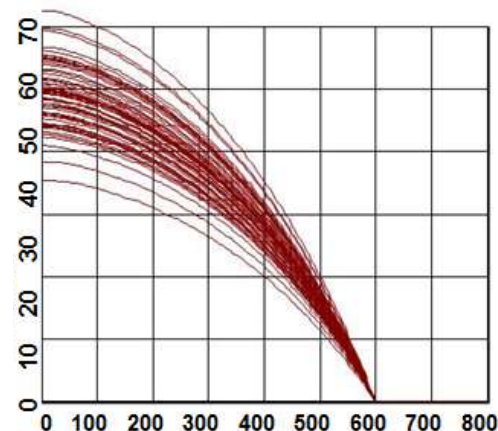
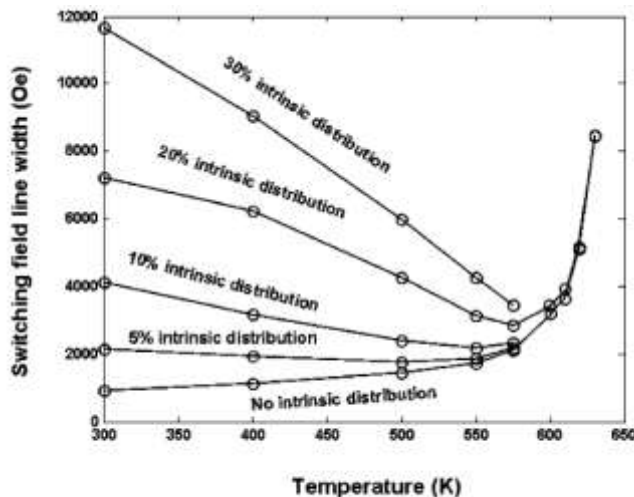
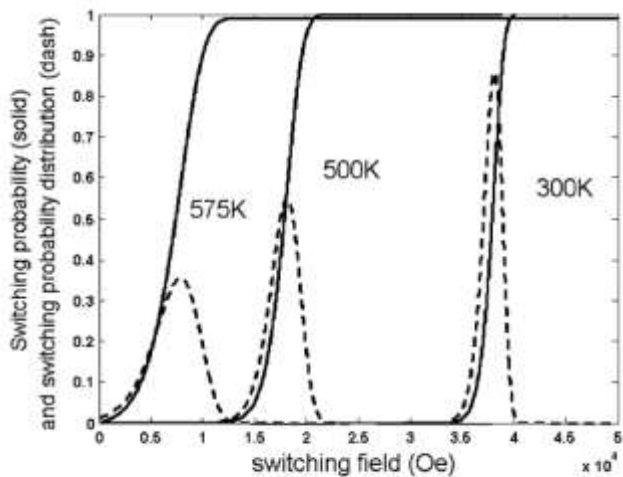
$$\frac{\sigma H_K}{H_K} = 10\% \text{ vs. } (\sigma H_K)/H_K = 30\%$$

Conventional perpendicular recording will have significant challenge as it approach 1Tb/in², the primary limiting factors is due to SFD, instead of SF (writeability).

HAMR still requires low SFD media

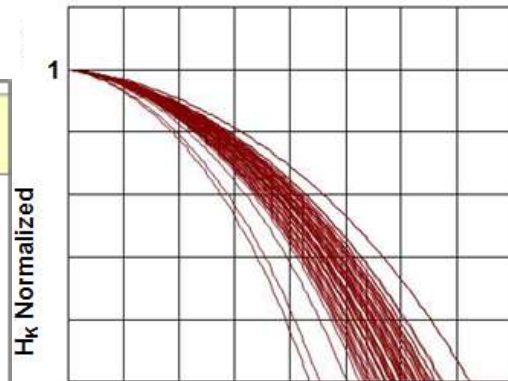
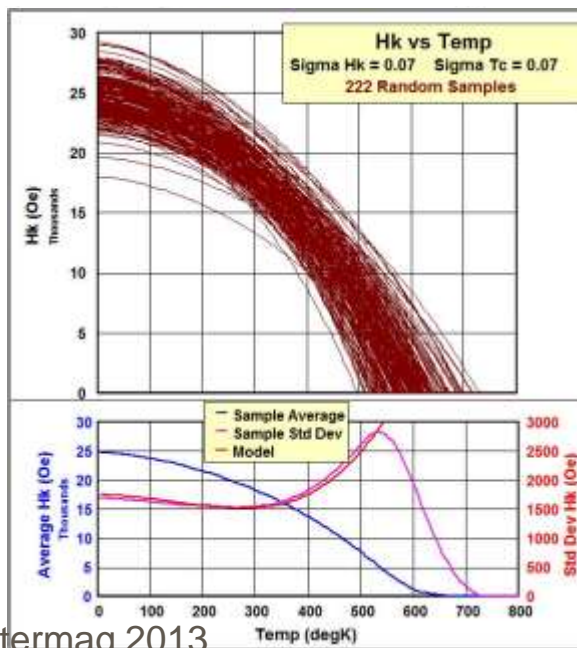
K. Z. Gao and H. N. Bertram, "Transition Jitter ...", IEEE Trans. Magn. vol. 39, no 2, p.704-9, 2003.

Switching Field Distribution at Elevated Temperature



Switching field distribution broadening at elevated temperature

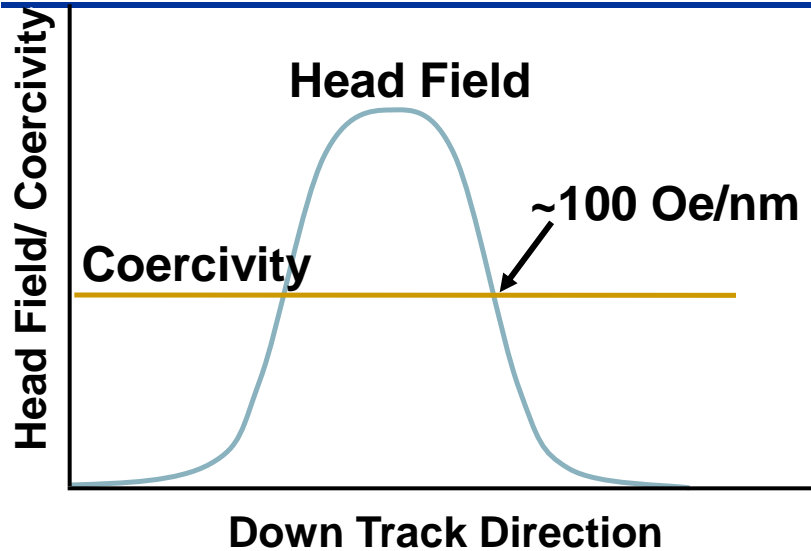
HAMR has additional SFD contributing factors during recording



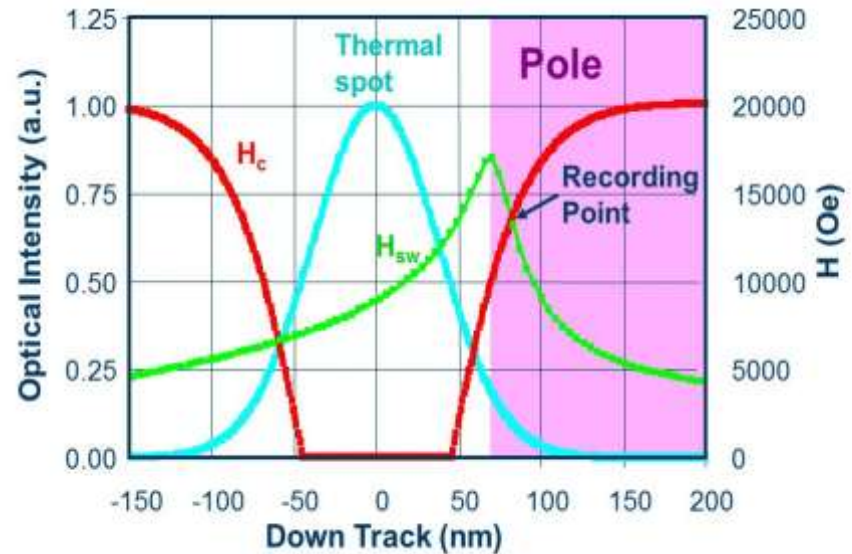
Impact of H_k and T_c distribution

HAMR benefit: ultra sharp write gradient

Traditional Recording



HAMR Recording



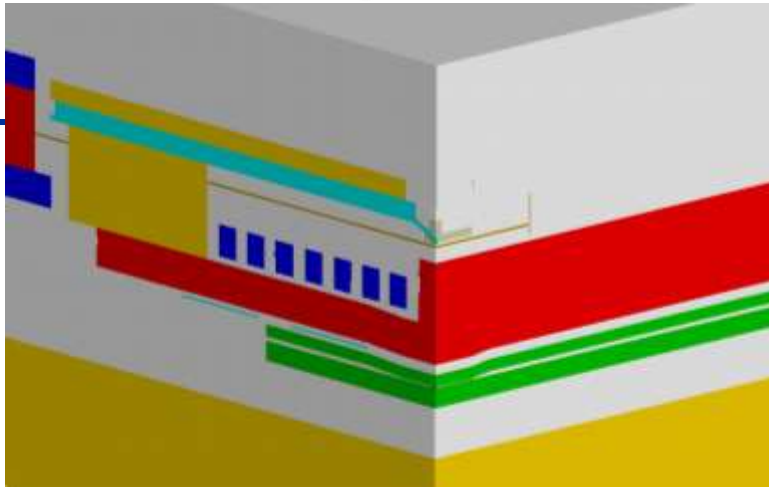
$$\text{write gradient} = \frac{dH_x}{dx}$$

$$\text{write gradient} = \frac{dH_x}{dx} - \frac{dH_x}{dT} \frac{dT}{dx}$$

Large effective write field gradients are advantageous in both cross track and down track directions.

Rausch et al., *IEEE Trans. Magn.* 40 (2004) 137

HAMR Reliability



Managing temperatures in the transducer is key.

- The media must reach its cure temp. 700-800K within 100's of ps.
- Experimental stress tests and modeling indicate that the transducer rapidly degrades at > 500K.

The optical resonant coupling enables temp. rise in the media to be 3X> temp. rise in head.

However the extreme localization of the heating source can still lead to localized protrusions that need to be managed.

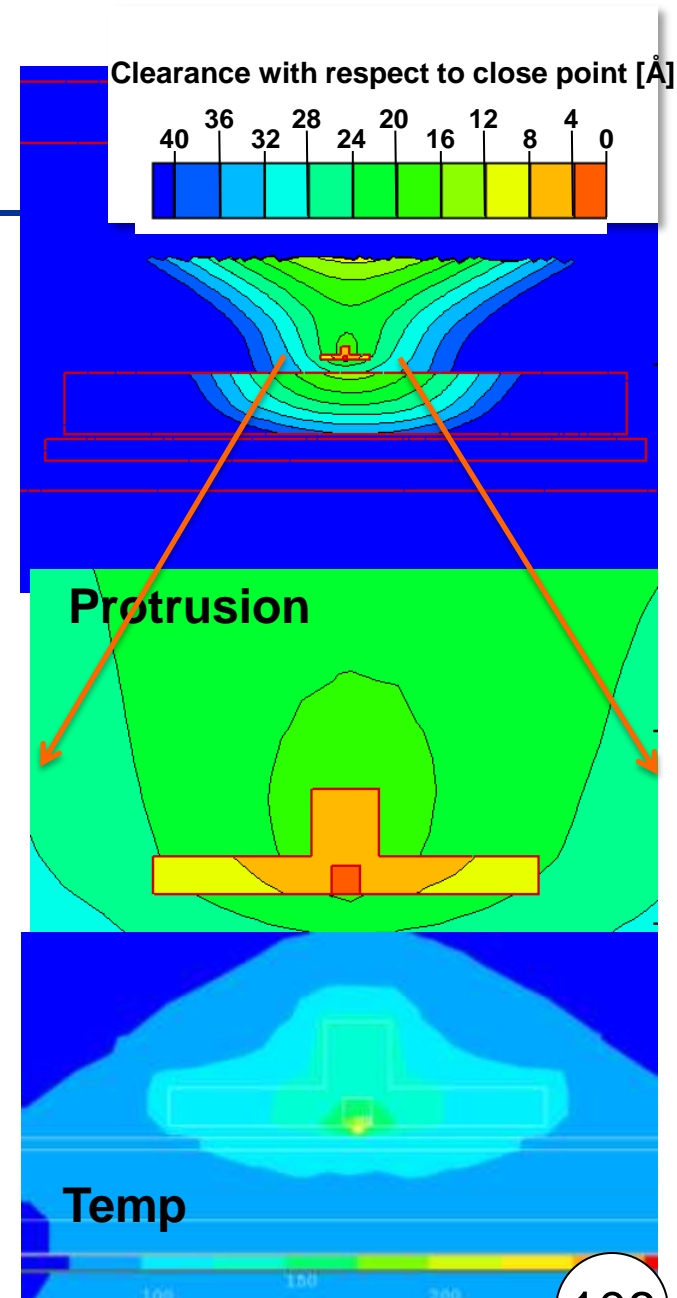
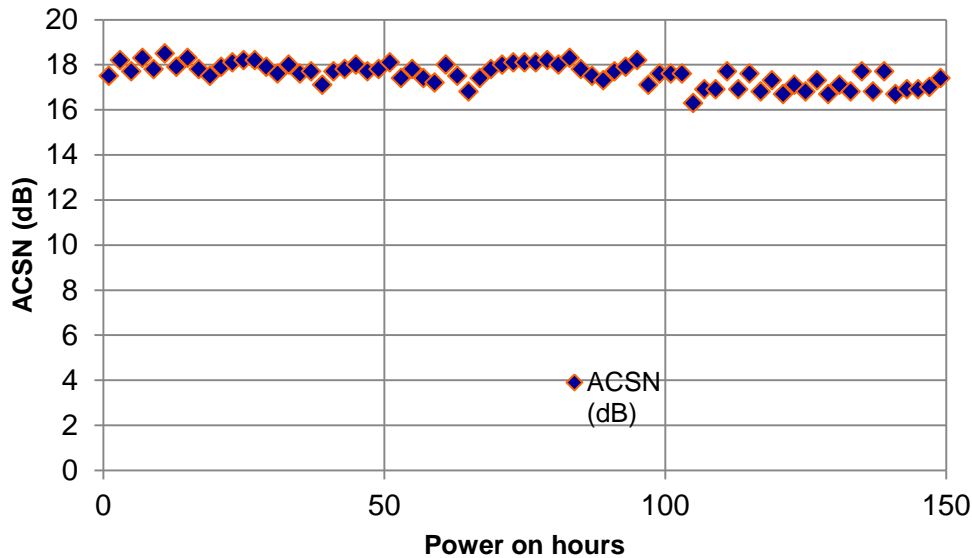


Illustration of at least 150 hours continuous writing.

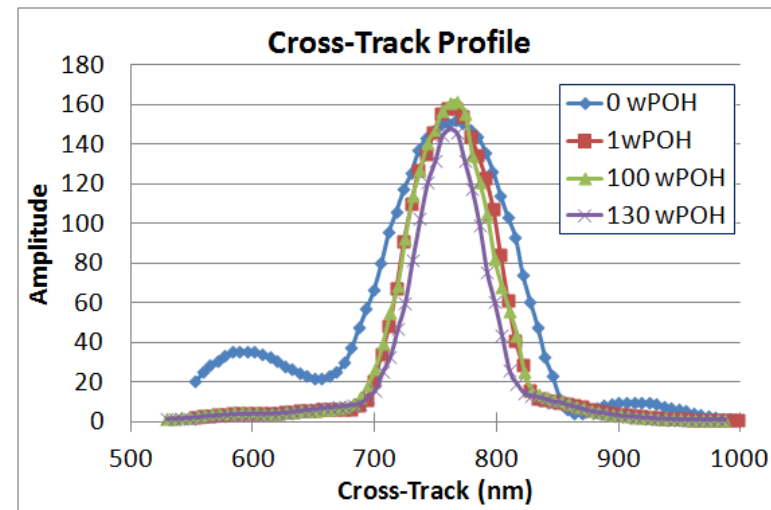
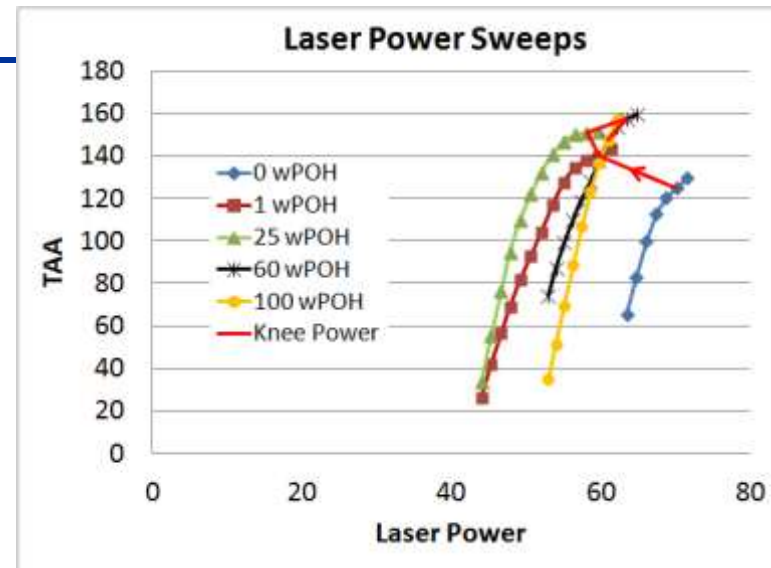
Reference SNR after power on writing



Spinstand measurements:

Optimal laser power initially drops after first hour of test, track confinement improves, and stabilizes.

Head failed beyond 150 hours.



Summary...

- PMR has replaced LMR within the past decade:
 - Due to significant reduction of media (SFD) and improved writeability, field gradient
 - After 5X areal density gain conventional PMR areal density slows down
- HAMR have been demonstrated at both spin stand level and in drive
 - After HAMR demo catches PMR in terms of areal density, HDD industry now working on HAMR for products from 1-5Tb/in² (ASTC)
 - New component technologies have been developed, such as NFT and FePt.
 - Significant challenges in SFD and recording head reliability are being addressed.
 - With continue growth in storage demand, there is more urgent need to productize HAMR beyond conventional perpendicular recording.
 - HAMR still have many practical challenges needs to be solved before launches as product.

Materials choices and ultimate limits of magnetic recording



Media Materials Options (Bulk Properties)



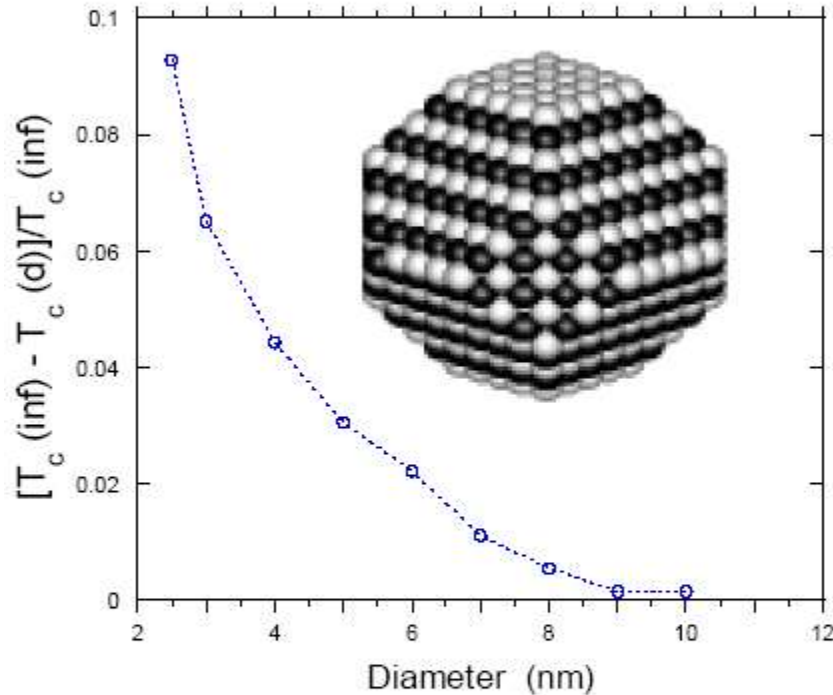
alloy system	material	K_1 (10^7erg/cm^3)	M_S (emu/cm^3)	H_K (kOe)	T_C (K)	$D_p^{(a)}$ (nm)	$D_p^{(b)}$ (nm)	$D_p^{(c)}$ (nm)	$D_p^{(d)}$ (nm)
	CoCr ₂₀ Pt ₁₅	0.25	330	15.2		15.5	12.4	15.3	7.8
Co-alloys	Co ₃ Pt	2	1100	36.4	1200	6.4	6.9	8.5	4.3
	(CoCr) ₃ Pt	0.39	410	19		12.4	10.6	13.2	6.7
	CoPt ₃	0.5	300	33.3	600	9.0	8.6	10.7	5.4
CoX/Pt(Pd)	Co2/Pt9	1	360	55.6	500	6.1	6.7	8.3	4.2
multilayers	Co2/Pd9	0.6	360	33.3	500	8.4	8.2	10.2	5.2
	FePd	1.8	1100	32.7	760	7.3	7.5	9.3	4.7
L1 ₀ phases	FePt	7	1140	122.8	750	2.4	3.6	4.4	2.3
	CoPt	4.9	800	122.5	840	2.8	3.9	4.9	2.5
	MnAl	1.7	560	60.7	650	4.9	5.7	7.1	3.6
rare-earth	Fe ₁₄ Nd ₂ B	4.6	1270	72.4	585	3.4	4.5	5.5	2.8
transition m.	SmCo ₅	20	910	439.6	1000	1.3	2.4	2.9	1.5

D_p : smallest possible thermally stable magnetic grain core size!

Particle Size Effects

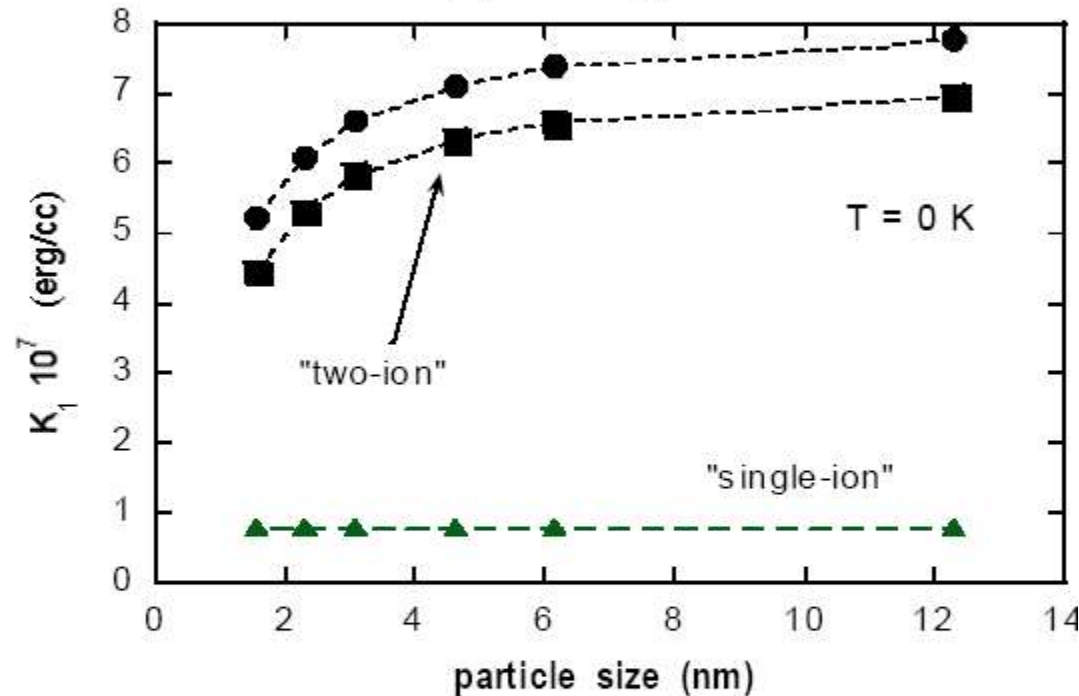
3d(Fe,Co)-5d/4d(Pt/Pd) High Anisotropy Alloys

Curie Temperature Reduction



Surface to volume fraction increases to 20-40% for 3 nm FePt particles (1000 atoms)

Anisotropy Energy Reduction



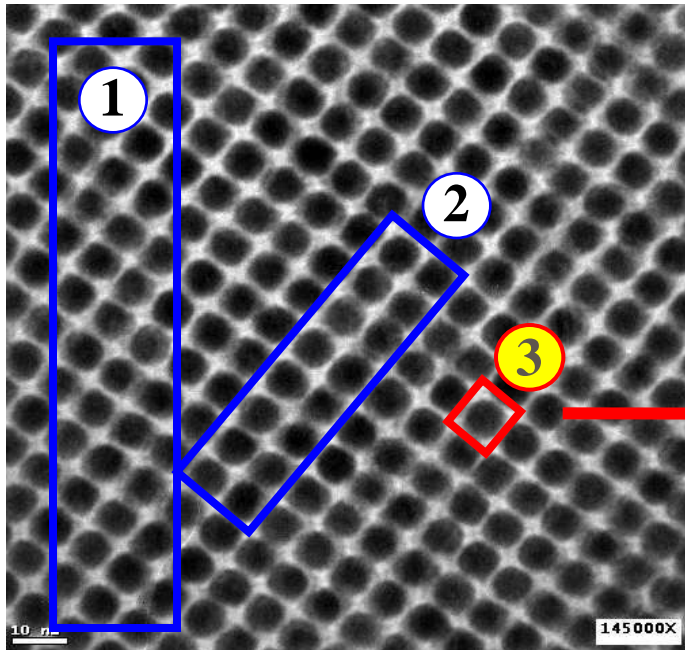
$$d_{ij}^{(2)} = \frac{k_{Pt}^{(0)}}{[J_{\mu}^0]^2} \sum_{\mu} J_{i\mu}^{Fe-Pt} J_{j\mu}^{Fe-Pt}$$

Finite size effects due to interactions mediated by induced Pt magnetic moment

O. Mryasov et.al., Europhy. Lett. 69, 805 (2005)

Ultimate size limits of magnetic recording

6nm FePt nanoparticles



S. Sun, C.B. Murray, D. Weller, L. Folks, and A. Moser,
Science **287** 1989-1992 (2000)

9 Tbit/in²

decrease particle size to 2.5nm,
center-to-center spacing to 3nm
⇒ 50 Tbit/in²

① Conventional Granular Media

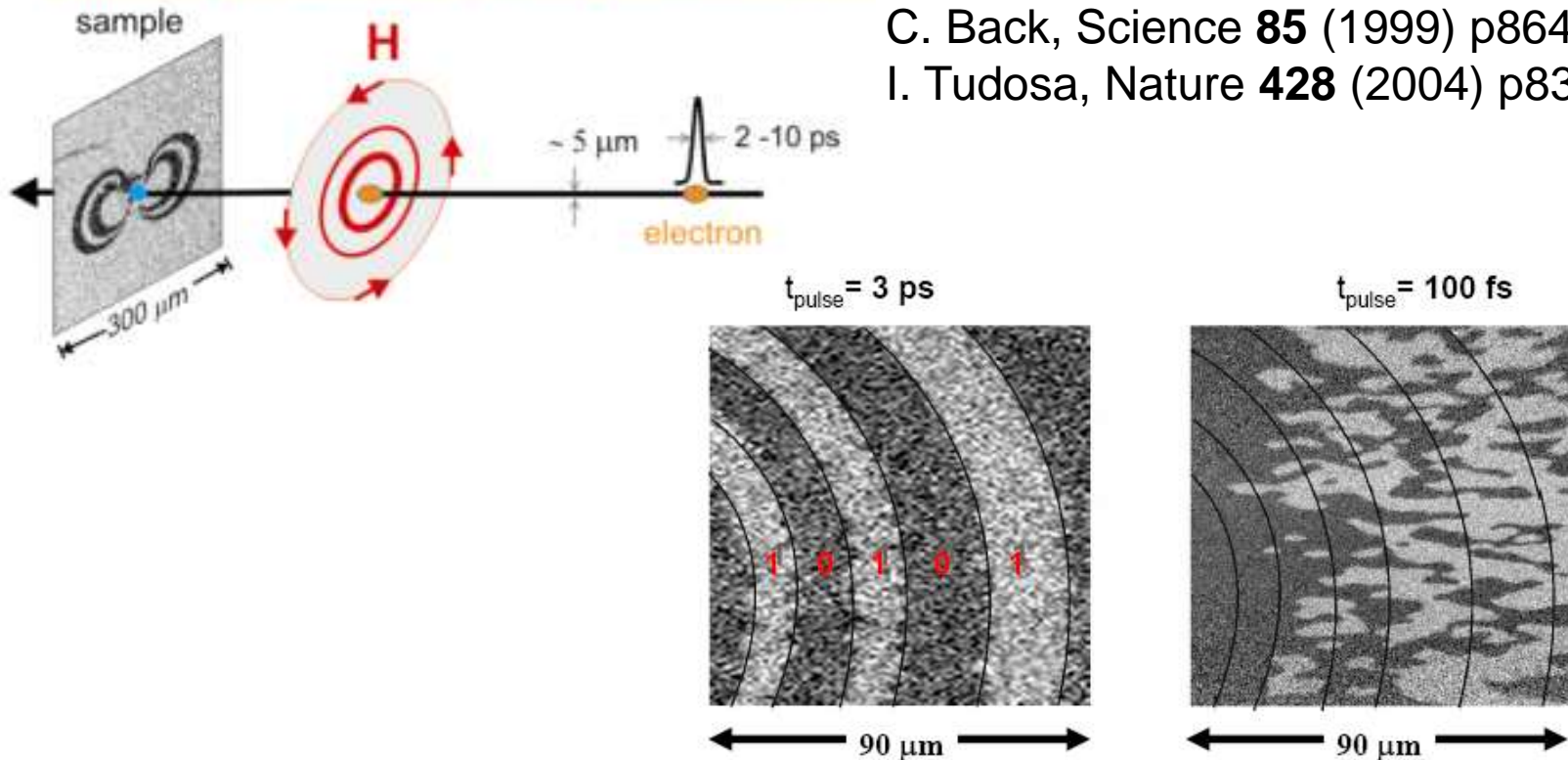
② Bit Patterned Media

③ Single-Grain-Per-Bit Patterned Media

The speed limit of magnetic recording

Ultrafast pulse – use electron accelerator

experiments at Stanford Linear Accelerator
C. Back, Science **85** (1999) p864
I. Tudosa, Nature **428** (2004) p831



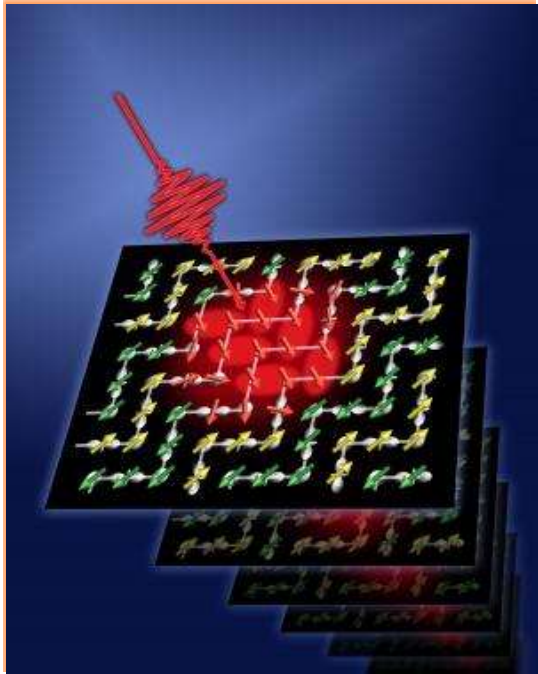
30 times faster than conventional
-- switching still works reliably --

1000 times faster than conventional
-- switching is not reliable --

There is a speed limit!

.. but we don't understand why

The speed limit of magnetic recording



Magnetic structure in a colossal magneto-resistive manganite is switched from antiferromagnetic to ferromagnetic ordering during about 100 femtosecond laser pulse photo-excitation. With time so short and the laser pulses still interacting with magnetic moments, the magnetic switching is driven quantum mechanically -- not thermally. This potentially opens the door to terahertz and faster memory writing/reading speeds.

Ames Laboratory, Iowa State University, and the University of Crete in Greece.

The discovery was reported in the April 4 issue of Nature, potentially opens the door to terahertz (10^{12} hertz) and faster memory speeds.

The ultimate limits of magnetic recording

